Development of recycled polypropylene plastic fibres to reinforce concrete

Thesis submitted by

Shi YIN (BEng, MEng)

for the degree of Doctor of Philosophy

in the College of Science, Technology & Engineering

James Cook University

Supervisors: Dr Rabin Tuladhar, A/Prof Nagaratnam Sivakugan

October 2015

Acknowledgements

I would like to thank my supervisory committee for their support and guidance throughout this multidisciplinary project.

I thank Dr. Rabin Tuladhar for giving me the freedom to pursue this stimulating and challenging project and providing a highly supportive and inspiring environment. Rabin's help extends far beyond the academic aspects of this project.

I wish to thank A/Prof Nagaratnam Sivakugan, my secondary supervisor, for his valuable expertise in all aspects of civil engineering.

I would like to acknowledge the financial support from Fibercon QLD. Thank you to Mr. Tony Collister and Mr. Mark Combe from Fibercon QLD for their unlimited availability and specialised knowledge in this field.

Special thank you to collaborators, A/Prof. Mohan Jacob, Prof. Robert A. Shanks, Dr. Madoc Sheehan, Mr. David Chung and Mr. Jacob Riella, who contributed their time, facilities and expertise to enable many of characterisations outlined in this thesis.

I would like to thank Mr. Warren O'Donnell, Mr. Tony Skalecki, Ms. Ruilan Liu and Ms. Melissa Norton for their assistance and patience in regards to laboratory testing and administration.

It would not have been possible to write this doctoral thesis without the help and support of my mum Xiangrong Yin, my dad Heng Shi, my brother and my friend Casey Maloney.

Statement of the Contribution of Others

Financial contribution towards this PhD project was received from:

1. Fibercon QLD (Living Expenses, for 3 years) AU$ 60,000

2. Graduate Research School, James Cook University AU$ 12,000

Apart from the financial assistance, the following have contributed to this PhD project as specified here under:

Dr. Rabin Tuladhar, supervised the entire PhD project and helped conceptualise the problem, suggested several ways of solving it and provided insights on the tools and technologies used in this thesis.

Abstract

In recent years, macro plastic fibres have widely been used to replace traditional steel reinforcement in the construction of concrete footpaths, precast elements and shotcrete tunnel linings, because of the ease of construction, reduced labour time and lower cost. They can effectively improve the performance of concrete, such as reducing drying shrinkage cracks and improving post-cracking performance of concrete elements. Recycled polypropylene (PP) fibres offer significant environmental benefits over virgin PP fibres or steel mesh. However, the recycled PP fibres have not yet been widely adopted by construction industries due to limited research and understanding on their mechanical properties, alkali resistance, and performance in concrete.

Since reinforcing effects of recycled PP fibres in concrete depend mainly on their tensile strength and Young's modulus, this research firstly explored the feasibility of using an improved melt-spinning and hot-drawing process to produce recycled PP fibres of high mechanical properties in an industrial scale. The 100% recycled PP fibre with high tensile strength (342 MPa) and Young's modulus (7115 MPa) was successfully produced in this research. The melt-spinning and hot-drawing process significantly improved crystallinity of the 100% recycled PP fibre from 51% to 82%. Since the 100% recycled PP fibre had higher crystallinity than that of virgin PP fibre, the recycle PP fibre showed higher Young's modulus. However, the 100% recycled PP fibre showed slightly lower tensile strength than that of virgin PP fibre, due to degradation from its repetitive processing and service life. In spite of the lower tensile strength, the 100% recycled PP fibre still has enough capacity to be used in concrete due to its high Young's modulus. An alkali resistance test was conducted and found that the 100% recycled PP fibre has minimum degradation in the concrete alkaline environment.

Performance of the 100% recycled PP fibre in different grades of concrete was studied and compared with virgin PP fibre. In order to increase bond with the concrete, line indentation was made on the surface of recycled PP fibre. Post-cracking performance of the fibre reinforced concrete was studied through the round determinate panel test (RDPT) and crack mouth opening displacement (CMOD) test. In the 40 MPa concrete

reinforced with 6 kg/m^3 of either 100% recycled or virgin PP fibre (normally used for precast concrete elements), most of the fibres were broken instead of being pulled out at the failure load. The 100% recycled PP fibre showed slightly lower performance than that of virgin PP fibre in the 40 MPa concrete. In 25 MPa concrete with 4 kg/m^3 of line-indent PP fibres (normally designed for concrete footpaths), majority of fibres were pulled out instead of being broken in the CMOD and RDPT tests. As the fibres did not reach ultimate tensile strength, their Young's modulus were more influential. The 100% recycled PP fibre had higher Young's modulus and hence, performed better than virgin PP fibre. The test results showed that the 100% recycled PP fibre has sufficient mechanical properties to be used to reinforce precast concrete elements and concrete footpaths.

In order to further improve fibre bonding with concrete, a new indentation of diamond shape was made on the fibre surface and compared with the commonly used line indentation. In the CMOD and RDPT tests, the diamond indents showed a better bonding with the concrete. Therefore, the diamond-indented 100% recycled PP fibre produced better post-cracking reinforcement in the concrete than that of line-indent 100% recycled PP fibre and virgin PP fibre and hence, can be used to replace steel reinforcing mesh (SRM) in concrete footpaths.

The environmental impacts of using 100% recycled PP fibres were assessed by using cradle to gate life cycle assessment (LCA) based on the Australian context. The LCA methodology is generally considered an excellent management tool for quantifying and comparing the eco-performance of alternative products. To reinforce 100 m^2 of concrete footpath, 364 kg of SRM and 40 kg of PP fibres can achieve the same degree of reinforcing in concrete. In this research, the environmental impacts of production of 40 kg 100% recycled PP fibres made by industrial PP waste and domestic PP waste were studied, and compared with those of production of 40 kg virgin PP fibre and 364 kg SRM. The LCA results showed that industrial 100% recycled PP fibre offers significant important environmental benefits over virgin PP fibre and SRM. Specifically, the industrial recycled PP fibre can save 93% of CO_2 equivalent, 97% of PO_4 equivalent, 99% of water and 91% of oil equivalent, compared to the SRM.

To showcase the industrial application of 100% recycled PP fibre produced in this research, the fibre performance was tested in various real-life applications which included concrete footpaths and precast concrete drainage pits. A 100 metre long footpath was casted in James Cook University by using 4 kg/m^3 of the diamond-indent 100% recycled PP fibre instead of traditionally used SRM. The fibre was directly mixed with the concrete in a concrete truck, and the ready-mixed concrete was poured into the formwork, which significantly reduced labour time and cost. Plastic shrinkage cracks did not appear after casting. The footpath has been used for half a year, and there are no drying shrinkage cracks as well. Concrete drainage pits reinforced by using 6 kg/m^3 of diamond-indent 100% recycled PP fibre were produced and found to have comparable testing results with the steel mesh reinforced concrete pits in the vertical loading tests.

In summary, this research has developed a methodology of producing recycled PP fibres with optimum mechanical properties for reinforcing concrete. The great potential of using these fibres in various concrete applications such as footpaths and precast concrete elements has been shown. This will not only help reduce consumption of virgin materials like steel or plastic but also provides attractive avenue of recycling plastic waste.

Table of Contents

List of Tables

List of Figures

List of Publications

The following is a list of publications by the candidate during the period of this thesis.

Journal articles

[1] S. Yin, R. Tuladhar, F. Shi, M. Combe, T. Collister, N. Sivakugan. Use of macro plastic fibres in concrete: A review. Construction and Building Materials. 2015, 93: 180-188. (Chapter 2)

[2] S. Yin, R. Tuladhar, F. Shi, R.A. Shanks, M. Combe, T. Collister, M. Jacob. Mechanical reprocessing of polyolefin waste: A review. Polymer Engineering and Science. 2015, 55(12): 2899-2909. (Chapter 2)

[3] S. Yin, R. Tuladhar, R. A. Shanks, T. Collister, M. Combe, M. Jacob, M. Tian and N. Sivakugan. Fiber preparation and mechanical properties of recycled polypropylene for reinforcing concrete. Journal of Applied Polymer Science. 2015, 132(16): 1-10. (Chapter 3)

[4] S. Yin, R. Tuladhar, J. Riella, D. Chung, T. Collister, M. Combe, N. Sivakugan. Comparative evaluation of virgin and recycled polypropylene fibre reinforced concrete. Construction and Building Materials. 2015 (Under review) (Chapter 4)

[5] S. Yin, R. Tuladhar, T. Collister, M. Combe, N. Sivakugan, Z. Deng. Post-cracking performance of recycled polypropylene fibre in concrete. Construction and Building Materials. 2015, 101(1): 1069-1077. (Chapter 5)

[6] S. Yin, R. Tuladhar, M. Sheehan, M. Combe, T. Collister. A life cycle assessment of recycled polypropylene fibre in concrete footpaths. Journal of Cleaner Production. 2016, 112(4): 2231-2242. (Chapter 6)

Conference papers

[1] S. Yin, R. Tuladhar, M. Combe, T. Collister, M. Jacob, R. Shanks. Mechanical properties of recycled plastic fibres for reinforcing concrete, In: Proceedings of the 7th

International Conference Fibre Concrete, pp. 1-10. From: 7th International Conference Fibre International Conference, September 12-13, 2013, Prague, Czech Republic.

[2] S. Yin, R. Tuladhar, T. Collister, M. Combe, N. Sivakugan. Mechanical Properties and Post-crack Behaviours of Recycled PP Fibre Reinforced Concrete, In: Proceedings of the 27th Biennial National Conference of the Concrete Institute of Australia, Construction Innovations, Research into Practice, pp. 414-421. From: 27th International Conference Concrete 2015, 30 August-2 September, 2015, Melbourne, Australia.

Other related paper

Zongcai Deng, Feng Shi, Shi Yin, Rabin Tuladhar. Characterisation of macro polyolefin fibre reinforcement in concrete through round determinate panel test. Construction and Building Materials. 2015 (Under review)

Chapter 1 Introduction

1.1 Rationale

Concrete is essentially a mixture of cement, aggregate and water. It is widely used in the construction industry because all the raw materials required are widely available and are of low cost. Concrete is very strong in compression, however, it has a very low tensile strength. To improve its tensile strength, steel reinforcing mesh (SRM) and steel bars are used in the concrete. Apart from traditional steel reinforcement, various fibres are also used to improve the properties of concrete, mainly for enhancing the tensile strength. There are four main types of fibres which can be used to reinforce concrete: steel fibre, glass fibre, natural fibre and synthetic fibre (Daniel et al., 2002).

In recent years, macro plastic fibres have widely been used in the construction of concrete footpaths (Alani and Beckett, 2013), precast panels (Peyvandi et al., 2013) and shotcrete mine tunnels (Kaufmann et al., 2013). Macro plastic fibres normally have a length of 30-60 mm, a cross section of 0.6-1 mm^2 (Yin et al., 2015b), a tensile strength of 300-600 MPa and a Young's modulus of 4-10 GPa (Hasan et al., 2011), depending on the raw materials and manufacturing techniques used. The macro plastic fibres can effectively control drying shrinkage cracks of concrete (Pujadas et al., 2014a). The drying shrinkage cracks occur in concrete due to loss of water molecules from hardened concrete (Jafarifar et al., 2014). This type of drying shrinkage cracks can occur in large flat areas like slabs in hot and dry environments, for example, in North Queensland, Australia. A SRM is normally used to prevent the drying shrinkage cracks; but it is now gradually being replaced by the macro plastic fibres due to ease of construction, reduced labour and lower cost. Another significant benefit of using macro plastic fibre is the improvement in post-cracking behaviour of concrete (Buratti et al., 2011). Brittle plain concrete has no effective post-cracking ductility, but the macro plastic fibres can considerably improve the post-cracking response of concrete, because the plastic fibres act as a crack arrester, and alter the intrinsically brittle concrete matrix into a tough material with better crack resistance and ductility. Therefore, when concrete cracks, the common large single cracks can be substituted by dense micro-cracks due to the presence of fibre reinforcement (Brandt, 2008).

Production of SRM involves significant carbon emissions. For instance, to reinforce 100 m^2 of concrete footpath (100 mm thick), typically, seven sheets of SL82 SRM are needed which produce about 1250 kg of carbon emission (BPIC, 2010; Strezov and Herbertson, 2006). However, 40 kg of polypropylene (PP) fibre can achieve the same degree of reinforcing in concrete, producing only 160 kg of carbon emissions (Chilton et al., 2010). Furthermore, the preparation required when using SRM such as laying, cutting and tying requires considerable labour time and cost compared to the use of plastic fibres which can be mixed directly into concrete trucks. Due to the ease of construction, and reduced labour cost, macro plastic fibers, such as PP (Ramezanianpour et al., 2013), high-density polyethylene (HDPE) (Zheng and Feldman, 1995) and polyethylene terephthalate (PET) fibres (Fraternali et al., 2014) have become attractive alternatives to SRM for reinforcing concrete (Pelisser et al., 2010).

Presently, thermoplastic waste from disposable consumer packaging and products is increasing, elevating the environmental pollution and wasting useful resources. According to the surveys done by the United States Environmental Protection Agency (U.S.EPA, 2014), plastic waste accounted for less than 1%·w/w of municipal solid waste stream in the 1960s, which considerably increased to 12.7%·w/w in 2012. Plastic bottles and plastic bags are becoming increasingly prevalent and have substituted glass bottles, metal containers and paper bags. Global plastic production was 288 and 299 million tonnes in 2012 and 2013, respectively (PlasticsEurope, 2015). However, the global recycling rate of plastic waste in this period was less than 5% (Velis, 2014). The recycling rate varied for different countries depending upon the maturity of the recycling process. For example, the recycling rates of Europe, Australia and the United State were 26% (PlasticsEurope, 2015), 20% (A'Vard and Allan, 2014) and 9% (U.S.EPA, 2014),respectively.

Consequently, increasing plastic production coupled with low recycling rates has led to a serious increase in pollution, including emission of powerful greenhouse gases (GHG) such as methane in landfill areas (Zhou et al., 2014), emission of toxic chemicals (e.g. bisphenol A and polystyrene) (Dodbiba et al., 2008), and poisoning of many marine species (La Vedrine et al., 2015). One of ways to address this problem is to develop various reusing and recycling techniques, such as material recycling (Castro et al.,

2014), feedstock recycling (Dormer et al., 2013) and energy recovery (Gallardo et al., 2014), for these materials. Improving the quality of recycled PP products (Eriksson et al., 2005) and extending their applications (Duval and MacLean, 2007) is also an effective way to promote the recycling rate. Therefore, preparing high-strength recycled plastic fibres and using them in concrete can be a unique way of reinforcing concrete while also decreasing plastic pollution.

Several techniques and methods have been developed to produce recycled plastic fibres (Fraternali et al., 2011; Gregor-Svetec and Sluga, 2005; Kim et al., 2008; Kim et al., 2010; Ochi et al., 2007). A common technique is extruding recycled plastic granulates into fibres, and then slowly stretching the fibres in an oven with a temperature of 130-170 ℃ (Ochi et al., 2007). Another popular processing technique is extruding recycled plastic granulates through a rectangular die to form film sheets. The resulting film sheets are then slit longitudinally into equal width tapes (Kim et al., 2008; Kim et al., 2010). de Oliveira and Castro-Gomes (2011) and Foti (2011) used a method to produce recycled lamellar PET fibres and 'O'-shaped PET fibres by simply cutting waste plastic bottles.

A common deficiency in these methods is that they are based mostly on laboratory processes, and they have low production rate resulting in high cost. Hence, these methods are not suitable to produce fibres for large-scale commercial applications. Moreover, the durability of recycled PET fibres in Portland cement matrix is still questionable (Silva et al., 2005). The PET fibres belong to polyester group, and polyester fibres degrade when embedded in Portland cement matrix (Alani and Beckett, 2013; Won et al., 2010). According to the degradation tests from EPC company (EPC, 2012), the PET fibre only could maintain its performance for 10 years in concrete, after that the strength of fibres decreased significantly. Although recycled PET fibres have recently become a focus of research, literatures on the use of recycled PP fibre in concrete is very limited. Recycled PP fibres have not yet been widely adopted by the construction industry due to limited research focusing on its mechanical properties and performance in concrete. Hence, this research focuses on the development of recycled PP fibre with sufficient mechanical properties like Young's modulus and tensile strength for the application in concrete. The research

also focuses on quantifying the post-cracking performance of recycled PP fibre reinforced concrete and comparing it with the performance of virgin PP fibre reinforced concrete.

In order to help decision makers choose reinforcing material that causes the lowest environmental impact, it is very important to carry out a comparative impact analysis. There are a variety of general and industry specific assessment methods, such as GMP-RAM (Jesus et al., 2006), INOVA Systems (Jesus-Hitzschky, 2007), and fuzzy logic environmental impact assessment method (Afrinaldi and Zhang, 2014). However, life cycle assessment (LCA) is the most comprehensive among the available tools and has been widely used. The LCA methodology is generally considered the best environmental management tool for quantifying and comparing the eco-performance of alternative products. Therefore, this research also studies and quantifies the environmental impacts of production of recycled PP fibres by using the LCA methodology, and compares these with the environmental impacts of production of traditionally used virgin PP fibre and SRM.

1.2 Research Objectives

This project aims to develop recycled PP fibres, which can be used to replace virgin PP fibre and SRM in the construction of concrete footpaths and precast elements. It includes production of recycled PP fibres of high tensile strength and Young's modulus in the industrial scale, investigation of reinforcing effects of the recycled PP fibres in concrete, assessment of environmental benefits of using recycled PP fibres, and industrial applications of the recycled PP fibre reinforced concrete. This is achieved by addressing the following objectives:

- To develop industrially feasible method of producing recycled PP fibres with high tensile strength and Young's modulus for application in concrete, and to assess durability of the recycled PP fibres in concrete alkaline environment.

- To quantify post-cracking performance of 100% recycled PP fibre in different concrete elements such as footpaths and precast drainage pits in comparison with virgin PP fibre. To develop high-performance recycled PP fibres, and study

the effects of tensile strength, Young's modulus and surface indents of these recycled PP fibres on their reinforcing effects in concrete.

- To explore the environmental benefits of using 100% recycled PP fibres produced by either domestic or industrial PP waste, and compare these with the environmental impacts of production of virgin PP fibre and SRM.

The outcomes of this project are expected to contribute to a sustainable development of construction industry.

1.3 Thesis Organisation

This thesis comprises eight chapters. Some chapters represent a manuscript or a series of manuscripts at various stages of publication joined by a common theme.

Chapter 1: This chapter provides the aim and objective, and also introduces the rationale for this project.

Chapter 2: In this chapter, current progress in the fields of recycled plastic fibre reinforced concrete is reviewed. In Section 2.1, various workable technologies in the mechanical reprocessing of PP waste, which have been successfully developed and widely applied in the recycling industry, are reviewed, and have been published as *S. Yin, R. Tuladhar, F. Shi, R.A. Shanks, M. Combe, T. Collister, M. Jacob. Mechanical reprocessing of polyolefin waste: A review. Polymer Engineering and Science. 2015, 55(12):2899-2909.* In Section 2.2, recent developments in the area of macro plastic fibre reinforced concrete are discussed, as published in *S. Yin, R. Tuladhar, F. Shi, M. Combe, T. Collister, N. Sivakugan. Use of macro plastic fibres in concrete: A review. Construction and Building Materials. 2015,93:180-188*. In Section 2.3, characterisation methods of toughness and post-cracking behaviour of fibre reinforced concrete are reviewed. Advantages and disadvantages of the current methods are presented. Based on the properties of recycled PP fibres in this research, the most suitable characterisation methods are chosen. The Section 2.4 reviewed current progress of life cycle assessment on recycling plastic waste.

Chapter 3: This chapter presents the production of fibre, and discusses about the development of a melt spinning and hot drawing technology, through which recycled PP fibres of high tensile strength and Young's modulus are successfully produced under the factory conditions. The findings have been published as *S. Yin, R. Tuladhar, R. A. Shanks, T. Collister, M. Combe, M. Jacob, M. Tian and N. Sivakugan. Fiber preparation and mechanical properties of recycled polypropylene for reinforcing concrete. Journal of Applied Polymer Science, 2015,132(16):1-10*.

Chapter 4: This chapter explores durability of 100% recycled PP fibre in concrete alkaline environment, studies reinforcement of the 100% recycled PP fibre in different concretes, designed for footpaths and precast panels, and proves the industrial feasibility of using 100% recycled PP fibre to replace virgin PP fibre. The results were submitted in *S. Yin, R. Tuladhar, J. Riella, D. Chung, T. Collister, M. Combe, N. Sivakugan. Comparative evaluation of virgin and recycled polypropylene fibre reinforced concrete. Construction and Building Materials. 2015 (Under review)*.

Chapter 5: In this chapter, ability of various newly developed recycled PP fibres to enhance post-cracking performance of concrete is ascertained. The effects of tensile strength, Young's modulus and surface indents of the different recycled PP fibres on their reinforcing effects in concrete are studied. The results of this investigation have been published as *S. Yin, R. Tuladhar, T. Collister, M. Combe, N. Sivakugan, Z. Deng. Post-cracking performance of recycled polypropylene fibre in concrete. Construction and Building Materials. 2015, 101(1):1069-1077.*

Chapter 6: This chapter assesses the environmental impacts of producing 100% recycled PP fibres from domestic and industrial plastic waste, compared with the production of virgin PP fibre and SRM. This study is based on Australian conditions and quantifies the environmental impacts in terms of material consumption, water use, and emissions to the environment by using life cycle assessment methodology. The outcomes of this study have been published in S*. Yin, R. Tuladhar, M. Sheehan, M. Combe, T. Collister. A life cycle assessment of recycled polypropylene fibre in concrete footpaths. Journal of Cleaner Production. 2016, 112(4): 2231-2242.*

Chapter 7: This chapter showcases the industrial application of 100% recycled PP fibre. The fibre performance is tested in various real-life applications which include concrete footpaths and precast concrete drainage pits.

Chapter 8: Concluding remarks and a recommendation for future work are presented in this chapter.

Chapter 2 Literature Review

2.1. Mechanical Reprocessing of Polypropylene Waste

Publication

S. Yin, R. Tuladhar, F. Shi, R.A. Shanks, M. Combe, T. Collister, M. Jacob. Mechanical reprocessing of polyolefin waste: A review. Polymer Engineering and Science. 2015, 55(12):2899-2909.

Thermoplastic waste from disposable consumer packaging and products is increasing, elevating the environmental pollution and wasting useful resources. Polypropylene (PP) is one of major types of thermoplastics used throughout the world in a wide variety of applications, such as toys, containers, pipes, automotive parts, electrical components, etc. In Australia, 0.23 million tonnes of PP products were consumed in 2013, while the recycling rate was only 24% (i.e. 0.056 million tonnes) (A'Vard and Allan, 2014). Legislations have been introduced around the world to limit disposal of the plastic wastes and to encourage more environmentally friendly options, to control plastic pollution (Achilias et al., 2008). Efficient recycling and recovery methods are therefore being researched and developed. According to Australian National Plastics Recycling Survey (A'Vard and Allan, 2014), mechanical recycling is the most widely practiced of these methods in Australia, since it is relatively easy and economical. Technology and infrastructure required for collection and mechanical reprocessing of plastic waste is also widely available.

Mechanical recycling refers to reprocessing plastic waste into secondary raw materials and products by physical means. The mechanical recycling involves a series of treatments and preparation steps (Yin et al., 2015c). Generally, the first stage of recycling process includes collecting, sorting, shredding, milling, washing and drying the plastic waste into recycled plastic pellets, powder or flakes (Al-Salem et al., 2009). Extensive research has been carried out in this stage, especially in terms of collection and sorting techniques (Carvalho et al., 2012), such as flotation, optical sorting, density

separation, electrical separation, etc. In the second stage the recycled plastic pellets, powder or flakes are molten and reprocessed into final products by resin moulding techniques (Demirel and Daver, 2013), including extrusion moulding, injection moulding, blow moulding, vacuum moulding, inflation moulding, etc.

Mechanically recycled products, however, often have mediocre mechanical properties in practice, which strongly limit their applicability and market demand (Khan et al., 2010). Two factors mainly lead to unsatisfactory performance of recycled plastic products. The first is degradation of the plastic waste (Sanchez et al., 2014). When plastics undergo high temperature or shearing during their processing stage, thermo-mechanical degradation occurs (Mbarek et al., 2006). Moreover, during the service life of plastic products, long exposure to the air, light, moisture, temperature and weathering gives rise to their natural aging. The second factor is heterogeneity of the plastic waste (Brems et al., 2012). Plastic waste is a mixture of various types and grades of polymers with distinct degrees of polymerization and chemical structures, which are mutually incompatible. Furthermore, contaminants, such as paper scraps and adhesive additives deteriorate the mechanical properties of recycled polymers and limit their applications. The more complex and contaminated the waste is, the more difficult it is to recycle it mechanically. Thus, a full separation of individual components is rarely implemented (Brachet et al., 2008).

In order to improve quality of end products of recycled PP, various workable reprocessing techniques in the second stage of mechanical recycling have been developed and widely applied in the recycling industry (Kabamba and Rodrigue, 2008). This chapter critically reviews the current reprocessing techniques of recycled PP. The degradation and crystallisation behaviour accompanying with the reprocessing processes is also presented. This would help us compare different reprocessing methods and choose the most suitable one for the production of recycled PP fibre.

2.1.1. Degradation and Crystallisation Behaviours of Reprocessing PP Waste

Reprocessing recycled PP is always accompanied with degradation, crystallisation, and consequent processability problems, which result from molecular chain scission, branching and crosslinking. The degradation behaviour decreases tensile strength and

impact strength, while the crystallisation behaviour increases Young's modulus and yield stress. Therefore, ultimate mechanical properties of the crystallisable plastics are determined by both degradation and crystallisation behaviours. In the recycling processes, the degradation behaviour is inevitable, but if the crystallisation behaviour can be taken full advantage of, the recycled plastic products still can maintain high quality and perform well (Andricic et al., 2008). Therefore, a good understanding of the degradation, crystallisation and processability is of scientific and technological importance for recycling PP waste.

2.1.1.1. Degradation Behaviour

Since PP is an organic polymer, undesirable chemical reactions, mainly caused by photo-oxidation and oxidation, frequently occur during their manufacture processes and service life (da Costa et al., 2007). The chemical reactions result in irreversible changes in the polymer structure, thus affecting the polymer performance. There are four types of distinguished degradation: chemical, thermal, mechanical and biological (Al-Salem et al., 2009). These degradation processes are very complex, and usually several types of degradation occur simultaneously. The phenomena, such as discoloration, loss of volatile components or smoking, and loss of mechanical properties, are frequently observed (Bahlouli et al., 2006).

During the processing stage, PPs are subjected to molecular chain damage, including crosslinking, chain scission and formation of double bonds. High shear forces, temperatures and presence of impurities and oxygen sever the polymer chains, producing highly reactive radicals at the end of chains. These radicals cannot recombine, but they can form peroxyl radicals and hydroperoxides with oxygen. Continuous degradation leads to serious molecular chain scission, branching and crosslinking, which may significantly change mechanical properties and processability of the recycled materials.

da Costa et al. (2005) studied PP degradation when it was submitted to multiple extrusion conditions. They found that under the condition of lower temperature (240 °C) and lower extrusion cycles (five cycles), the PP still remained with several entanglement points, and the mechanical chain breaking did not reach a level where

extensive degradation occurred. When the PP was under the conditions of higher die zone temperature (270 °C) and higher processing cycles (nineteen cycles), chain scission massively happened, and the material behaved as a liquid-like material of low viscosity, which resulted from the considerable reduction of molar mass, long chains and entanglements. Their further research (da Costa et al., 2007) found that the degradation process considerably reduced the break properties of PP, such as break strain, break stress and energy to break, while the small strain properties, like yield stress and yield modulus, were just slightly affected.

In many operations, the recycled PPs are pelletised first in plastic reprocessing plants. The extruded PP pellets are then delivered to plastic manufacturing plants for the production of end products. The double heating and reprocessing in the plastic reprocessing and manufacture plants cause more serious degradation. If this could be undertaken as only one heating cycle, the deterioration would be minimised. Residence time during extrusion or other heating processes would therefore be lowered and the plastics would be subjected to less overall heating. Cold processes, such as shredding and crumbing, are recommended to prevent the degradation in the hot processes, such as pelletisation.

2.1.1.2. Crystallisation Behaviour and Mechanical Properties

There is a potentially misleading idea that during the recycling process there is a continuous deterioration on mechanical properties of the recycled plastics. However, after repetitive reprocessing for a low numbers of cycles, Young's modulus and yield stress of the recycled PP increase due to augmentation of crystallinity (da Costa et al., 2007). Ha and Kim (2012) successfully applied recycled PP as refrigerator plastics due to the comparable mechanical properties with the virgin PP, and obtained about 50% cost-merit.

Aurrekoetxea et al. (2001) mimicked procedures of recycling PP through repetitively injection moulding for several cycles. With the increase of recycling cycles, the crystallinity increased from 44.5% (the first cycle) to 48.5% (the sixth cycle), and remained at 48.5% until the tenth cycle. When the recycling increased from one cycle to six cycles, the Young's modulus grew from 1700 MPa to 2000 MPa, and the yield

stress rose from 34.8 MPa to 36.4 MPa, because of the increase of crystallinity. However, the elongation at break decreased from 66% to 45%, and fracture toughness also decreased from 2.24 $MPa \cdot m^{1/2}$ to 1.98 $MPa \cdot m^{1/2}$ due to the decrease of molar mass and tie-molecule density. They explained that the repetitively reprocessing breaks the molecular chain and allows the strained or entangled macromolecules to be released. The crystallisation is then developed by the rearrangement of these freed macromolecules segments. The crystalline structures hindered rotations of molecular segments, leading to the increase of stiffness.

2.1.2. Melt Blending

Melt blending is one of the most frequently-used ways of mechanically recycling plastic waste. It refers to blending recycled plastics with similar type of virgin plastics or different types of recycled plastics in the melt process. Blending recycled PP with virgin PP not only can reduce cost, but the new blended PP can maintain equal performance with the virgin plastic products (Yin et al., 2013). However, plastic waste collected from kerbside is a mixture of various types and qualities of polymers, thus extensive research has been carried out on reprocessing commingled plastic waste.

Blending recycled plastics with virgin plastics of similar components is often used for mechanically recycling industrial plastic waste, which is industrial plastic scrap off-cuts and off-specification items obtained from processing operations. The mechanical recycling of industrial plastic waste has been widely adopted due to ease of separation of different types of plastics, the low level of impurities present, and their availability in large quantities. Meran et al. (2008) mixed recycled PP with its virgin material. As shown in Fig. 2.1.1, tensile strength of recycled PP can be effectively improved by mixing its virgin plastic. They believed that recycled PPs have the capacity of being as good as any engineering grade under optimised mixing rates and reprocessing conditions.

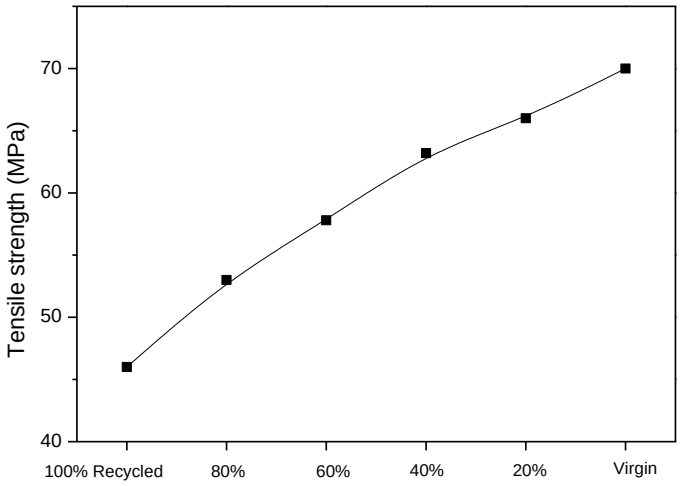

Fig. 2.1.1 Tensile strength of recycled PP blended with its virgin material (Meran et al., 2008)

Domestic plastic waste, consisting mostly of packaging materials from kerbside recycling collections, contains various types of polymers. A segregation of the plastic waste before recycling is time- and cost- consuming, and never fully separated. Therefore, the study on reprocessing the commingled plastic waste from roughly sorted waste is very practical. Table 2.1.1 shows mechanical properties when recycled PP is blended with recycled low-density polyethylene (LDPE) and HDPE (Hasanah et al., 2014; Strapasson et al., 2005). The mechanical properties show similar trends when the recycled PP is mixed with recycled LDPE and recycled HDPE. With the decrease of PP rate, the yield strength and Young's modulus of the materials are decreasing, thus the materials are becoming more ductile. Elongation at break dramatically decreases when 50% of PP is mixed with 50% HDPE or LDPE, due to incompatibility of the different blends.

Table 2.1.1 Mechanical properties of the recycled PP–LDPE and PP–HDPE composites

	Blending rate	Yield strength (MPa)	Young's modulus (MPa)	Elongation at break (%)
PP–LDPE composites (Strapasson et al., 2005)	100:0	25.1	1304	600–700
	75:25	22.8	1149	100
	50:50	13.8	845	3.7
	25:75	11.4	435	400–529
	0:100	7.6	157	111
PP–HDPE composites (Hasanah et al., 2014)	100:0	45	2340	14
	80:20	34	1690	8
	60:40	29	1290	7
	50:50	29	1250	6
	40:60	27	1200	15
	20:80	26	920	25
	0:100	25	900	25

2.1.3. Filler Reinforcement

Filler reinforcement can effectively reduce cost, and enhance mechanical and thermal properties of the recycled plastics. A variety of fillers, such as natural fillers, inorganic fillers and elastomers, have been successfully applied to reinforce recycled plastics.

Natural fillers have substantial inherent advantages, such as low density, low abrasion of processing equipment, relatively good specific mechanical properties, biodegradability and low cost. The natural fillers, including wood, bagasse, phormium tenax and wheat straw have been widely used. The natural filler-based recycled polyolefins now have been used in construction applications, such as decking and furniture, and automotive ones, including door panels and seat frames. However, incompatibility, processability and thermal degradation are the main problems which limit applications of the natural fillers in the recycled polyolefins (Mengeloglu and Karakus, 2008). Extensive research has been carried out to solve these problems and improve mechanical properties of the composites.

The addition of inorganic fillers to plastics results in remarkable improvements in morphological, mechanical, rheological and thermal properties, compared to neat polymer matrices. Unlike natural fillers, the properties can be significantly improved even upon using small amount of inorganic fillers. Various inorganic fibres have been developed and widely used in the plastic reprocessing industry. They are calcium carbonate, mica, glass beads, glass fibre, talc, silver, zinc oxide, titanium dioxide, cement, fly ash, and clays. The properties of inorganic filler reinforced recycled polyolefins strongly depend on size, shape, and distribution of the fillers in the plastic matrix, and also to the extent of interfacial adhesion between the fillers and the matrix.

Elastomer fillers can effectively improve toughness and impact resistance, but have side effects of decreasing tensile strength and Young's modulus (Clemons, 2010). Elastomers, such as poly(ethylene-co-propylene) rubber (EPR), poly(ethylene-co-octene) rubber (EOR), and poly(ethylene-co-propylene-co-diene monomer) (EPDM) are often used to improve the toughness and elongation at break of recycled materials, but the yield strength, tensile strength and Young's modulus would decrease (Liu et al., 2010). Therefore, sometimes inorganic fillers are used as well to compensate the side effect of the elastomers.

2.1.4. Mechanochemistry

Due to the degradation and immiscibility of the plastic waste, high content of stabilisers, compatibilisers, and fillers have to be used, which is not economically feasible for the recycling industry. Mechanochemistry is a good alternative method, where reactive blending occurs in the mechanical pulverization of polymers without using any additives (Streletskii et al., 2015). The mechanochemistry denotes the chemical and physicochemical transformation of substances during the agglomeration caused by the mechanical energy. The technique includes a variety of reactions, such as fast decomposition and synthesis, graft modification, and polymorphic transformation. The advantages include simple process, ecological safety and possibility of obtaining a product in the metastable state. This technology has thus attracted wide focus (Guo et al., 2010).

Mechanical milling, typically ball milling, refers to the process that utilizes high-energy ball milling technology to co-pulverize shredded recycled plastic, resulting in a considerable decrease in the polymer size (Kaupp, 2009). The mechanical effects generated in the process, such as impact, compression, fracture, extension and shearing, can induce chain scission and hydrogen abstraction within the material particles, thus producing a large number of free radicals. The free radicals from different molecular chain species react with each other to induce chemical crosslinking and coupling (Liu et al., 2013).

Solid-state shear pulverization (S^3P) is a novel, continuous and one-step cryogenic extrusion process to recycle plastic waste (Akchurin and Zakalyukin, 2013). The normally incompatible plastic waste is subjected to high shearing forces to shred the carbon-chain backbone of plastic, thus generating a large amount of free radicals, which can form graft copolymers. The pulverized particles are then used to prepare high-quality products through the injection moulding, rotational moulding, powder coatings, or blending with virgin plastics (Guo et al., 2010). Lebovitz et al. (2003) prepared recycled PPs through the S^3P process. The mechanical properties can be seen in Table 2.1.2.

Table 2.1.2 Properties of blends of postconsumer plastics (Lebovitz et al., 2003)

Feedstock	S^3P	Tensile properties		Izod impact (J/m)	Flexural properties	
		Ultimate (MPa)	Elongation (%)		Modulus (MPa)	Strength (MPa)
Recycled PP	Yes		375	32	1710	64.3
Recycled PP	No		330	37	1900	59.3
Virgin PP		28.2	38	21	1430	48
HDPE–recycled PP 70:30	Yes	19.6	8	11	960	27
LLDPE–recycled PP 70:30	Yes	12.9	8	32	510	19

The mechanochemical process only requires simple devices, and is a time-saving, cost-saving and eco-friendly process. The technology will contribute considerably to economy, industry and environment in the future. But presently, the technology is just in the experimental stage, and still needs investigations for commercialization.

2.2 Use of Macro Plastic Fibres in Concrete

Publication

S. Yin, R. Tuladhar, F. Shi, M. Combe, T. Collister, N. Sivakugan. Use of macro plastic fibres in concrete: A review. Construction and Building Materials. 2015,93:180-188.

Concrete is very strong in compression, however, it has a very low tensile strength. To improve its tensile strength, reinforcing steel is often used in the concrete. Apart from traditional steel mesh and bars, various fibres, such as steel fibre, glass fibre, natural fibre and synthetic fibre, have also been used to improve the properties of concrete.

Steel fibres can greatly improve the tensile strength and the flexural strength of concrete due to their ability to absorb energy (Beglarigale and Yazici, 2015) and control cracks (Buratti et al., 2013). Their electric (Dai et al., 2013), magnetic (Al-Mattarneh, 2014) and heat (Sukontasukkul et al., 2010) conductivity properties make them suitable for some special applications, such as shielding electromagnetic interference . However, corrosion of steel fibres can be detrimental and lead to rapid deterioration of concrete structures (Soylev and Ozturan, 2014). Glass fibre has an excellent strengthening effect (Tassew and Lubell, 2014) but poor alkali resistance (Sayyar et al., 2013). Natural fibres, such as wood (Torkaman et al., 2014), sisal (Silva et al., 2010), coconut (Ali and Chouw, 2013), sugarcane bagasse (Alavez-Ramirez et al., 2012), palm (Abd Aziz et al., 2014), and vegetable fibres (Pacheco-Torgal and Jalali, 2011), are cheap and easily available, but they have poor durability. Synthetic fibres can be made of polyolefin (Alberti et al., 2014), acrylic (Pereira-De-Oliveira et al., 2012), aramid (Vincent and Ozbakkaloglu, 2013), and carbon (Chaves and Cunha, 2014). They can prevent plastic shrinkage cracks in fresh concrete (Cao et al., 2014) and improve post-cracking behaviour of concrete (Pujadas et al., 2014b).

The schematic diagram in Fig. 2.2.1 shows the different failure modes associated with the fibre reinforced concrete (Zollo, 1997). Fibre rupture (1), pull-out (2) and debonding of fibre from matrix (4) can effectively absorb and dissipate energy to stabilise crack propagation within concrete. Fibre bridging the cracks (3) reduces stress

intensity at the crack tip. In addition, the fibre bridging can decrease crack width, which prevents water and contaminants from entering the concrete matrix to corrode reinforcing steel and degrade concrete. Fibre in the matrix (5) prevents the propagation of a crack tip. Consequently, minor cracks will be distributed in other locations of the matrix (6). Although every individual fibre makes a small contribution, the overall effect of three-dimensional reinforcement is cumulative (Zollo, 1997). Therefore, the fibres can effectively control and arrest crack growth, hence preventing plastic and dry shrinkage cracks (Yoo et al., 2013), retaining integrity of concrete (Yoo et al., 2014), and altering the intrinsically brittle concrete matrix into a tougher material with enhanced crack resistance and ductility (Park, 2011). In order to achieve considerable reinforcement, the fibres should have high tensile strength and Young's modulus (Yin et al., 2013).

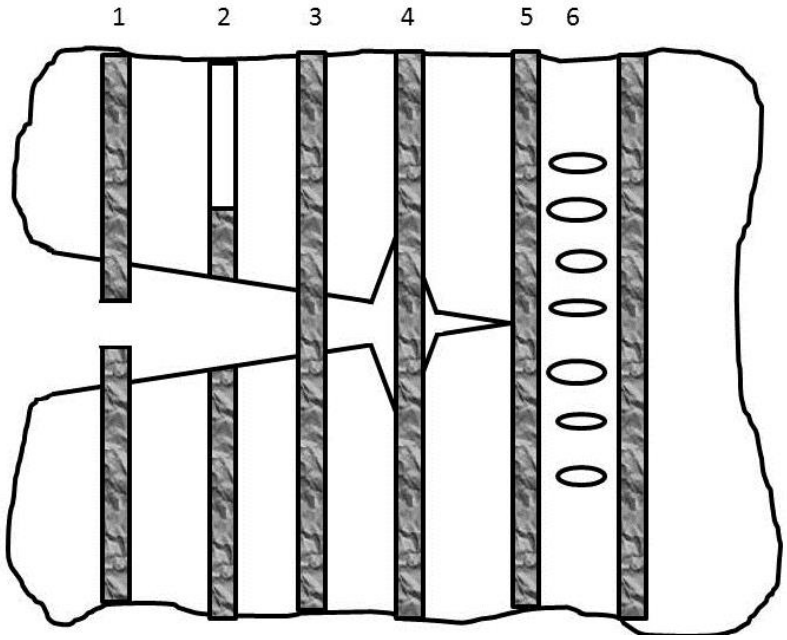

Fig. 2.2.1 Failure mechanisms in fibre reinforced concrete. 1. Fibre rupture; 2. Fibre pull-out; 3. Fibre bridging; 4. Fibre/matrix debonding; 5. Fibre preventing crack propagation; 6. Matrix cracking (Zollo, 1997)

Plastic fibres are synthetic fibres, which can be in the form of micro plastic fibres or macro plastic fibres. The micro plastic fibres refer to the plastic fibres whose diameter ranges from 5 to 100 μm and length is 5-30 mm (Nili and Afroughsabet, 2010). These micro fibres can effectively control plastic shrinkage cracking (Soutsos et al., 2012),

which is caused by shrinkage of fresh concrete during the first 24 hours after placement due to excessive evaporation of bleed water (Guneyisi et al., 2014). However, they normally do not have obvious effects on the properties of hardened concrete, as reported by Pelisser et al. (2010) and Habib et al. (2013). It is noteworthy that some micro plastic fibres, such as nylon fibres, can provide good thermal energy storage to concrete (Ozger et al., 2013), effectively controlling shrinkage of concrete (Song et al., 2005), and also significantly improving tensile strength and toughness of concrete (Spadea et al., 2015).

The macro plastic fibres normally have a length of 30-60 mm and cross section of 0.6-1 mm^2 (Yin et al., 2015b). The macro plastic fibres are not only used to control plastic shrinkage cracks (Chavooshi and Madhoushi, 2013), but also mostly used for controlling drying shrinkage cracks (Pujadas et al., 2014a). Another significant benefit is the post-cracking performance provided by the macro plastic fibres (Buratti et al., 2011). The macro plastic fibres now have become increasingly popular in the construction of concrete footpaths (Alani and Beckett, 2013), precast elements (Peyvandi et al., 2013) and shotcrete mine tunnels (Kaufmann et al., 2013).

2.2.1 Preparation and Properties of Plastic Fibres

The macro plastic fibres can be virgin and recycled polypropylene (PP), high-density polyethylene (HDPE) or polyethylene terephthalate (PET) fibres. PP fibres have been widely used in the concrete industry, due to its ease of production, high alkali resistance (Santos et al., 2005), and high tensile strength and Young's modulus (Yin et al., 2013). However, their low density (around 0.9 g/cm^3) may make the fibres 'float up' to the surface of concrete matrix (Auchey, 1998). Low hydrophilic nature of PP fibres, which can be reflected by low wetting tension of about 35 mN/m, also significantly deteriorates workability of fresh concrete and bonding between the fibres and the concrete (Ochi et al., 2007). HDPE fibres have slightly higher density (around 0.95 g/cm^3) and are more hydrophilic than PP fibres. However, HDPE fibres have low tensile strength (ranging from 26 to 45 MPa), which significantly limits their applications (Auchey, 1998). PET fibres have much higher density at 1.38 g/cm^3 and better wetting tension of 40 mN/m than PP fibres, so they are easier to be mixed with

concrete than the PP or HDPE fibres. They also have high tensile strength and Young's modulus (Ochi et al., 2007), which can effectively improve post-cracking performance of concrete. However, PET granules must be dried for at least 6 hours before being processed into fibres. The PET granules are also easily crystallised and stick on the inner wall of extruder. Hence, it is more difficult and costly to process PET than either of PP or HDPE. Moreover, alkali resistance of the PET fibres is questionable (EPC, 2012; Silva et al., 2005). Therefore, the PP fibres have become the most common commercial concrete fibre, and PET fibres have attracted extensive research, but HDPE fibres are still rare in practice with very little research being reported in the literature. From the environmental and cost-saving perspective, researchers are now also investigating the use of recycled plastic fibres in concrete (Siddique et al., 2008). However, recycled plastics have uncertain processing and service history, impurities and varying degrees of degradation, leading to processing difficulties and unstable mechanical properties (Wang et al., 1994).

The physical and chemical characteristics of the macro plastic fibres vary widely depending upon the manufacturing techniques. A popular technique involves melt spinning plastic granules into filaments and then hot drawing the monofilaments into fibres (Fraternali et al., 2011). In the study conducted by Ochi et al. (2007), PET granules were melted and extruded into monofilaments with a fineness of 60,000 dtex (dtex: grams per 10,000 m length). Then the monofilaments were hot drawn into 5000 dtex through a film orientation unit shown in Fig. 2.2.2 (Ochi et al., 2007). The resulting monofilaments were then indented and cut into fibres of 30-40 mm long. This melt spinning and hot drawing process highly oriented the molecular chains of the PET fibres, inducing high crystallinity and thus significantly improving tensile strength and Young's modulus. Through this method, PET (Fraternali et al., 2011) and PP (Yin et al., 2015b) fibre of tensile strength above 450 MPa can be obtained.

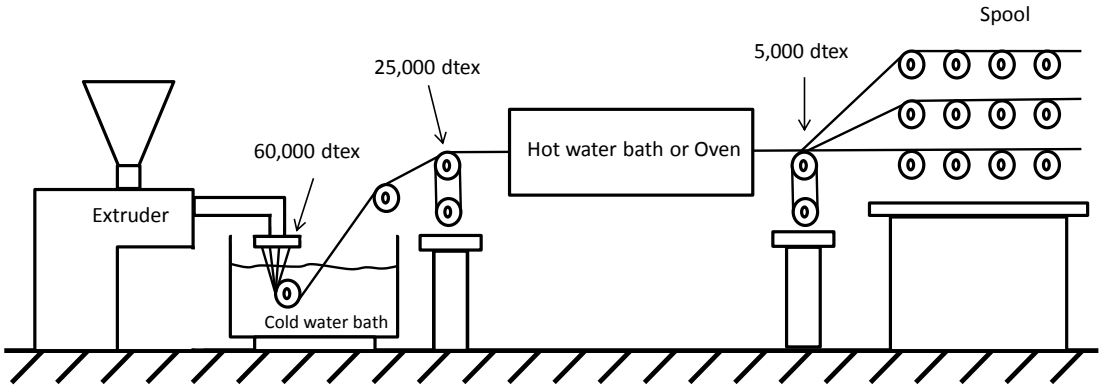

Fig. 2.2.2 Apparatus for PET fibre extrusion (Ochi et al., 2007)

Another popular processing technique is extruding PET, PP or HDPE granules through a rectangular die to form film sheets (0.2-0.5 mm thick). The resulting film sheets are then slit longitudinally into equal width tapes (1.0-1.3 mm wide) by a slitting machine. The tapes are then mechanically deformed using a patterned pin wheel, such as crimped and embossed. In some cases, the fibrillated tapes are also twisted before cutting to desired lengths (40-50 mm) (Kim et al., 2008). Kim et al. (2010) used this technique to successfully prepare recycled PET fibre with 420 MPa tensile strength and 10 GPa Young's modulus.

In order to reduce manufacturing costs, researchers have explored the potential of producing recycled plastic fibres just by mechanically cutting PET bottles, as reported by Fraternali et al. (2013), de Oliveira and Castro-Gomes (2011) and Foti (2011). Foti (2011) produced lamellar fibre and 'O'-shaped annular fibre by this method. The special shape of the 'O'-fibre can assist to bind the concrete on each side of a cracked section, thus improving ductility of the concrete. This technique though economical in smaller scale, cannot be used for a large-scale production. Firstly, the bottles should be washed before or after cutting which makes this process labour-intensive. Secondly, waste bottles have different history and degradation, which results in variable and poorer mechanical properties of the fibres. Moreover, the fibres produced through this technique only has a tensile strength of around 160 MPa and low Young's modulus of about 3 GPa (Foti, 2013), which are much lower than those of the fibres produced by the other two techniques.

2.2.2. Macro Plastic Fibre Reinforced Concrete

2.2.2.1. Fresh Concrete Properties

2.2.2.1.1. Slump

Workability of fresh concrete can be determined through a slump test (AS1012.3.9, 1993). Table 2.2.1 shows slump test results of macro plastic fibre reinforced concrete. The results indicate addition of macro plastic fibres decreases slump, thus decreasing workability of fresh concrete. This is due to the fact that the addition of fibres can form a network structure in the concrete matrix, thus restraining mixture from segregation and flow. Moreover, due to high content and large surface area of the fibres, the fibres can easily absorb cement paste to wrap around, hence increasing viscosity of the concrete mixture (Soroushian et al., 2003). Mazaheripour et al. (2011) made following two suggestions to improve the workability of fibre reinforced concrete: (a) to limit the volumetric content of macro plastic fibres to a range of 0.1% to 1% and (b) to add more water. However, addition of water will negatively affect concrete strength; hence plasticiser or water reducing admixtures are often used in fibre reinforced concrete to improve workability without increasing water content (Hasan et al., 2011).

Table 2.2.1 Properties of macro plastic fibre reinforced concrete

Macro plastic fibre	Fibre dimension	Fibre volumetric content (%)	Slump (mm)	Compressive strength (MPa)	Splitting tensile strength (MPa)
Macro PP fibre, wavelength shape (Choi and Yuan, 2005)	0.9mm in diameter, 50 mm in length	0	102	35.0	2.2
		1	38	35.4	3.2
		1.5	6.5	30.7	3.2
PP fibre, 620 MPa tensile strength and 9.5 GPa Young's modulus (Hasan et al., 2011)	40mm x 1.4mm x 0.11mm	0	N/A	38.9	3.6
		0.33	N/A	40.5	3.9
		0.42	N/A	41.4	4.1
		0.51	N/A	41.6	4.1

2.2.2.1.2. Plastic Shrinkage

Plastic shrinkage cracking is caused by moisture loss after casting (Banthia and Gupta, 2006). Generally, if the moisture evaporation rate exceeds 0.5 kg/m^2/hr, it causes negative capillary pressure inside the concrete, resulting in internal strain (Uno, 1998). Plastic shrinkage can cause cracks during the initial stages, when the concrete has not yet developed adequate strength (Sanjuan and Moragues, 1997). Kim et al. (2008) reported that although the macro plastic fibres do not affect the total moisture loss or rate of moisture loss, they still can effectively control the plastic shrinkage cracking by improving integrity of the fresh concrete. They also found that once the fraction of fibre volume exceeds 0.5%, a sufficient number of fibres are involved in controlling plastic shrinkage cracking, so the fibre geometry had no further effect. Najm and Balaguru (2002) studied the effects of fibre aspect ratio on the plastic shrinkage crack areas. They found that longer fibres (aspect ratio with length/width = 167) were extremely efficient and provided a crack-free surface at a fibre dosage of 9 kg/m^3,

while shorter fibre (aspect ratio with length/width = 67) could eliminate 94% cracking at a dosage of 18 kg/m^3.

2.2.2.2. Hardened Concrete Properties

2.2.2.2.1. Compressive Strength

As shown in Table 2.2.1 (Choi and Yuan, 2005; Hasan et al., 2011), the macro plastic fibres have no significant effects on the compressive strength, which is consistent with what was reported by Hsie et al. (2008), Campione (2006), Fraternali et al. (2011), and de Oliveira and Castro-Gomes (2011). Ochi et al. (2007) reported that there is no significant variation in the values of compressive strength associated with varying PET fibre contents. Moreover, during the compression tests, the plain concrete failed catastrophically, while as reported by Brandt (2008) the macro plastic fibre reinforced concrete cylinders failed with many minor cracks on the surface. The plastic fibres still held the concrete together at the failure load. Fig. 2.2.3 shows stress-strain curves of a compressive test on concrete cylinders conducted by Hasan et al. (2011). The samples with fibres showed a more ductile mode of failure and a post failure structural performance. This is attributed to ability of the fibres to distribute stresses and slow down the crack propagation process.

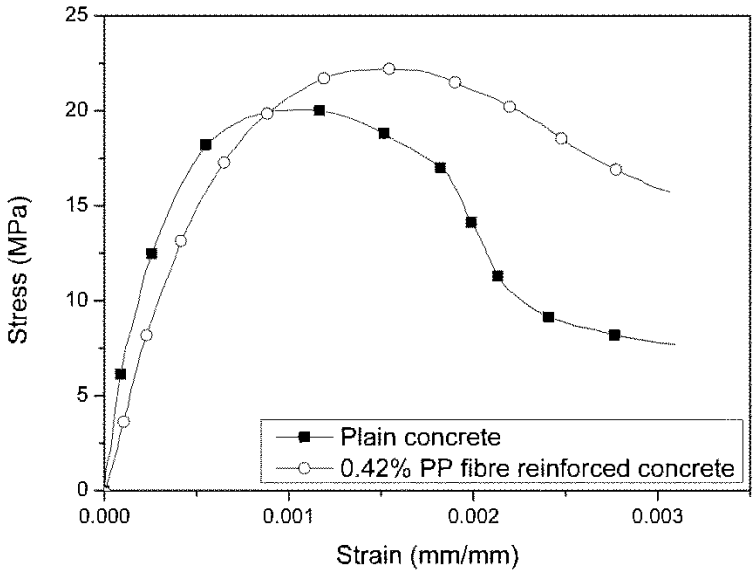

Fig. 2.2.3 Average stress-strain curves for concretes with macro plastic fibres (Hasan et al., 2011)

2.2.2.2.2. Splitting Tensile Strength

The split-cylinder test is an indirect test to obtain tensile strength of concrete (AS1012.10, 2000). As can be seen in Table 2.2.1 (Choi and Yuan, 2005; Hasan et al., 2011), the macro plastic fibres improve the splitting tensile strength of concrete. In the split-cylinder test, when the stress in concrete reaches tensile strength of concrete, the stress is transferred to the macro plastic fibres. The fibres can arrest the propagating macro cracks, thus improving the splitting tensile strength (Hsie et al., 2008). It was shown that plain concrete cylinders failed abruptly once the concrete cracked, whereas macro plastic fibre reinforced concrete could retain its shape even after concrete cracked. This shows that the macro plastic fibre reinforced concrete has the ability to absorb energy in the post-cracking state (Hasan et al., 2011).

2.2.2.2.3. Flexural Strength

Flexural test is another indirect tensile test which measures the ability of concrete beam to resist failure in bending (AS1012.11, 2000). Three-point loading and four-point loading are normally used in the flexural tests. For the three-point loading flexural test, results are more sensitive to specimens, because the loading stress is concentrated under the centre loading point (Alani and Beckett, 2013). However, in the four-point loading flexural test, maximum bending occurs on the moment span (Soutsos et al., 2012). Research has found that the macro plastic fibres have no obvious effects on the flexural strength, which is dominated by the matrix properties (Soroushian et al., 2003). The main benefit of using macro plastic fibres lies in improved ductility in the post-cracking region and flexural toughness of concrete (de Oliveira and Castro-Gomes, 2011). Brittle behaviour is always associated with plain concrete (Berndt, 2009). When the first crack is produced, the specimen cracks and collapses almost suddenly, with very small deformations and no prior warning. However, in plastic fibre reinforced concrete specimens, the failure progresses with bending, but without any sudden collapse as seen in plain concrete. When flexural tensile cracks occur, the load is transmitted to the plastic fibres. The fibres prevent the spread of cracks as shown in Fig. 2.2.1 and hence delay the collapse (Foti, 2011).

Hsie et al. (2008) tested the flexural strength of macro PP fibre reinforced concrete. The PP fibre had diameter of 1 mm, length of 60 mm, tensile strength of 320 MPa and Young's modulus of 5.88 GPa. As can be seen in Fig. 2.2.4, the plain concrete showed a brittle failure. The flexural strength reached the maximum at a deflection of around 0.05 mm without any post-crack performance. The PP fibre slightly increased the maximum flexural strength to 5.5 MPa at the same deflection point as the plain concrete. However, after the maximum flexural strength, the load is transferred to the PP fibres, thus becoming stable around 1.5 MPa. Similar trends were reported by de Oliveira and Castro-Gomes (2011), Ochi et al. (2007), Meddah and Bencheikh (2009), and Koo et al. (2014).

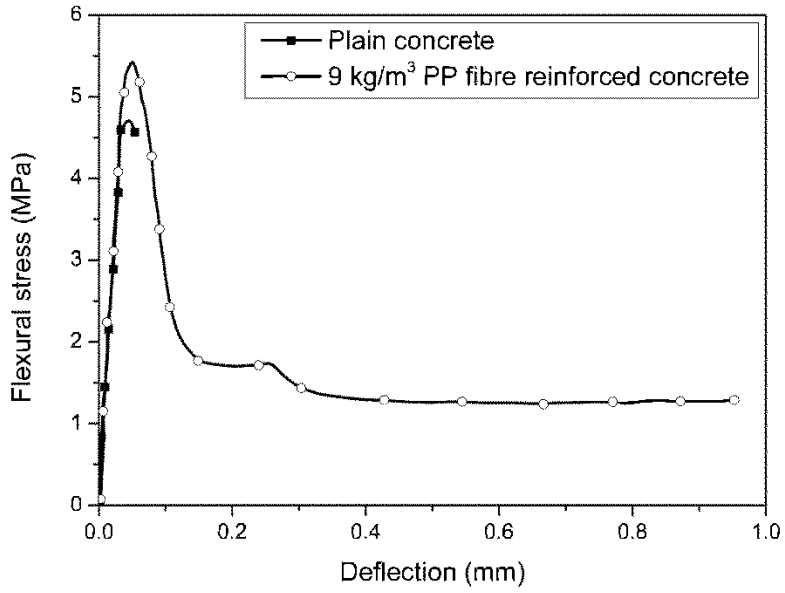

Fig. 2.2.4 Load-deflection curves of PP fibres reinforced concretes (Hsie et al., 2008)

2.2.2.2.4. Post-cracking Performance

Crack Tip Opening Displacement (CTOD) and Crack Mouth Opening Displacement (CMOD) tests are normally used to study the effect of fibres on the post-cracking behaviour of concrete (Fraternali et al., 2011). According to ASTM E1290 (ASTM, 2008b), CTOD is the displacement of the crack surfaces normal to the original (unloaded) crack plane at the tip of the fatigue pre-crack. However, due to inherent difficulties in the direct determination of CTOD, CMOD test is a preferred test to assess

post-crack performance of fibre reinforced concrete (Zhijun and Farhad, 2005). According to BS EN 14651:2005+A1:2007 (BSI, 2007), CMOD test measures the opening of the crack at mid-span using a displacement transducer mounted along the longitudinal axis. Both tests can clearly display the ability of fibres to redistribute stresses and bridge the cracks formed.

Fraternali et al. (2011) performed CTOD tests on PP and recycled PET fibre reinforced concrete specimens. The PP fibre had 1.04 mm^2 of cross section, 47 mm of length, 250 MPa of tensile strength, 1.1 GPa of Young's modulus, and 29% of ultimate strain, while the recycled PET fibre had 1.54 mm^2 of cross section, 52 mm of length, 274 MPa of tensile strength, 1.4 GPa of Young's modulus, and 19% of ultimate strain. The results can be seen in Fig. 2.2.5 (Fraternali et al., 2011). The peak load was reached at a corresponding CTOD of less than 0.6 mm for all the specimens. However, compared to the plain concrete, ductility of the specimens after the peak load was significantly improved in the PP and PET fibre reinforced specimens. This clearly exhibits the ability of macro plastic fibres to improve post-cracking performance of concrete.

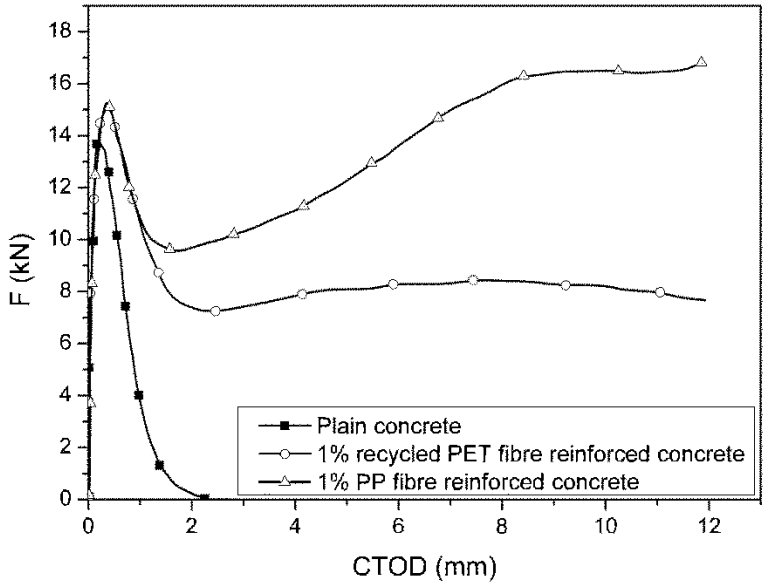

Fig. 2.2.5 Load-CTOD curves of recycled PET and PP fibres reinforced concrete (Fraternali et al., 2011)

Round Determinate Panel Test (RDPT) is considered to better represent the relative behaviour of different fibre reinforced concretes. This test has a significantly lower variation in post-cracking performance than that of either CMOD or CTOD test (Bernard, 2002). The panel-based performance assessment is desirable because panels fail through a combination of stress actions that reflects the behaviour of a fibre reinforced concrete more closely than other mechanical tests (Cengiz and Turanli, 2004). RDPT, based on ASTM C1550 (ASTM, 2012), involves bi-axial bending in response to a central point load, and shows a mode of failure related to the in-situ behaviour of structures such as concrete slabs-on-grade and sprayed tunnel lining construction (Parmentier et al., 2008).

Cengiz and Turanli (2004) compared the shotcrete panels reinforced by macro PP fibre, steel mesh and steel fibre. The PP fibre had a length of 30 mm, a diameter of 0.9 mm, a tensile strength of 400 MPa, a Young's modulus of 3.5 GPa, and ultimate strain of 11%. The steel fibre had a length of 30 mm, a diameter of 0.6 mm, a tensile strength of 1.2 GPa, a Young's modulus of 200 GPa, ultimate strain of 0.6%, and flattened ends with a round shaft. The steel mesh had a diameter of 8 mm and intervals of 150 mm. As can be seen from Fig. 2.2.6, 0.45% of steel fibre reinforced concrete showed 65 kN of peak load and 664 J of energy absorption until 25 mm deflection, while 0.78% of PP fibre reinforced concrete showed better post-cracking performance with 70 kN of peak load and 716 J of energy absorption. Steel mesh showed much more brilliant post-cracking performance (1308 J in energy absorption) than either of steel or PP fibres. However, until deflection of 2.5 mm, the PP fibre reinforced concrete exhibited comparable load with that reinforced with steel mesh.

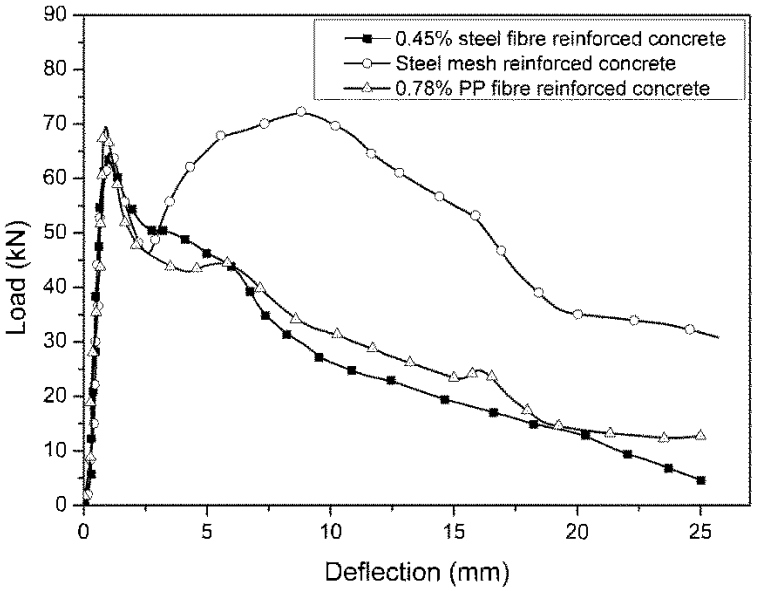

Fig. 2.2.6 Comparison of RDPT results for concrete reinforced with steel mesh, steel fibre and PP fibre (Cengiz and Turanli, 2004)

2.2.2.2.5. Drying Shrinkage

Soroushian et al. (2003) tested the restrained drying shrinkage of plastic fibre reinforced concrete, according to ASTM C157 (ASTM, 2008a). They found that the average maximum crack width of plain concrete was 0.3 mm at the 90^{th} day, while 0.19% of PP fibre effectively restrained the crack width to 0.15 mm, and delayed the initiation of cracking. As reported by Najm and Balaguru (2002) and Hsie et al. (2008), the plain concrete can withstand only small drying shrinkage strain, which is usually neglected. However, the addition of plastic fibres significantly increases the strain capacity of concrete, thus contributing to a reduction in crack widths and a delayed crack occurrence time.

2.2.2.2.6. Pull-out Behaviour of Plastic Fibres

Fibre debonding and pull-out (sliding) at the interface have a substantial impact on total energy absorption during the crack propagation. Therefore, the bond of fibre and matrix significantly affects capacity of the fibres to stabilise the crack propagation in concrete matrix (Singh et al., 2004). Low mechanical bonding strength may not provide

sufficient bridging force to control crack development. Moreover, the weak bonding strength also can cause internal micro-cracks in the interfacial areas (Ochi et al., 2007).

Oh et al. (2007) explored optimum shape among the various plastic fibres as shown in Fig. 2.2.7. In their pull-out tests, the crimped-shape plastic fibres exhibited the highest energy absorption capacity. Kim et al. (2008) reported that the embossed fibre had high bonding strength at 5 MPa due to its high surface energy and friction resistance. The crimped fibre also had high bond strength at 3.9 MPa, but its crimped part was stretched fully during the pull-out tests, thus leading to a rapid increase in displacement and low initial stiffness. The straight fibre had lowest bond strength at 1.7 MPa.

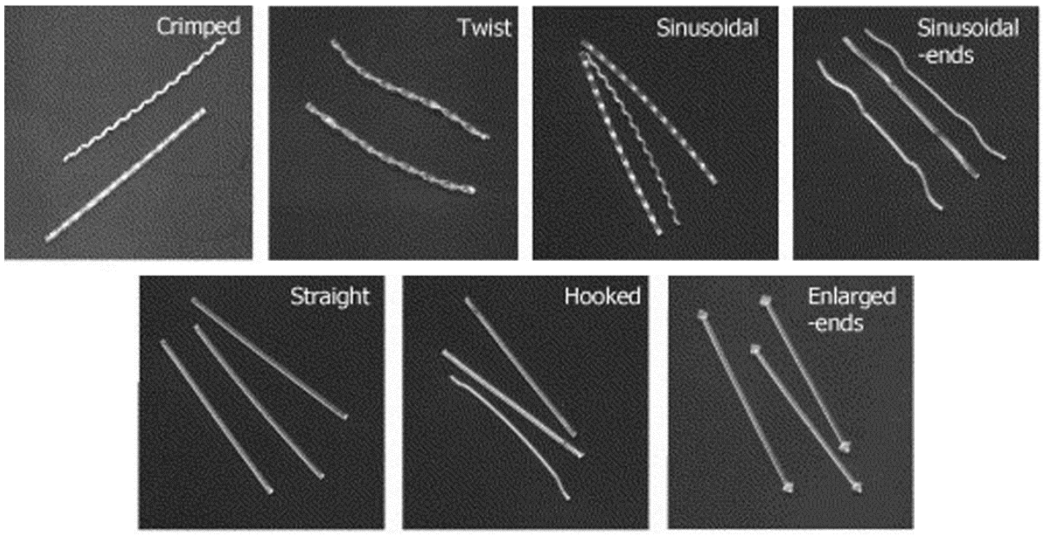

Fig. 2.2.7 Various types of plastic fibres for pull-out tests (Oh et al., 2007)

2.2.2.2.7. Degradation of Plastic Fibres in Concrete

PP has a high resistance to chemical attack due to its non-polar nature (Ha and Kim, 2012). For example, PP is resistant to alcohol, organic acids, esters and ketones, inorganic acids and alkalis. However, it swells when exposed to aliphatic and aromatic hydrocarbons and by halogenated hydrocarbons (da Costa et al., 2007).

Brown et al. (2002) studied long-term properties of virgin PP fibres in the concrete under a reactive environment. When PP fibres were exposed to an ionic environment of sodium and chloride ions created by salt water at different temperatures of 71 °C

and -7 °C for six months, the tensile properties of the PP fibres remained unchanged. Roque et al. (2009) immersed PP fibre reinforced concrete in simulated saltwater conditions for 33 months, and found that rate of stiffness reduction was only 2.34%, which was much lower than those of steel fibre (14.0%) and polyvinyl alcohol (PVA) (59.9%) reinforced concrete. It was concluded that PP has the best durability for non-structural applications in the saltwater environment. Elasto Plastic Concrete (EPC) company (EPC, 2012) did advanced alkalinity testing for their product olefin fibre. The fibres were subjected to an alkaline solution, which simulates a concrete environment. They reported that their olefin fibre could last up to 100 years in an alkaline environment without any decrease of strength.

The olefin fibres, including PP and HDPE, show high resistance to alkaline environment, while there is no agreement about the durability of PET fibres in Portland cement matrix. The PET fibres belong to the polyester group, and polyester fibres degrade when embedded in Portland cement matrix (Alani and Beckett, 2013; Won et al., 2010). The degradation tests from EPC company showed that the PET fibre only could perform well for 10 years in the concrete, after that the strength of fibre decreased significantly (EPC, 2012). However, Ochi et al. (2007) and the ACI 544 (Daniel et al., 2002) reported good alkali resistance of PET fibres in mortar and concrete. Moreover, Won et al. (2010) reported recycled PET fibres and recycled PET fibre reinforced concrete are highly resistant to salt, $CaCl_2$, and sodium sulphate, and have no significant difference in chloride permeability and repeated freeze-thaw tests compared to plain concrete.

Ochi et al. (2007) immersed recycled PET fibre into an alkaline solution, which was prepared by dissolving 10 g of sodium hydroxide in 1 dm^3 of distilled water, for 120 h at 60 °C. The results showed that the tensile strength of PET fibre after immersion was 99% of that before immersion, showing minimal deterioration. Fraternali et al. (2013) did the same test on the recycled PET fibre obtained by mechanically cutting post-consumer bottles, and found that the tensile strength of the PET after alkali attack was 87% of that before attack. Therefore, the recycled PET fibre was considered to have sufficient alkali resistance in both their studies.

Silva et al. (2005) immersed recycled PET fibres in a Lawrence solution (0.48 g/l $Ca(OH)_2$ +3.45 g/l KOH+0.88 g/l NaOH, pH=12.9), which simulates a fully hydrated cement paste. Through micrographs they found that surface of the recycled PET fibres became rough after being immersed for 150 days at 50 °C. Toughness of the PET fibre reinforced concrete decreased with the age due to the degradation of PET fibres inside the concrete. Fraternali et al. (2014) submerged recycled PET fibre reinforced concrete in the Italian Salerno harbour seawater for a period of 12 months. Through the CTOD tests, the energy absorption in the heavily cracked regime (CTOD 0.6-3 mm) was found significantly decreased by 52.1%.

2.2.3 Cost and Environmental Benefits of Using Macro Plastic Fibres

In recent years, macro plastic fibres have become an attractive alternative to traditional steel reinforcement in construction industry due to multiple reasons. Firstly, plastic fibres have significantly low cost compared to steel. For instance, based on our previous study (Yin et al., 2015a), 100 m^2 of concrete footpath (100 mm thick) typically requires seven sheets of SL82 steel mesh (364 kg of total weight). Whereas, 40 kg of plastic fibre (4 kg/m^3) can achieve the same degree of reinforcement in concrete footpath of same area. As of current price in Australia, the cost of 40 kg PP fibre is AU$ 600 (Fibercon, 2015), while seven sheets of SL82 steel mesh cost AU$ 800 (OneSteel, 2015). This shows the clear saving of price when using macro plastic fibres. Furthermore, preparation required when using steel mesh such as laying, cutting and tying requires considerable labour time and cost compared to the use of plastic fibres, which can be directly added to the agitator of an agitator truck and combined with the ready-mixed concrete. Ochi et al. (2007) reported that the process of using traditional steel reinforcement in a footpath of size 100 m^2 and thickness of 150 mm includes steel mesh preparation, and concrete placing and finishing, which requires 20 worker-hours (i.e. 0.2 man-h/m^2). However, the PP fibres can be directly mixed with concrete, eliminating the need of preparation of steel, which significantly reduces worker-hours to 10 h, (i.e. 0.1 man-h/m^2).

Thirdly, steel is highly corrosive in nature; corrosion of steel reinforcement in concrete structures can lead to their deterioration and failure. However, plastic fibres,

especially PP fibres, as we discussed before, are highly resistant to corrosion, thus having a long-term durability. Moreover, handling plastic fibres are much safer and lighter than using steel.

Last but not least, the production of plastic fibres can significantly reduce carbon footprint compared to that of producing steel. For instance, producing 40 kg of PP fibre can emit 140 kg carbon dioxide equivalents (Shen et al., 2010), while the production of 364 kg of steel has a 1250 kg of carbon emission (Strezov and Herbertson, 2006).

2.2.4. Applications of Plastic Fibre Reinforced Concrete

Reinforcing steel is expensive and its placement in concrete is labour and time intensive, often requiring placement in difficult and dangerous locations. Moreover, steel is highly corrosive in nature, which commonly deteriorates concrete. Therefore, macro plastic fibres are increasingly used in concrete and shotcrete industries for construction of footpaths, non-structural precast elements (pipes, culverts, cable pits and other small components), tunnels and underground structures, to partially or totally substitute steel reinforcement.

At mines, some locations, such as bedrock, are very difficult to support and are susceptible to collapse. In these cases, there is a long-standing demand to increase the support by increasing the fiber content. In the case of steel fiber reinforced concrete, difficulty of mixing and formation of fiber balls have prevented the use of higher fiber contents (Yang et al., 2012). However, plastic fiber reinforced concrete can be produced with fibre dosage more than 1% within the normal mixing time without any fibre ball formation and pipe clogging issues (Ochi et al., 2007).

Steel reinforcing mesh is conventionally used in the footpath applications to prevent drying shrinkage cracks (Abas et al., 2013). However, some roads, such as passages in tunnels under construction, passages through underground structures, urban alleyways, and bush roads, are commonly narrow, winding, and steep. It is desirable to apply fibre reinforced concrete to the pavement of such narrow sections of road. Unfortunately, traditional steel fibre can puncture tires, corrode and also can reduce

workability of concrete. Therefore, plastic fibres are now gradually replacing steel reinforcing mesh for such usage, because of ease of construction, and for saving labour and cost (Cengiz and Turanli, 2004). Table 2.2.2 lists some applications of PET fibre in mines and pavements in Japan (Ochi et al., 2007).

Table 2.2.2 Example applications of the PET fibres reinforced concrete in Japan (Ochi et al., 2007)

Prefecture	Location	Concrete sprayed/ placed	Water/ Cement (%)	Fibre length (mm)	Fibre content (%)	Remark
Kagoshima	Mine gateway	Sprayed	50	30	0.3	Replacement of steel fibre. First trial to use PET fibre in Japan. Found to be very easy to handle.
Kanagawa	Bush road	Placed	64	40	0.75	Replacement of wire mesh. Considerable laboursaving.
Ibaragi	Bush road	Placed	64	40	1	Applied successfully to road with 10% gradient.
Ehime	Slope	Sprayed	50	30	0.3	Replacement of steel fibre on the sea front.
Fukuoka	Tunnel	Placed	52	40	0.3	Applied to tunnel support for the first time.
Tottori	Tunnel	Placed	52	40	0.3	A new fibre content analyser was developed and used.
Kanagawa	Bridge pier	Placed	50	30	0.3	Crack extension was substantially decreased.
Shiga	Tunnel	Placed	52	40	0.3	A new fibre injector was developed and used.

Macro plastic fibres are also an appealing alternative to steel for reinforcing precast concrete elements, such as pipes (Haktanir et al., 2007), sleepers (Ramezanianpour et al., 2013) and pits (Snelson and Kinuthia, 2010). Fuente et al. (2013) produced fibre reinforced concrete pipes with internal diameter of 1000 mm, thickness of 80 mm and length of 1500 mm. PP fibre with continuously embossed indents (54 mm in length, 0.9 mm in diameter, 10 GPa Young's modulus and 640 MPa tensile strength) was used at 5.5 kg/m^3 dosage to reinforce the pipes. Through a crush test, they found that the peak strength of 50 kPa was achieved at the deflection of 1 mm, with the strength dropping to 30 kPa at the deflection of 2 mm, which kept constant until 10 mm. They reported that the traditional pipe production systems can be adapted while using PP fibre reinforced concrete, and the pipes can meet required strength classes without resorting to conventional rebar reinforcement.

2.3. Characterisation of Toughness and Post-cracking Behaviour of Fibre Reinforced Concrete

The macro plastic fibres do not have obvious effects on the compressive strength of concrete (de Oliveira and Castro-Gomes, 2011), but they can effectively improve the toughness and post-cracking performance of concrete (Fraternali et al., 2011). Therefore, a good characterisation of the toughness and post-cracking behaviour is of scientific and technological importance for the macro plastic fibre reinforced concrete.

The toughness of fibre reinforced concrete materials can be considered as their energy absorption capacity. It is conventionally characterised by the area under the load-deflection curve obtained experimentally. Various testing methods, such as tensile, compressive and flexural tests, have been developed to study the energy absorption and toughness of the fibre reinforced concrete. The most straightforward way to characterise a material regarding its post-cracking behaviour in tension is by performing uniaxial tension tests under closed-loop displacement control (de Montaignac et al., 2012). However, such test procedure is complicated to carry out as compared to bend tests, and requires equipment that is not generally available. Using the flexural tests to characterise the toughness has been widely adopted and become the most popular, since the tests are easy to operate and can simulate most of engineering situation. Therefore, various kinds of flexural toughness tests have been developed, and are of common use in different parts of the world.

No Australian standards exist at present to determine toughness and post-cracking performance of fibre reinforced concrete. Most of the available European and American standards and guidelines recommend the use of unnotched beam specimens subjected to four-point loading, such as ACI Committee 544 (544, 1988), ASTM C1018 (ASTM, 1997), ASTM C1399 (ASTM, 2011a), and ASTM C1609 (ASTM, 2011b). Load versus mid-span deflection curves are used in these standards to study the toughness of fibre reinforced concrete. Load-crack opening diagrams are recommend by some standards, including ASTM E1290 (ASTM, 2008b) and BS EN 14651 (BSI, 2007), through a three-point bending test on a notched specimen. ASTM C1550 (ASTM, 2012) suggests testing the toughness on a concrete round panel instead of a beam. Other

standards, such as JSCE-G551 (JSCE, 2005a), JSCE-G552 (JSCE, 2005b), and RILEM TC162-TDF (RILEM, 2002) are also used to evaluate the toughness of fibre reinforced concrete. Facing with such a large amount of standards and guidelines, it is important to choose appropriate testing methods to characterise the toughness and post-cracking behaviour of macro plastic fibre reinforced concrete.

2.3.1 Four-point Flexural Tests on the Unnotched Beams

2.3.1.1 ASTM C1018

For many years ASTM C1018 (ASTM, 1997) was the most common testing method for evaluating the toughness of fibre reinforced concrete. As shown in Fig. 2.3.1, a four-point loading is carried on an unnotched beam of 350 mm x 100 mm x 100mm. The specimen net mid-span deflection is used to control the rate of increase of deflection using a closed-loop, servo-controlled testing system. The deflection of specimen at the mid-span increases at a constant rate within the range of 0.05 to 0.10 mm/min.

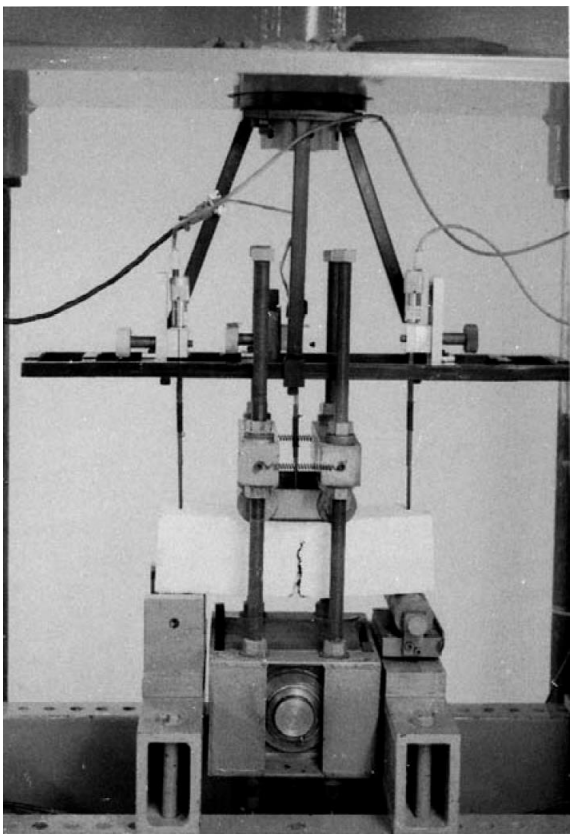

Fig. 2.3.1 Typical four-point flexural tests based on ASTM C1018 (ASTM, 1997)

The toughness indexes were defined in terms of the ratio of the area under the load vs. deflection curve out to some specified deflection to the area under the curve out to the point of first crack. As shown in Fig. 2.3.2, the toughness index I_5, I_{10}, and I_{30} are the numbers obtained by dividing the area up to a deflection of 3, 5.5 and 15.5 times the first-crack deflection (δ_f) respectively by the area up to first crack.

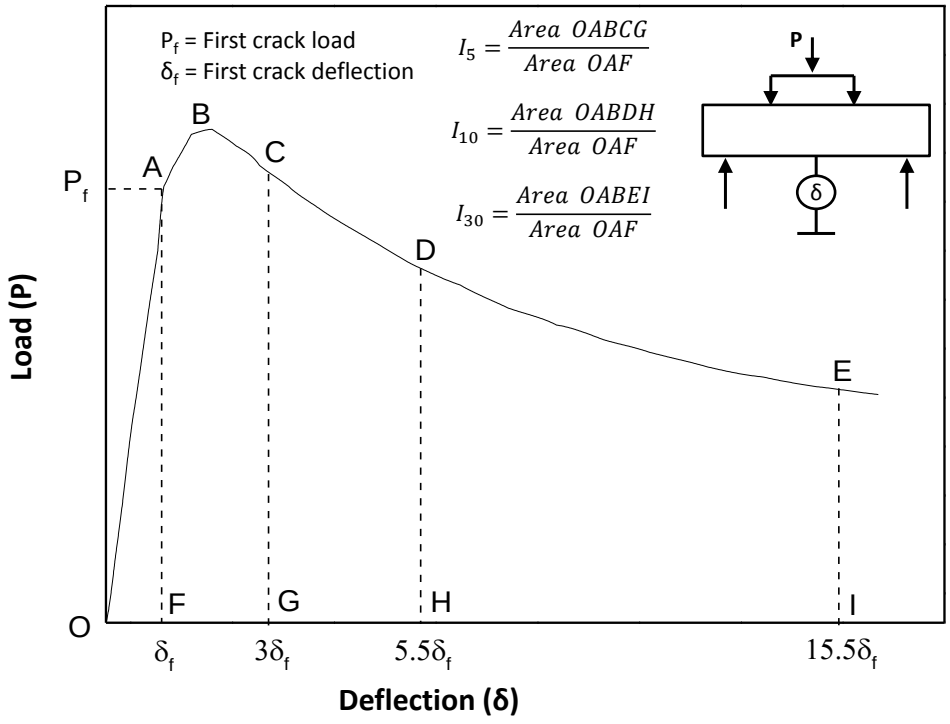

Fig. 2.3.2 Definition of ASTM C1018 toughness parameters (Gopalaratnam et al., 1991)

The first crack point is defined as 'the point of the load-deflection curve at which the form of the curve first becomes non- linear'. When using first crack deflection as part of a method for characterising toughness, an objective, accurate, and practical definition for the first crack point is important. However, the location of this point in practice is ambiguous and depends upon the resolution of the recording device and the judgement of the operator. Thus, errors can be introduced due to the difficulty of accurate definitions of the first crack point (Mindess et al., 1994). Moreover, these errors can be propagated and magnified when this deflection is multiplied by several numerical factors to calculate the toughness indexes. Equally important is an exact determination of the beam deflections both before and after the first crack. However, this is often difficult, due to various extraneous deflections that may occur due to

machine deformations and seating of the specimen on the supports (El-Ashkar and Kurtis, 2006). Other limitations include: the wide range of parameters that have been used to interpret test results (Banthia and Trottier, 1995), the greater variation in the recorded deflections in four-point bend tests compared with three-point bend tests (Taylor et al., 1997), and the influence of size effects on the test results (Gopalaratnam et al., 1991). As a result of these problems, ASTM C1018 was withdrawn in 2006.

2.3.1.2 ASTM C1399

ASTM C1399 (ASTM, 2011a) is a very useful method of assessing the toughness of fibre reinforced concrete, especially for the concrete reinforced by relatively low fibre volumes (Banthia and Dubey, 1999). This test is an open-loop test, so the testing machine does not need a displacement control. It was found by Bathia and co-workers (Banthia and Dubey, 2000; Banthia and Dubey, 1999) that the load vs. deflection curves obtained in this way were very similar to those obtained using a closed-loop testing machine with proper displacement control.

As shown in Fig. 2.3.3, a four-point loading is carried on a beam of 350 mm x 100 mm x 100 mm, which is the same size with the beam in ASTM C1018. Different with the ASTM C1018, a steel plate is used under the beam before concrete cracks. After the beam is cracked, the steel plate is removed and the cracked beam is reloaded to obtain data to plot a reloading load-deflection curve. An open-loop testing system is used with the rate of displacement of loading head at 0.65 mm/min.

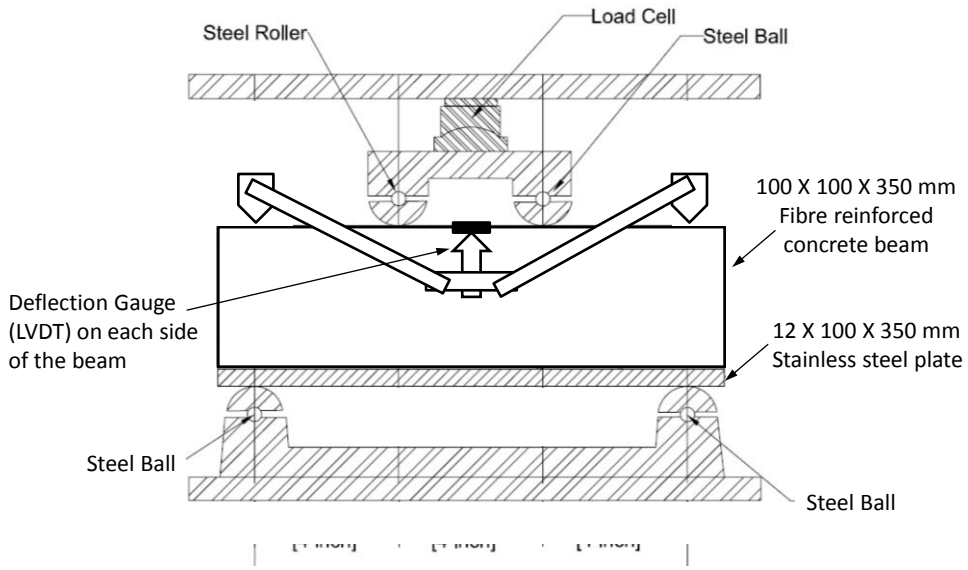

Fig. 2.3.3 Schematic of ASTM C1399 (ASTM, 2011a)

ASTM C1018 uses relative toughness value descriptions, which normalise the energy absorbed up to a specified deflection by the energy absorbed up to the first crack, while the ASTM C1399 describes absolute toughness values, which involve the average energy absorption (i.e. average residual strength (ARS)). The ARS is calculated using the loads determined at reloading curve (Fig. 2.3.4) deflections of 0.50, 0.75, 1.00, and 1.25 mm as follows:

$$\mathrm{ARS}=\frac{P_A+P_B+P_C+P_D}{4}\times\frac{L}{bd^2} \qquad (1)$$

where:

ARS = average residual strength, MPa,

$P_A + P_B + P_C + P_D$ = sum of recorded loads at deflections of 0.50, 0.75, 1.00, and 1.25 mm, N,

L = span length, mm,

b = average width of beam, mm, and

d = average depth of beam, mm.

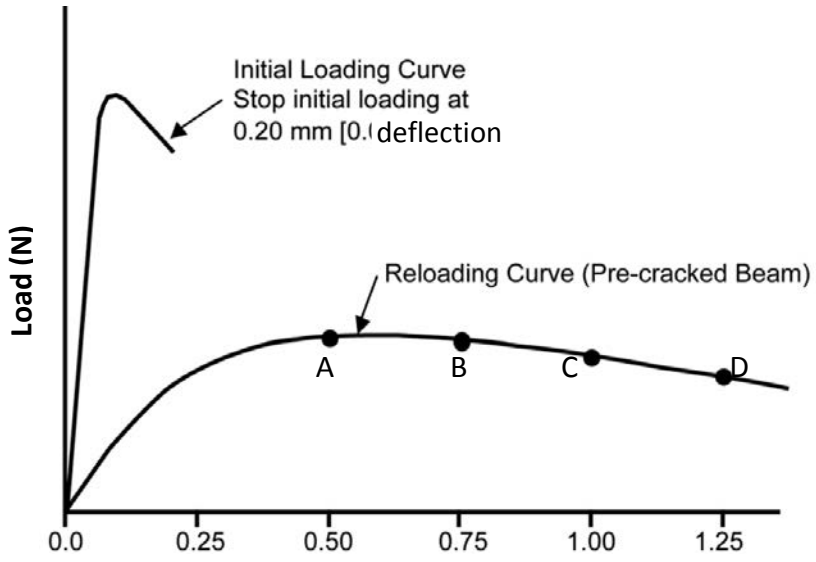

Fig. 2.3.4 Load-deflection curves (ASTM, 2011a)

This standard, however, has some disadvantages (Banthia and Mindess, 2004). Firstly, since the test procedure is divided into two parts, the effect of the fibres on the behaviour just after first cracking is lost. Another concern is that in an uncontrolled open-loop test, during initial loading, the deflection is very hard to control and the net deflection requirements are seldom met. This is of particular concern for very high strength matrices. Doubts are often raised as to the capacity of the pre-cracking procedure (with steel plate) to effectively replace proper re-loading test setup. Moreover, the length of the pre-crack obtained is unknown, and is variable for different fibre reinforced concrete systems. This makes comparison between different fibre reinforced concrete beams difficult.

2.3.1.3 ASTM C1609

Due to the drawbacks of ASTM C1018, this standard has been replaced by ASTM C1609 (ASTM, 2011b) since 2005. The ASTM C1609 has similar procedures with ASTM C1018 for obtaining the load vs. deflection curve, but the resulting curve is analysed in a totally different way. Therefore, the faults in the ASTM C1018 were excluded.

Based on the ASTM C1609, toughness tests are carried out on concrete beams with size of 350 mm x 100 mm x 100 mm and 500 mm x 150 mm x 150 mm. A closed-loop, servo-controlled testing system and roller supports are used in this test. Flexural load is applied under constant rate of displacement (not exceeding 0.05 mm/min) at one-third of test specimen spans. As shown in Fig. 2.3.5, a frame (referred to as a ‘yoke’) is mounted to the beam specimens, which allows direct measurement of the net central deflection of the beams. The use of the ‘yoke’ eliminates extraneous deflections arising from support settlements and results in load-deflection curves which are considerably different from those obtained by using the cross-head displacement of the testing machine.

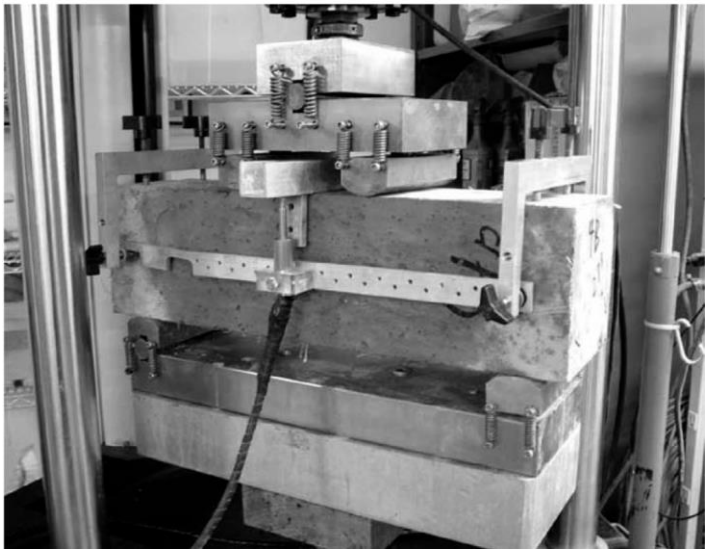

Fig. 2.3.5 Test apparatus of ASTM C1609 (ASTM, 2011b)

Different to ASTM C1018, this standard calculates residual strength (f^D_{600} and f^D_{150}) at net deflection of L/600 and L/150, respectively. Absolute toughness (T^D_{150}) and equivalent flexural strength ratio ($T^D_{T,\,150}$) are also presented. As shown in Fig. 2.3.6, this test uses first-peak instead of first-crack, which is more accurate and objective. The equivalent flexural strength ratio, which is based on the first-peak strength, is more accurate. However, some difficulties still arise when this standard is applied to ultra-high performance fibre reinforced concrete containing very high volume fraction of fibre and exhibiting deflection-hardening behaviour (Wille et al., 2014). The peak load in ASTM C1609 is defined as the first point on the load-deflection curve where the slope is zero. Clearly, deflection-softening fibre reinforced concrete exhibits such a response. However, a deflection-hardening fibre reinforced concrete may have a stable deflection-hardening response without a sudden load drop after peak load, so there is no point with a zero slope (Yehia, 2009).

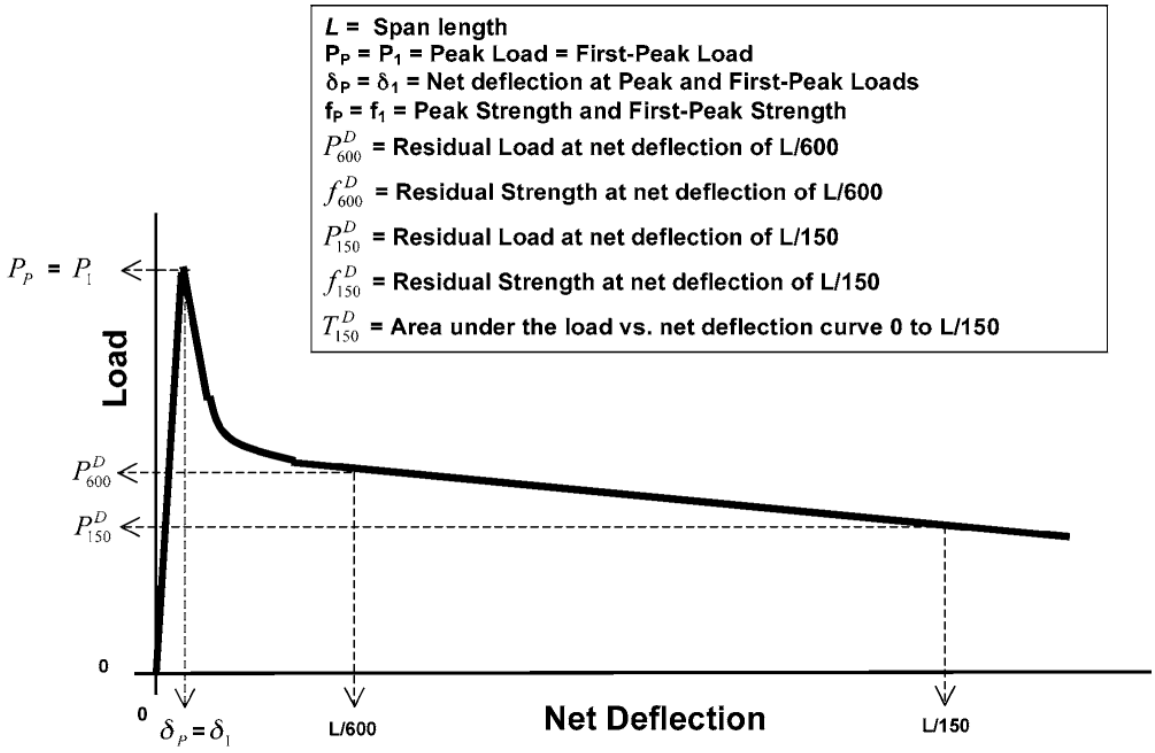

Fig. 2.3.6 Load-deflection curve of ASTM C1609 (ASTM, 2011b)

2.3.2 Three-point Flexural Tests on the Notched Beams

The stress-strain relation from the four-point flexural test on the unnotched beams is considered to be the most desirable since it can be directly used in engineering calculations. However, it does not represent the actual post-cracking behaviour of fibre reinforced concrete and cannot be retrieved directly from a characterisation test. Moreover, during the test, there is a momentary loss of stability when the concrete matrix cracks, even under displacement control, and while using relatively stiff conventional testing machines (Barr et al., 1996). Therefore, the unnotched beams through a four-point flexural test normally have a great variation in the recorded deflections.

Notched beam tests offer a promising alternative to characterise toughness of fibre reinforced concrete. The tests avoid many of the problems associated with the four-point test on unnotched beams, and thus guarantee stability throughout the tests even for unreinforced and high-strength low fibre-content concretes (Shaheen and

Shrive, 2007). A mid-point loading configuration is obviously more appropriate for notched beam specimens than the four-point loading (Ding, 2011).

For the notched mid-point loaded specimen, crack initiates at the notch-tip and propagates along the notch plane and hence, deformation is always localised at the notch-plane and the rest of the beam does not undergo significant inelastic deformations (Mahmud et al., 2013). This minimises the energy dissipated over the entire volume of the specimen and, therefore, all the energy absorbed can be directly attributed to fracture along the notch plane. Consequently, the energy dissipated in these tests can be directly correlated to material response (i.e. fibre reinforcement) (Stynoski et al., 2015). Moreover, the stress-crack opening relation from the tests naturally expresses the real post-cracking behaviour of fibre reinforced concrete. The stress-crack opening properties are also independent of the structural member size (de Montaignac et al., 2012). Therefore, three-point flexural test on the notched beams are considered as the best way of studying toughness, crack propagation and the associated fibre reinforcement.

Crack Tip Opening Displacement (CTOD) and Crack Mouth Opening Displacement (CMOD) tests are common three-point flexural tests on the notched beams. According to ASTM E1290 (ASTM, 2008b), CTOD is the displacement of the crack surfaces normal to the original (unloaded) crack plane at the tip of the fatigue precrack. However, due to inherent difficulties in the direct determination of CTOD, CMOD test is a preferred test to assess post-cracking performance of fibre reinforced concrete (Zhijun and Farhad, 2005). According to BS EN 14651:2005+A1:2007 (BSI, 2007), CMOD test measures the opening of the crack at mid-span using a displacement transducer mounted along the longitudinal axis.

During the last ten years many laboratories have been using closed-loop servo-hydraulic machines to test concrete specimens in fracture tests. In such machines the opening of the crack mouth is used to control the test. In such tests, the CMOD can be used directly as a measure of the response of the beam, thus eliminating the need to monitor the actual central deflection of the test specimen via a ‘yoke’ arrangement (Aslani and Bastami, 2015). The load-CMOD curves directly represent the deformation

of the critical section. Though this requires more sophisticated testing equipment than that required for load-displacement curves, such testing equipment results in stable post-peak response and avoids the effects of energy dissipation outside the cracking zone (Bordelon et al., 2009). Therefore, in our research CMOD tests were carried out to study the reinforcing effects of the recycled plastic fibres in concrete, rather than using the four-point flexural tests on the unnotched beams.

Fig. 2.3.7 shows the test set-up and the schematic of the controls. A CMOD transducer monitors the crack opening displacement and supplies the feed-back signal to the servo-controller. A Japanese yoke is mounted around the specimen to record the net deflections so that the extraneous deflections resulting from settlement of supports, crushing at load points, and load-fixture deformation are automatically eliminated. Averaged data from two LVDTs placed on either side of the specimen are used to record the net deflection of the beam at the mid-span (de Montaignac et al., 2012). A load-CMOD relationship can be obtained from the test. Using this type of relationship, the load at the limit of proportionality and the residual flexural tensile strength parameters can be obtained.

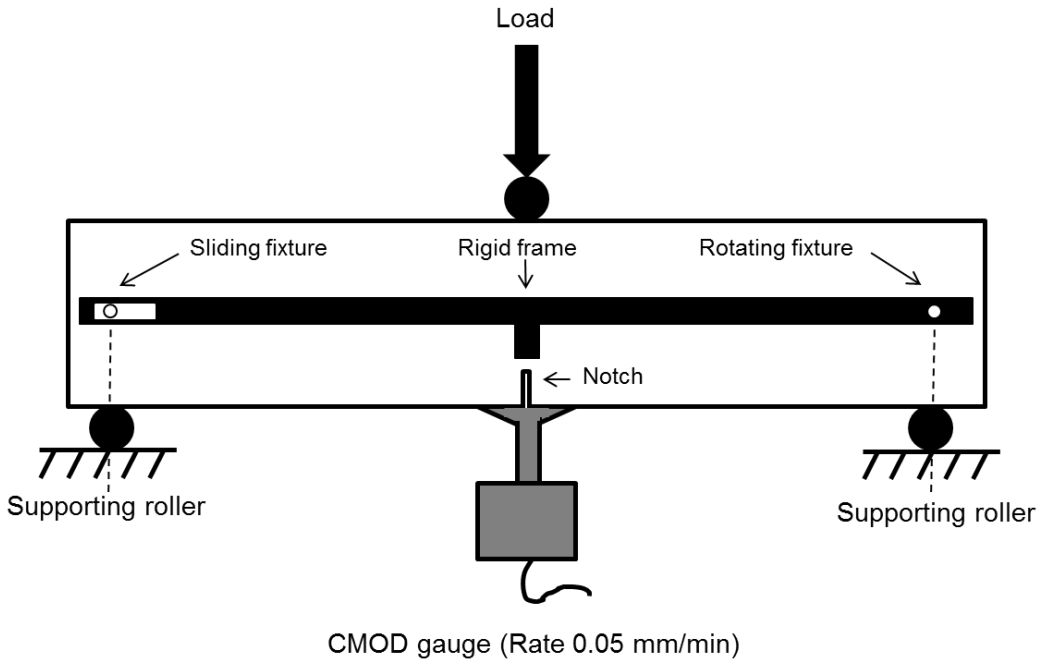

Fig. 2.3.7 Schematic of BS EN 14651

2.3.3 Flexural Tests on the Round Panel

Round determinate panel test (RDPT), according to ASTM C1550, involves a centre point loading of a large circular plate (800 mm in diameter and 75 mm in thickness) supported on three points. The specimen toughness is assessed in terms of the energy absorbed in loading the plate to some selected values of central deflection. This test has become popular for fibre reinforced shotcrete due to its high precision in post-cracking performance evaluation (Wang et al., 2004), and is often used in the mining industry (Decker et al., 2012). Its panel-based performance assessment is desirable because panels fail through a combination of stress actions that reflect an in situ behaviour of concrete footpaths more closely than other mechanical tests in the laboratory (Parmentier et al., 2008). This test has a significantly lower variability in post-cracking performance than other tests, and therefore energy absorption in the round determinate panel is considered the most reliable test method of post-cracking performance assessment (Zi et al., 2014). Therefore, in our research the RDPT is another effective method chosen to assess the reinforcement of recycled plastic fibres in concrete.

As shown in Fig. 2.3.8, a load is applied to the centre of the panel by a hemispherical-ended steel piston. The load is controlled by a programmable logic controller to maintain a constant deflection rate of 4.0 ± 1.0 mm/min. The panel rests on three pivots, evenly spaced around its circumference, and deflection is carried out until a central displacement of at least 40 mm is achieved. The energy absorbed is recorded at deflections of 10, 20, 30, and 40 mm (de Montaignac et al., 2012).

(a)

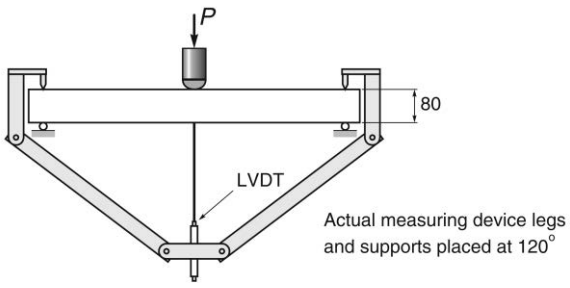

(b)

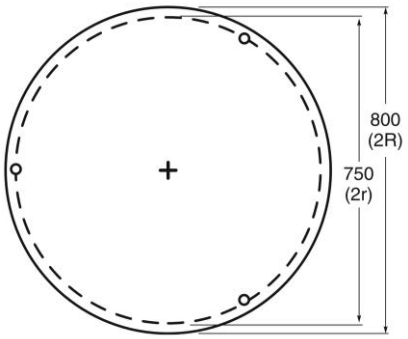

Fig. 2.3.8 Side view (a) and top view (b) of the RDPT apparatus setup according to ASTM C1550

2.4. Life Cycle Assessment

In order to help decision makers correctly consider the comparative environmental impacts of virgin PP fibre, recycled PP fibres and steel reinforcing mesh in concrete footpaths, it is very important to carry out environmental impact assessment (EIA). The environmental impact assessment is a formal process used to predict the positive or negative environmental consequences of a project prior to making decisions (Achilleos et al., 2011; Carvalho et al., 2014). There are a variety of general and industry specific assessment methods, such as GMP-RAM (Jesus et al., 2006), INOVA Systems (Jesus-Hitzschky, 2007), fuzzy logic EIA method (Afrinaldi and Zhang, 2014; Peche and Rodriguez, 2009). However, life cycle assessment (LCA) (Sandin et al., 2014) is the most comprehensive among the available tools and widely adopted and used in a wide variety of applications. For example, the LCA is widely used in building assessment (Gabel et al., 2004; Ingrao et al., 2014; Iribarren et al., 2015; Silvestre et al., 2014) and its implementation must adhere to standards ISO 14040: 2006 (ISO14040, 2006) and ISO 14044: 2006 (ISO14044, 2006).

Life cycle assessment is commonly used to identify and measure the impacts associated with all the stages of a product's life from-cradle-to-grave (i.e., from raw material extraction and raw materials processing, to product manufacture, distribution, use, repair and maintenance, and ending with disposal or recycling). It considers all stages to evaluate the environmental burdens associated with a product, process, or activity by identifying and quantifying energy consumed, materials used and waste released to the environment (Sandin et al., 2014). The LCA methodology is generally considered the best environmental management tool for quantifying and comparing alternative eco-performances of products, as well as recycling and disposal systems (Lasvaux et al., 2014). The structure of Life cycle assessment consists of four distinct phases: goal and scope definition, inventory analysis, impact assessment and interpretation (Dodbiba et al., 2007).

The goal of an LCA states the intended application, the reasons for carrying out the study, the intended audience, and where the results are going to be used. The scope should be sufficiently well defined to ensure that the breadth, depth and details of the

study are compatible and sufficient to address the stated goal. It includes the following items: the product system to be studied; the functional unit; the system boundary; allocation procedures; impact categories and methodology of impact assessment, and subsequent interpretation to be used; data requirements; assumptions; limitations; initial data quality requirements; and format of the report required for the study.

Inventory analysis involves data collection and calculation procedures to quantify relevant inputs and outputs of a product system. Data for each unit process within the systems boundary can be classified under major headings, including energy inputs, raw material inputs, ancillary inputs, other physical inputs; products, co-products and waste; emissions to air, discharges to water and soil, and other environmental aspects. Following the data collection, calculation procedures, including validation of data collected, the relating of data to unit processes, and the relating of data to the reference flow of the functional unit, are needed to generate the results of the inventory of the defined system for each unit process and for the defined functional unit of the product system that is to be modelled.

The impact assessment phase of LCA aims at evaluating the significance of potential environmental impacts using the life cycle impact (LCI) results. In general, this process involves associating inventory data with specific environmental impact categories and category indicators, thereby attempting to understand these impacts. Interpretation is the phase of LCA in which the findings from the inventory analysis and the impact assessment are considered together. The interpretation phase should deliver results that are consistent with the defined goal and scope and which reach conclusions, explain limitations and provide recommendations (Viksne et al., 2004).

Perugini et al. (2005) studied the LCA for recycling of Italian household plastic packaging waste. Their study quantified the overall environmental performances of mechanical recycling of plastic containers in Italy and compared them with conventional options of landfilling or incineration, as well as comparing with other innovative processes of feedstock recycling (low-temperature fluidized bed pyrolysis, and high-pressure hydrogenation). Their results confirmed that recycling scenarios were always preferable to those of non-recycling. Arena et al. (2003) also studied the

Italian system of collecting and mechanically recycling the post-consumer polyethylene (PE) and polyethylene terephthalate (PET) liquid containers. They found that the production of recycled PET can save between 29 % and 45 % of energy compared to virgin PET production, depending on whether the process wastes (mainly coming from sorting and reprocessing activities) were used for energy recovery. Moreover, 39 % - 50 % reductions in energy use were observed in the production of recycled PE compared to virgin PE.

Shen et al. (2010) assessed the environmental impact of PET bottle-to-fibre recycling. Four recycling cases, including mechanical recycling, semi-mechanical recycling, back-to-oligomer recycling and back-to-monomer recycling were analysed. The LCA results showed that recycled PET fibres offered important environmental benefits over virgin PET fibre, including energy use savings of 40 % - 85 %.

2.5 Conclusions

1. In order to decrease the plastic pollution and conserve non-renewable fossil fuel, efficient technology for recycling plastic waste has become increasingly important. Mechanical recycling is relatively easy and economic, and infrastructure for collection and reprocessing has been well established. In order to improve quality of end products of recycled plastics, various workable reprocessing techniques in the second stage of mechanical recycling have been developed and widely applied in the recycling industry. Reprocessing recycled polypropylene is always accompanied with degradation, crystallisation, and consequent processability problems, which result from molecular chain scission, branching and crosslinking. The degradation behaviour decreases tensile strength and impact strength, while the crystallisation behaviour increases Young modulus and yield stress. This chapter critically reviews the current reprocessing techniques of recycled polypropylene, including melt blending, filler reinforcement and mechanochemistry. Each method has inherent context, application and specific recycling advantages. However, reprocessing recycled polypropylene into fibre has limited research. The degradation and crystallisation behaviour in the reprocessing of fibre production is unknown.

2. This chapter then presents the current state of knowledge and technology of preparation techniques and properties of macro plastic fibres. It also reviews the reinforcing effects of macro plastic fibres in concrete and applications of plastic fibres reinforced concrete. The macro plastic fibres decrease workability of fresh concrete, but effectively control plastic shrinkage cracking of fresh concrete. The macro plastic fibres have no obvious effects on compressive and flexural strength, which are dominated by the concrete matrix properties. The main benefit of using macro plastic fibres lies in improved ductility in the post-cracking region and flexural toughness of concrete. The macro plastic fibres reinforced concrete shows excellent post-cracking performance and high energy absorption capacity. The macro plastic fibres also have good crack controlling capacity of dry shrinkage. The macro plastic fibres offer significant cost and environmental benefits over traditional steel reinforcement, thus have been widely used in the construction of pavements, precast elements and tunnel linings. However, there is a very limited study on the performance of recycled PP fibres in concrete.

3. The macro plastic fibres do not have obvious effects on the compressive strength of concrete, but they can effectively improve the toughness and post-cracking performance of concrete. This chapter critically compares various testing methods of characterisation of the toughness and post-cracking behaviour, including four-point flexural tests on the unnotched beams (ASTM C1018, ASTM C1399 and ASTM C1609), three-point flexural tests on the notched beams (ASTM E1290 and BS EN 14651) and flexural tests on the round panel (ASTM C1550). After comparing different standards and guidelines, the crack mouth opening displacement test based on BS EN 14651 and round determinate panel test based on ASTM C1550 were considered as appropriate testing methods of ascertaining the ability of recycled PP fibres to enhance the post-cracking performance of concrete.

4. The environmental impact assessment is a formal process used to predict the positive or negative environmental consequences of a project prior to making decisions. There are a variety of general and industry specific assessment

methods, such as GMP-RAM, INOVA Systems, fuzzy logic EIA method. Life cycle assessment is the most comprehensive among the available tools and widely adopted and used in a wide variety of applications. The literature on LCA of recycling plastic waste are very limited, and are strongly influenced by final product types, plastic sources, and by local characteristics of procedures for collecting and reprocessing plastic waste. Hence, these studies cannot be extrapolated to Australian conditions, where there is limited information on comparative LCA of recycling plastic wastes. In order to help decision makers correctly consider the comparative environmental impacts of virgin PP fibre, recycled PP fibres and SRM in concrete footpaths, it is very important to carry out life cycle assessment.

Chapter 3 Production and Characterisation of the Physical and Mechanical Properties of Recycled PP Fibers

Publication

S. Yin, R. Tuladhar, R. A. Shanks, T. Collister, M. Combe, M. Jacob, M. Tian and N. Sivakugan. Fiber preparation and mechanical properties of recycled polypropylene for reinforcing concrete. Journal of Applied Polymer Science, 2015,132(16):1-10.

This chapter explored the industrial feasibility of using melt spinning and hot drawing process to produce PP fibre under factory conditions instead of laboratory conditions. Virgin PP fibre of high tensile strength and Young's modulus was successfully produced by this method. However, the production of recycled plastics with sufficient mechanical properties is still a major challenge due to degradation during their service life and heat processing stage. The aim of this chapter is to improve the tensile strength and Young's modulus of fibres from recycled PP produced through the melt spinning and hot drawing process, and establish a relationship between mechanical properties of PP fibres with their crystallinity, crystal structure and orientation. Besides 100% recycled PP fibre, 50% of virgin PP and 5% of HDPE were mixed into the recycled PP fibre to produce 50:50 Virgin-Recycled PP fibre and 5:95 HDPE-Recycled PP fibre, respectively. The mechanical properties of these recycled fibres produced by the melt spinning and hot drawing process were presented and compared with the virgin PP fibre. The effects of 50% of virgin PP and 5% of HDPE on fibre from recycled PP were studied in terms of crystal structure and crystallinity by differential scanning calorimetry (DSC) and wide-angle X-ray scattering (WAXS).

3.1. Fibre Production and Measurement

3.1.1. Raw Materials for Fibre Production

Raw materials for producing virgin PP, recycled PP and HDPE used in this study are commercial grade granules. Their characteristics given in the manufacturer

specifications are presented in Table 3.1 (LyondellBasell, 2013; Martogg, 2013; PTTPM, 2013).

Table 3.1 Characteristics of raw materials of plastic fibres

Raw material	Virgin PP granule	Recycled PP granule	HDPE granule
Density (g/cm³)	0.90	0.90-0.92	0.957
Melt flow index (MFI, 2.16 kg, dg/min)	3.5 (at 230 °C)	13 (at 230 °C)	0.4 (at 190 °C)
Tensile stress at yield (MPa)	31	35	31.4
Flexural modulus (GPa)	1.25	1.48	0.8
Notched izod impact strength (23 °C, type 1, Notch A, kJ/m²)	4.7	3.5	5.8

3.1.2. Preparation of PP Fibres

As shown in Fig. 3.1, the plastic granules are fed into a single-screw extruder and melted. Temperatures of five heating zones of the extruder are set at 218, 223, 225, 233 and 235 °C. Fibres are then extruded into a water bath from the nozzle at the tip of the extruder. The extruded fiber is pulled to a chill roll and hot-drawn in the oven at 120-150 °C. The resulting fibres through the second chill roll are smooth and have a circular cross-section of around 0.9 mm^2. An indented roller die is used to mark indents on the fibres, in order to increase the bond strength between the fibres and concrete. After indentation, fibers are cut into a length of 47 mm. Table 3.2 lists the virgin and recycled PP fibres produced through this method. They were 100% virgin PP fibre, 5:95 HDPE-virgin PP fibre, 100% recycled PP fibre, 5:95 HDPE-recycled PP fibre, and 50:50 virgin-recycled PP fibre. Their details can be seen in Table 3.2.

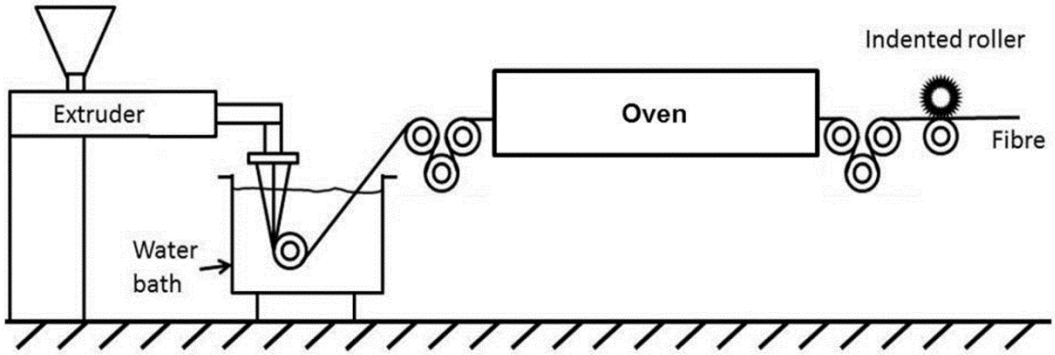

Fig. 3.1 Extrusion apparatus for monofilaments

Table 3.2 Details of PP fibres

Specimen	Details
100% virgin PP fibre	100% virgin PP
5:95 HDPE-virgin PP fibre	mixture of 5% of HDPE and 95% virgin PP
100% recycled PP fibre	100% recycled PP
5:95 HDPE-recycled PP fibre	mixture of 5% of HDPE and 95% recycled PP
50:50 virgin-recycled PP fibre	mixture of 50% of virgin PP and 50% recycled PP

3.1.3. Tensile Strength of PP Fibres

Since there is no specific tensile test guidelines for fibres in Australian Standards, tests for tensile strength and Young's modulus are performed on the virgin and recycled PP fibres according to ASTM D3822-07 (ASTM, 2007c). The tensile test instrument used for the tests was United STM 'Smart' Test System (STM-50KN) from United Calibration Corporation and was equipped with a 2 kN load cell and data acquisition software (Fig. 3.2). Distance between the clamps was adjusted to obtain a gauge length of 25.4 mm, and extension speed was set as 60% of the gauge length/min (15.24 mm/min). 30 specimens were tested for each sample. Testing temperature was 20 ±2 °C.

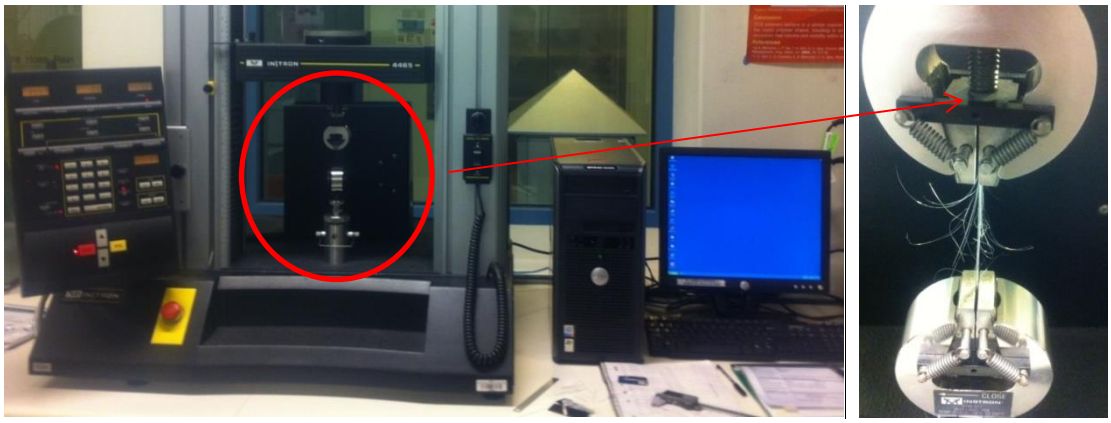

Fig. 3.2 Test apparatus for fibre tensile test

3.1.4. Fourier Transform Infrared Spectroscopy

Fourier transform infrared spectroscopy (FTIR) measurements were carried out with a Perkin-Elmer spectrum 100 FTIR Spectrometer. FTIR is a technique which is used to obtain an infrared spectrum of absorption, emission, photoconductivity or Raman scattering of a material, as shown in Fig. 3.3. Since the FTIR measures how well a sample absorbs light at each wavelength, molecular orientation of the recycled PP fibre and its raw material can be measured by using FTIR spectra with radiation parallel and perpendicular to the fibre and raw material. Through this test, we can see how the melt spinning and hot drawing process affect the molecular chains of the PP fibres. The intensity of absorption brands at 998 and 1153 cm^{-1} are used to calculate the contents of crystal and amorphous, respectively (Parthasarthy et al., 2002). For quantitative estimation of orientations, the dichroic ratios of 998 and 1153 m^{-1} bands, R_{998} and R_{1153}, were calculated with dividing the intensity of absorption brands in parallel direction ($A_{parallel}$) by the intensity in perpendicular direction ($A_{perpendicular}$), that is, $R = A_{parallel} / A_{perpendicular}$. The degree of orientation f of crystal and amorphous was further calculated through Equation (2) (Li et al., 2014)

$$f = (R-1)/(R+2) \qquad (2)$$

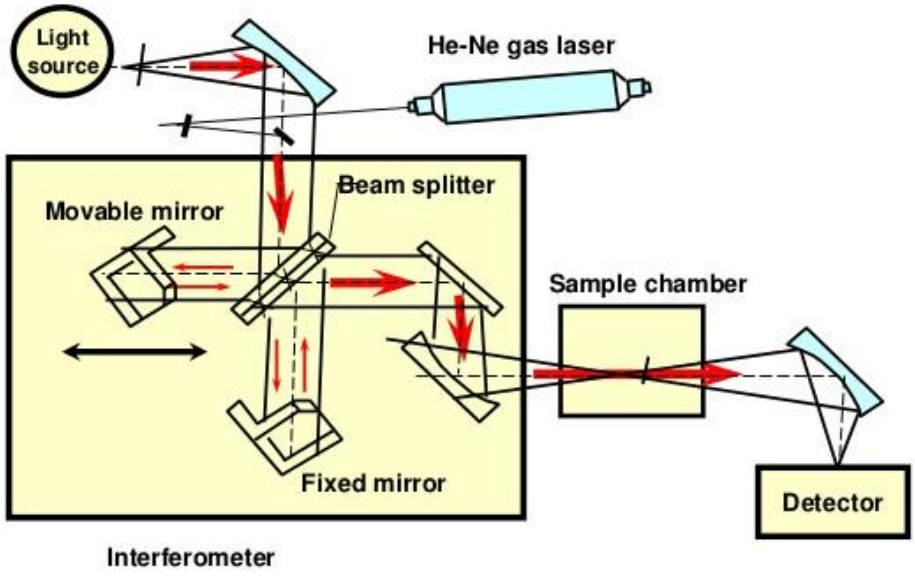

Fig. 3.3 Mechanism of FTIR (Myllari et al., 2015)

3.1.5. Differential Scanning Calorimeter

Non-isothermal crystallisation and melting behaviour of the fibres are studied using a Perkin-Elmer Pyris-1 differential scanning calorimeter (DSC), as shown in Fig. 3.4. DSC is a thermoanalytical technique in which melting and crystallisation behaviour of the fibres can be measured with the increase and decrease of temperature, respectively. About 3 mg of PP fibre is weighed accurately and encapsulated in an aluminium pan. Samples are heated from 30 °C to 220 °C at the heating rate of 10 K/min to study the melting behaviour of the fibres. The crystallinity and crystalline structure of the PP fibres can be calculated through this heating. The samples are then kept at 220 °C for 5 min to eliminate their thermal history. Subsequently, the samples are cooled to 30 °C at the rate of 10 K/min to study their crystallisation behaviour with temperature; and reheated to 220 °C at the heating rate of 10 K/min to study their melting behaviour with temperature. All measurements are carried out under a nitrogen atmosphere to avoid thermal-oxidative degradation. In both crystallisation and melting experiments the peak temperatures are obtained for crystallisation temperature (T_c) and melting temperature (T_m), respectively. Crystallinity refers to the degree of crystallisation of the PP fibres. The crystallinity has a significant influence on hardness, density and transparency. The crystallinity of the PPs is calculated using Equation (3) (Cerqueira et al., 2006)

$$Crystallinity = \frac{\Delta H_f}{\Delta H_f^0} \times 100 \qquad (3)$$

Where, ΔH_f is the heat of fusion of PP fibres and ΔH_f^0 is the heat of fusion of a totally crystalline PP taken as 207 J/g (Yeo et al., 2003).

Fig. 3.4 Test apparatus for the DSC test

3.1.6. Wide-angle X-ray Scattering

Wide-angle X-ray scattering (WAXS) is an X-ray-diffraction technique that is often used to determine the crystalline structure of polymers, as shown in Fig. 3.5. This technique specifically refers to the analysis of diffraction peaks scattered to wide angles, which implies that they are caused by sub-nanometer-sized structures. The diffraction pattern generated are used to determine the chemical composition or phase composition of the film, the texture of the film (preferred alignment of crystallites), the crystallite size and presence of film stress. According to this method the sample is scanned in a wide-angle X-ray goniometer, and the scattering intensity is plotted as a function of the 2θ angle.

In this research, the WAXS measurements are performed in reflection mode at ambient temperature using an X-ray diffractometer (Bruker D4 Endeavor). The generator is set at 40 kV and 40 mA and the copper Cu-Kα radiation was selected using

a graphite crystal monochromator. The α- and β- content of the PPs are calculated via the K-value of Chen et al. (2002):

$$K_\alpha = \frac{I_\alpha}{I_{HDPE} + I_\alpha + I_\beta} \tag{4}$$

$$K_\beta = \frac{I_\beta}{I_{HDPE} + I_\alpha + I_\beta} \tag{5}$$

Accordingly, K_α = 1 and K_β = 1 for the fully α- and β-crystalline PP, respectively. The overall crystallinity (X_c) is determined by:

$$X_c = \frac{A_c}{A_c + A_a} \times 100 \tag{6}$$

Where A_c and A_a are the areas under the crystalline peaks and amorphous halo, respectively (Cerqueira et al., 2006). The α-crystallinity is given by $K_\alpha X_c$, whereas for the β-crystallinity $K_\beta X_c$ holds.

Fig 3.5 Test apparatus for the WAXS test

3.2. Mechanical Properties of PP Fibres

As can be seen in Fig. 3.6, all the fibres produced by the melt spinning and hot drawing process show a brittle mode of failure, with a short elastic period of steep slope and a regime of sharply rising specific stress until fracturing occurred at strains between 8 and 16%. Table 3.3 presents average of the tensile strength, Young's modulus and extension of these fibres and their standard deviation. Compared with the mechanical properties of virgin and recycled PP raw materials in Table 3.1, the melt spinning and hot drawing process offers the PP fibres much higher mechanical properties. As shown in Table 3.3, the virgin PP fibre obtains highest tensile strength at 457.1 MPa and very high Young's modulus at 7526 MPa, while the recycled PP fibre exhibits 341.6 MPa of tensile strength.

As the raw material properties in Table 3.1, the melt flow index (MFI) of raw recycled PP is 13 dg/min, which is much higher than that of raw virgin PP (only 3.5 dg/min). This means that the fibre from recycled PP has much lower molar mass and hence shorter molecular chains than the virgin PP fibre (da Costa et al., 2007). During the service life of PP products, the recycled PP materials normally have natural aging from long exposure to the air, light, moisture, temperature and weathering (Villain et al., 1995). Moreover, the multiple processes under high shear forces and temperatures, and the presence of impurities and oxygen severely damage molecular chain of PPs, including crosslinking, chain scission and formation of double bonds (Hinsken et al., 1991). The chain scissions and degradation make the molecular chain easier to be pulled out, forming disentanglement and promoting nucleation of micro-voids and micro-cracks (Bahlouli et al., 2006). Therefore, the recycled PP fibre had much lower tensile strength and extension than the virgin PP fibre.

When 5% HDPE was mixed with both the recycled and virgin PP fibre, the Young's modulus of both fibres were decreased and the tensile elongations were increased compared with the 100% recycled and virgin PP fibre. This indicated that the HDPE brought ductility to the PP fibres. However, when 50% of the virgin PP was mixed with 50% of the recycled PP, the Young's modulus was considerably increased to 9016 MPa, which was even higher than that of virgin PP fibre, and the tensile strength remained

as high as the virgin PP fibre at 435.5 MPa. Therefore, the recycled PP fibre can obtain good ductility from the 5% of HDPE and can be well modified to obtain high tensile strength and Young's modulus by mixing with 50% of virgin PP.

It is worth to note that there is a high variation on the Young's modulus of all the fibres. The Young's modulus of PP fibre is very sensitive to its crystallisation. As a macromolecule polymer, the location, length and entanglement of the molecular chains of PP are not even through the whole PP materials, thus the crystallisation of PP is not consistent, especially for the PP fibres. Virgin PP materials have more homogeneous molecular chains, thus showing lower variation than that of recycled PP fibres, which has some degradation from service life and repetitive processing.

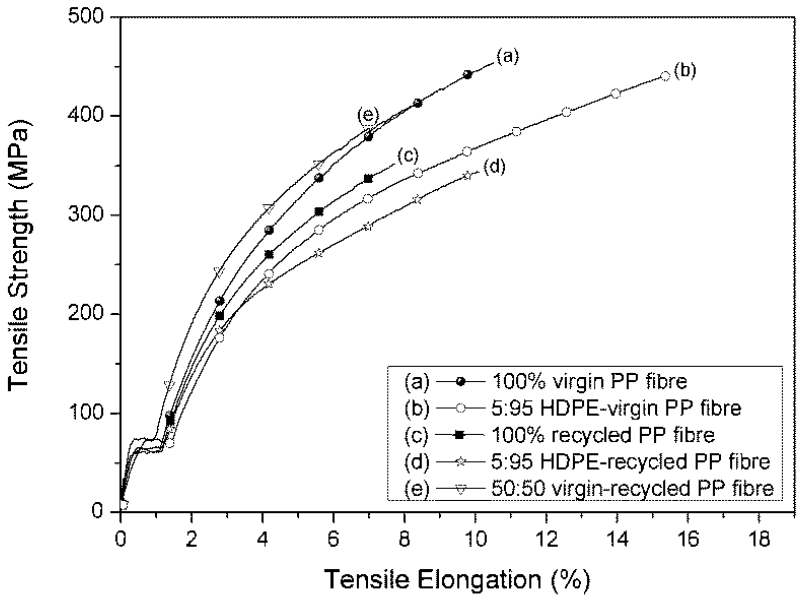

Fig. 3.6 Typical stress-strain curves of the PP fibres

Table 3.3 Tensile properties of the PP fibres

PP compositions	Tensile strength (MPa)		Young's Modulus (MPa)		Elongation at break (%)	
	Mean	Standard deviation	Mean	Standard deviation	Mean	Standard deviation
100% virgin PP fibre	457.1	31.7	7526	2011	10.6	1.4
5:95 HDPE-virgin PP fibre	436.0	23.2	6837	1538	16.5	2
100% recycled PP fibre	341.6	29.3	7115	2083	8.4	2.2
5:95 HDPE-recycled PP fibre	341.9	27.6	6467	2326	9.4	1.7
50:50 virgin-recycled PP fibre	435.5	26.5	9016	1919	8.1	1.4

3.3. Molecular Orientation by FTIR

As shown in Equation (2), the closer to zero the absolute value of f is, the less orientation the molecules have, and vice versa. As can be seen in Fig. 3.7.a, the recycled PP raw granule in both parallel and perpendicular directions shows similar intensity of absorption brands at 998 and 1153 cm^{-1}. The f_{998} and f_{1153} were calculated as -0.09 and 0.05, respectively. Therefore, the raw material has not obvious molecular orientation. However, after the melt spinning and hot drawing process, the intensities of absorption brands at 998 cm^{-1} of the recycled PP fibre exhibit significant difference on the both directions as Fig. 3.7.b. The f_{998} was calculated as -0.5, thus the crystal phase of the recycled PP fibre exhibits considerable molecular orientation.

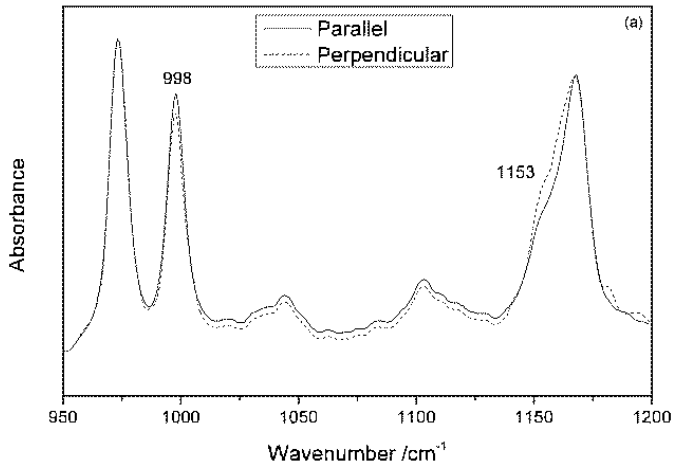

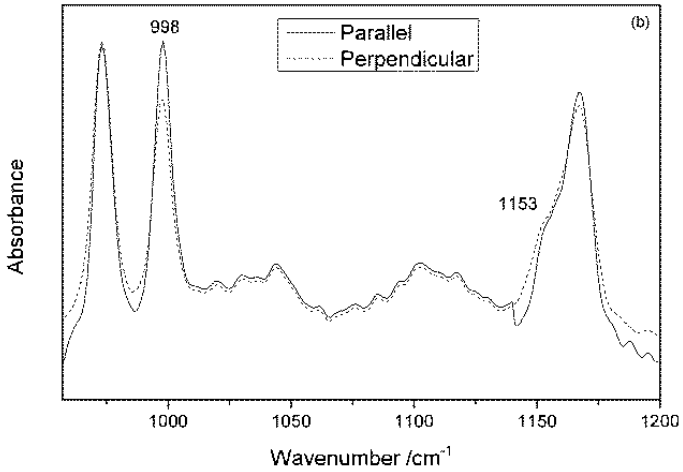

Fig. 3.7 FTIR spectra of (a) recycled PP raw granule and (b) recycled PP fibre on parallel and perpendicular directions to the raw material and the fibre

3.4. Crystal Structure and Crystallinity by DSC

The crystal structure of the PP fibres was studied by DSC. As shown in Fig. 3.8.a and Fig. 3.8.b, the raw material of recycled PP has a broader melting endotherm than that of the virgin PP, which indicates that the raw recycled PP has more crystals of different sizes, and the raw virgin PP has more uniform crystal sizes. From the Table 3.4 the raw recycled PP exhibits higher heat of fusion (ΔH) than the raw virgin PP, indicating the raw recycled PP has higher crystallinity. This is why the raw recycled PP has higher mechanical properties than the raw virgin PP as Table 3.1. As Table 3.1, the raw recycled PP has much higher MFI than the raw virgin PP, indicating that the raw recycled PP has lower molar mass and shorter molecular chains. In the processing stage and service life of the recycled PP, chain scissions frequently occur, thus significantly reducing the molar mass and shortening the molecular chains. The lower molar mass and shorter molecular chains are easier to rearrange, orient and form into crystals than the longer molecular chains of the raw virgin PP (Gonzalez-Gonzalez et al., 1998).

As shown in Table 3.4, the ΔH and crystallinity of the raw virgin PP are very small (only 76.2 J/g and 36.8%, respectively). However, after the melt spinning and hot drawing process, the ΔH and crystallinity of the virgin PP fibre are increased dramatically to

106.7 J/g and 51.5%, respectively. Similar with the recycled PP, the process improved the crystallinity of the recycled PP from 41.5% to 50.9%. Furthermore, as Fig. 3.8.c the virgin and recycled PP fibres exhibit a double melting endotherm at around 154 and 168 °C. The peak located at 154 °C is ascribed to the β-form crystals and the other is to the α-form crystals (Tabatabaei et al., 2009). According to Huo et al. (2005), this oriented molecular chains formed α row-nuclei and the oriented α row-nuclei can induce to form β-crystals. Somani et al. (2005) reported that the PP fibres which have a double melting endotherm show a specific shish-kebab structure. The shish in PP had a melting temperature of about 5-10 °C higher than that of the kebabs and about 15-20 °C higher than that for spherulites.

On the α-form crystallisation in Table 3.4, the virgin PP fibre exhibited higher peak melting temperature (T_m) than its raw material. As Zhao and Ye (2011), the high-temperature endotherm represents the melting of the highly chain-extended and the highly oriented crystalline blocks formed during the hot drawing process and the low-temperature endotherm is due to the melting of strained non-crystalline region and some partially oriented lamellar. According to Elias et al. (2000), the hot drawing process also can result in a connectivity of molecular chains in the shish or fibrils, thus increasing the crystal thickness. Therefore, a higher melting point was obtained by the virgin PP fibre. However, the recycled PP fibre had slightly lower peak temperature of melting than its raw material probably because of molecular defects and lower purity.

As seen in Table 3.4, the recycled PP fibre and virgin PP have similar *ΔH*s (105.4 J/g and 106.7 J/g, respectively) and similar crystallinity (50.9 and 51.5, respectively). However, as Fig. 3.8.a and Fig. 3.8.b the recycled PP fibre has much higher *ΔH* on β-form crystals than the virgin PP fibre. The β-form crystals are much less stable than the α-form crystals (Hirose et al., 2000). Due to a large amount of β-form crystals, the recycled PP fibre showed lower tensile strength and Young's modulus. Although the oriented α row-nuclei of the virgin PP fibre induced some β-crystals, the α-form crystals were still dominant and the *ΔH* of β-form crystals was very low in the virgin PP fibre. Therefore, the virgin PP fibre had a large amount of stable α-form crystals, thus showing higher tensile properties.

When 5% of HDPE was mixed with the virgin PP fibre as Fig. 3.8.a, the ΔH of α-form crystals was decreased and the α-form crystallisation was significantly affected by the heterogeneous structure between HDPE and virgin PP. Moreover, the HDPE offered nucleation sites for β-form crystals, thus improving rate of the β-form crystals. Therefore, the tensile strength and Young's modulus of the virgin PP fibre was weakened by the HDPE. On the contrast, the 5% of HDPE restrained the formation of β-form crystals in the recycled PP fibre, more stable α-form crystals were produced by adding the HDPE as Fig. 3.8.b. The recycled PP normally has more molecular defects and lower purity due to the degradation in its service and processing history. The HDPE can act as a compatibilizer, which changes rough phase structure of the molecular defects and some impurities, thus more stable α-form crystals were obtained.

When 50% of virgin PP was mixed with 50% of recycled PP as Fig. 3.8.c, a double-melting endotherm is found on the α-form crystallisation. One peak is located on 167 °C, which is close to the T_m of α-crystals of recycled PP fibre; the other peak at 169.8 °C, which is similar with the T_m of α-crystals of virgin PP fibre. Moreover, the ΔH of β-form crystals on 154.3 °C is much lower than that of recycled PP fibre and slightly higher than that of virgin PP fibre. Therefore, the 50% of virgin PP not only retains high crystallinity and crystal structure, but effectively restrains the formation of β-form crystals in the recycled PP fibre. Finally, the 50:50 virgin-recycle fibre shows very high tensile strength and Young's modulus as shown in Table 3.4.

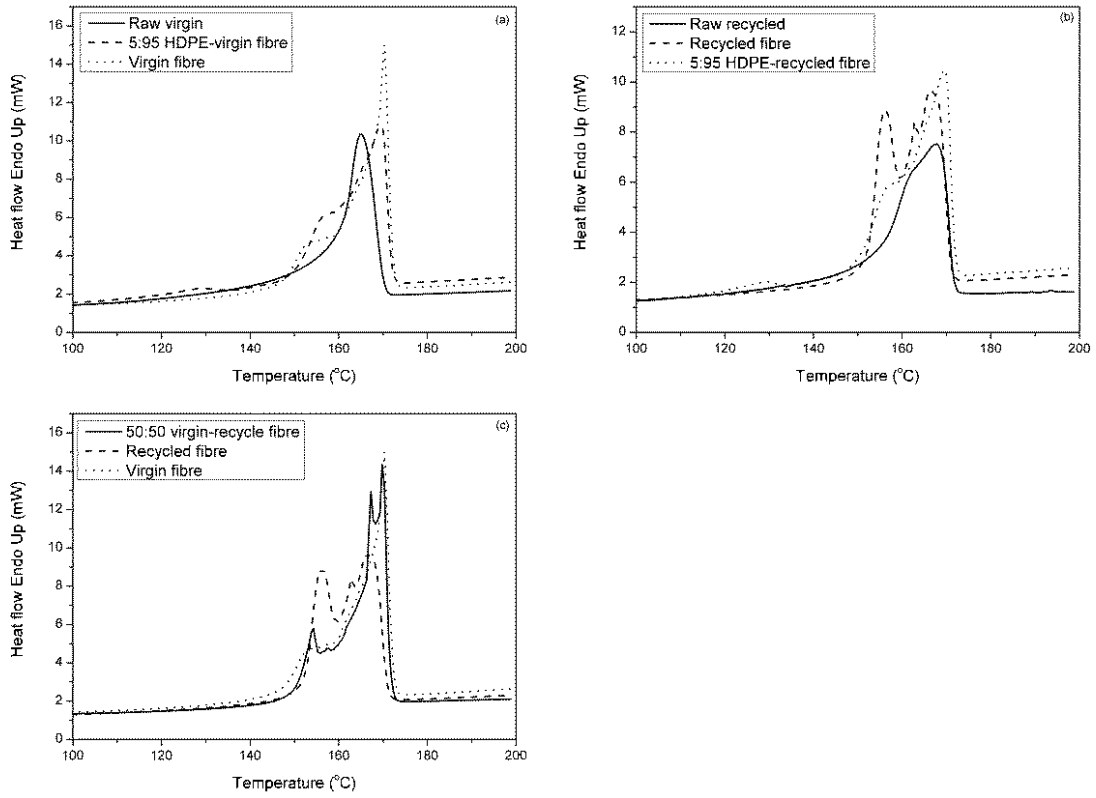

Fig. 3.8 DSC heating curves of the PP fibres and their raw materials (First round of heating from 30 to 220 °C)

Table 3.4 Peak temperatures of melting and heat of fusion for the α- and β-form crystals (first heating from 30 to 220 °C)

PP compositions	T_m of α-form crystals (°C)	T_m of β-form crystals (°C)	Total ΔH (J/g)	Crystallinity (%)
raw material of virgin PP	166.3		76.2	36.8
100% virgin PP fibre	170.3	152.8	106.7	51.5
5:95 HDPE-virgin PP fibre	169.8	153.3	100.5	48.6
raw material of recycled PP	167. 8		85.9	41.5
100% recycled PP fibre	166.3	156.3	105.4	50.9
5:95 HDPE-recycled PP fibre	169.2	157.3	99.7	48.2
50:50 virgin-recycle fibre	169.8	154.3	104.8	50.6

The samples were then held at 220 °C for 5 min, and cooled from 220 °C to 30 °C at a scan rate of 10 K/min. As seen in Fig. 3.9.a and b, and Table 3.5, the raw material of recycled PP has lower T_c (114.8 °C) than the raw virgin PP (119.8 °C), indicating that the raw recycled PP is easier to crystallise and can crystallise at a lower temperature. This is due to the lower molar mass and shorter molecular chains of recycled PP, which can be reflected by its lower MFI in Table 3.1. According to Horvath et al. (2013), the shorter molecular chains are easier to be released from the strained or entangled macromolecules, thus the crystallisation can be further developed by the rearrangement of these freed macromolecules segments. The heat of fusion of raw recycled PP is 87.9 J/g, which is lower than that of the raw virgin PP (88.4 J/g), indicating that the raw recycled PP released less thermal energy, formed fewer crystals and less perfect crystals than the raw virgin PP, because the raw recycled PP has more defective molecules and impurity.

As Table 3.5 and Fig. 3.9, after the melt spinning and hot drawing process, both the virgin PP and recycled fibres obtained much higher T_c (124.8 °C) and more narrow crystalline peaks than their raw materials, indicating the hot drawing process highly oriented and aligned the crystal structures. When the temperature cooled down from the 220 °C, the ordered molecular structure was more active at higher T_c and thus formed more perfect crystals than the raw materials, which leads to significantly improved mechanical properties of the fibres.

The heat of fusion of recycled PP fibre was also improved to 89.4 J/g, because its short oriented molecular chains can be crystallised easily and quickly. However, the virgin PP fibre obtained lower heat of fusion (87.6 J/g) than its raw material. The oriented molecular chains of virgin PP fibre is more likely to form perfect crystals than its raw material, but it needs more time due to the long molecular chains. However, because of the same cooling rate in the DSC tests, the virgin PP fibres did not have enough time to form perfect crystals, thus obtained lower heat of fusion (Zhang et al., 2011). Moreover, the long molecular chains were easier to entangle and entwist together, thus deceased molecular order degree and crystallinity (Zhong and Mao, 2009).

When 5% of HDPE was mixed with the recycled and virgin PP fibres, their *ΔH*s were improved to 93.8 and 97.8 J/g, respectively, indicating the HDPE had heterogeneous nucleation effect on the PP crystallisation. The crystallisation of HDPE, which can be seen on the small peaks around 118.8 °C in Fig. 3.9.a and b, also contributed to the *ΔH*s. When 50% of the virgin PP was mixed with 50% of the recycled PP, the T_c and *ΔH* was slightly decreased probably due to compatible problems between the virgin and recycled PPs.

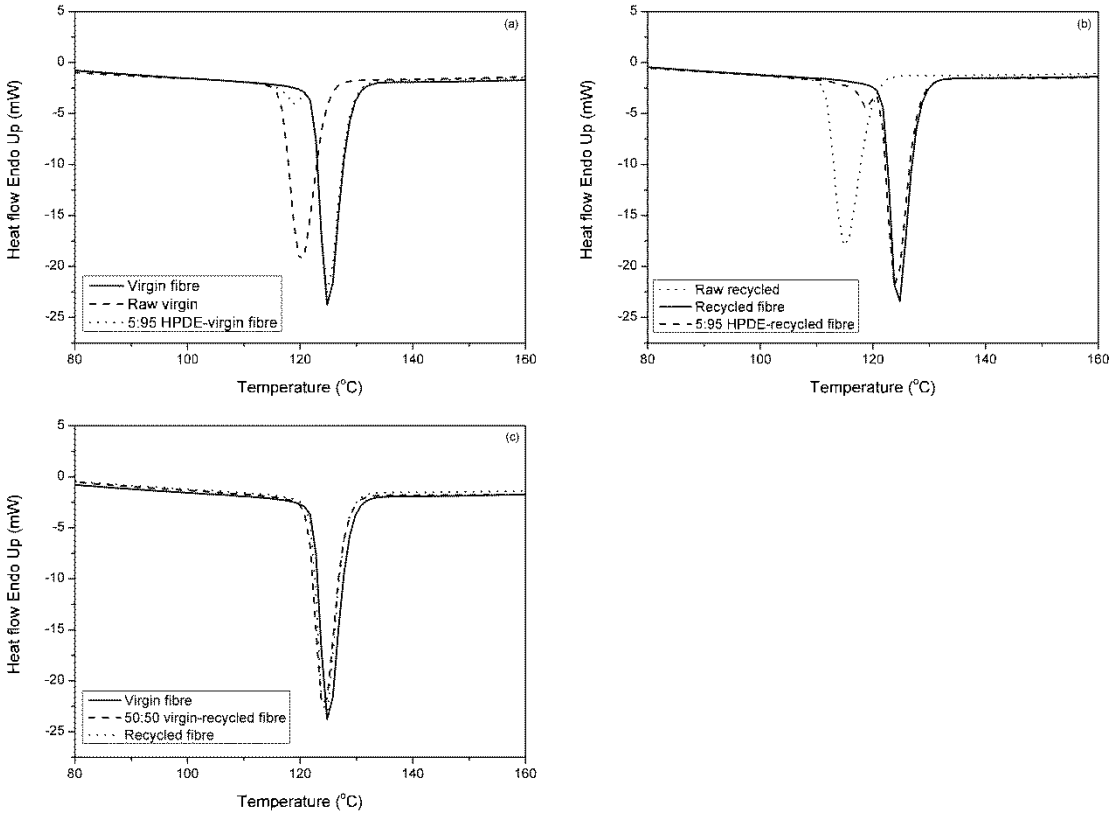

Fig. 3.9 DSC heating curves of the PP fibres and their raw materials (cooling from 220 to 30 °C)

Table 3.5 Peak temperature of crystallisation and heat of fusion (cooling from 220 to 30 ^{o}C)

PP compositions	T_c (°C)	ΔH (J/g)
raw material of virgin PP	119.8	88.4
100% virgin PP fibre	124.8	87.6
5:95 HDPE-virgin PP fibre	124.8	97.8
raw material of recycled PP	114.8	87.9
100% recycled PP fibre	124.8	89.4
5:95 HDPE-recycled PP fibre	123.8	93.8
50:50 virgin-recycle fibre	123.8	87.3

Thermal history of all the samples was eliminated through heating and cooling process, and then the samples were reheated from 30 to 220 °C. As seen in Fig. 3.10.a and b, the raw materials still have broad peaks, which are related to three-dimensional crystals known as spherulites and/or rows of lamellae (Somani et al., 2005). Further, the raw material of the recycled PP has a broader peak than the raw material of the virgin PP, which indicates the crystals of recycled PP have broader size distribution. However, all the fibres show narrow peaks, because the highly chain-extended and the highly oriented crystalline blocks formed fibrils during the hot drawing process. The thermal history of highly extended and oriented molecular chain is hard to be fully eliminated in the first round of heating and cooling (Zhao and Ye, 2011). Small melting peaks from the HDPE can be found for the 5:95 HDPE-virgin PP fibre and 5:95 HDPE-recycled PP fibre. As Table 3.6 the T_ms of all the fibres are only about 165 °C, which are much lower than the T_m of α-form crystals from the first heating in Table 3.4, indicating that the hot drawing process highly extended and oriented crystalline blocks. Furthermore, the ΔHs of all the fibres in Table 3.6 are much lower than those in Table 3.4, indicating that the hot drawing process significantly improved the crystallinity of the fibres.

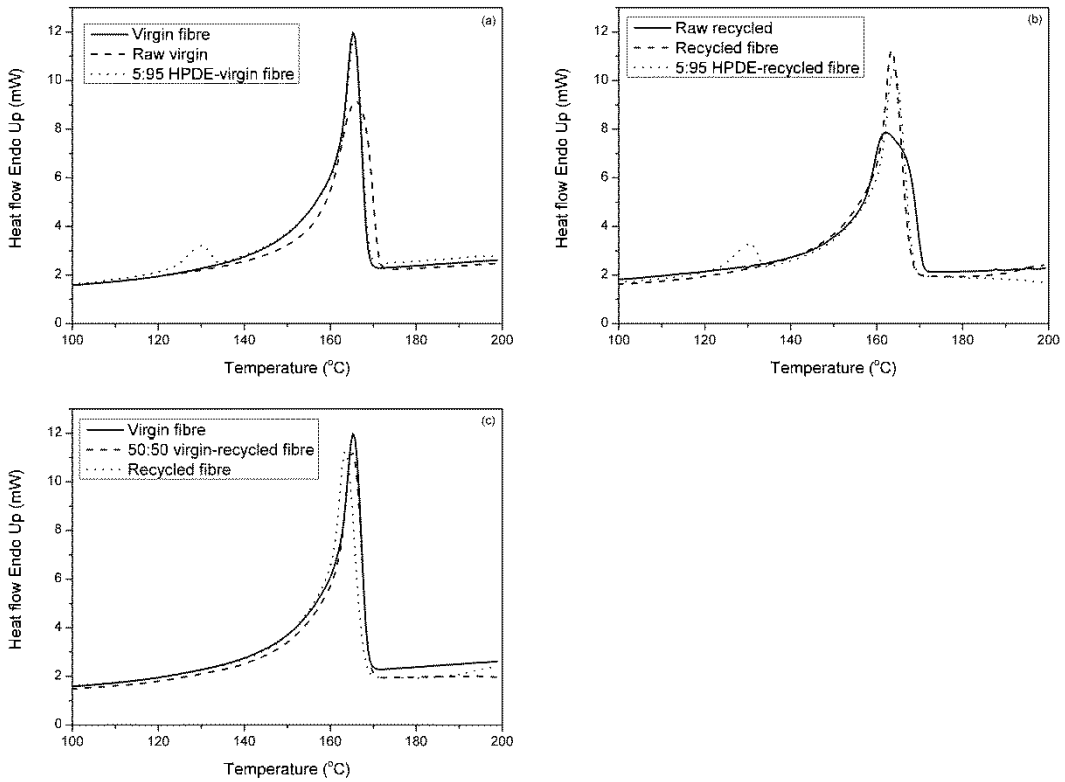

Fig. 3.10 DSC heating curves of the PP fibres and their raw materials (second round of heating from 30 to 220 °C)

Table 3.6 Peak temperature of melting and heat of fusion (second round of heating from 30 to 220 °C)

PP compositions	T_m (°C)	ΔH (J/g)
raw material of virgin PP	164.8	83.2
100% virgin PP fibre	165.3	90.9
5:95 HDPE-virgin PP fibre	165.3	94.6
raw material of recycled PP	161.8	84.3
100% recycled PP fibre	163.8	91.2
5:95 HDPE-recycled PP fibre	164.3	95.4
50:50 virgin-recycle fibre	165.3	92.8

3.5. Crystallinity by WAXS

Crystallinity of all the fibres and their raw materials was determined using wide-angle X-ray scattering (WAXS) measurements. In the Fig. 3.11, the raw materials of virgin and recycled PP have four distinct diffraction peaks at 2θ = 14.2°, 17°, 18.8°, and 21.4° /21.9°. According to the research of Huang et al. (2005), the 2θ = 14.2°, 17°, 18.8°, and 21.4°/21.9° associated with the (110), (040), (130) and (111)/(041) planes, respectively. The peaks at 2θ=21.4° and 21.9° are the co-diffractions of β phase and α phase. The virgin and recycled PP fibres obtain five diffraction peaks at 2θ = 14.2°, 17°, 18.8°, 25.5° and 28.4°.

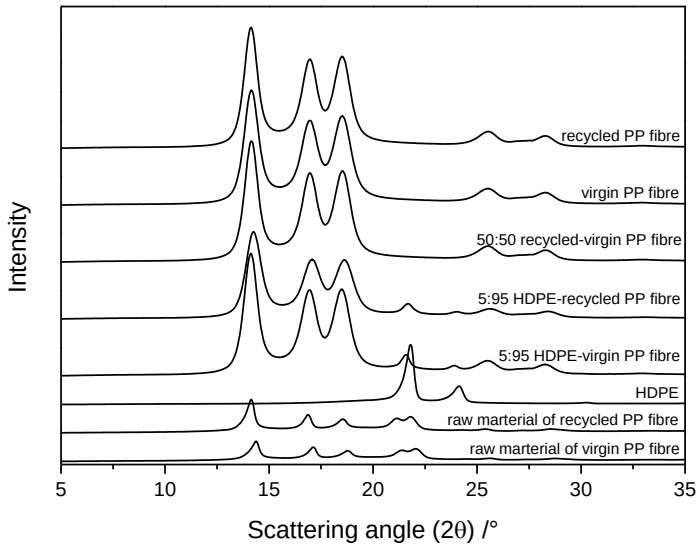

Fig. 3.11 WAXS profiles of the polypropylenes

The crystallinity values derived from the WAXS measurements are summarized in Table 3.7. As can be seen, the raw material of recycled PP has slightly higher crystallinity (51.2%) than the raw material of virgin PP (47.2%), because the raw material of recycled PP has lower molar mass, shorter molecular chains and more impurities. The lower molar mass and shorter molecular chains were easier to align and form into crystals, and the impurities greatly decreased the free enthalpy required for the formation of a critical nucleus, which further reduced the critical size of the nucleus and then led to the formation of heterogeneous nuclei (Aurrekoetxea et al., 2001). However, the hot drawing process can considerably improve the crystallinity of

the virgin and recycled PP fibre to 82.7% and 81.7%, respectively. The α-crystallinity (given by $K_\alpha X_c$) of the virgin and recycled PP fibres were significantly improved, while the β-crystallinity (given by $K_\theta X_c$) kept similar to their raw materials.

Table 3.7 Crystallinity of the polypropylenes

Composition	Crystallinity (X_c)	α-crystallinity ($K_\alpha X_c$)	β-crystallinity ($X_c K_\beta$)
Raw material of virgin PP	0.472	0.40	0.077
100% virgin PP fibre	0.827	0.75	0.078
5:95 HDPE-virgin PP fibre	0.820	0.68	0.063
Raw material of recycled PP	0.512	0.43	0.078
100% recycled PP fibre	0.817	0.74	0.074
5:95 HDPE-recycled PP fibre	0.799	0.66	0.060
50:50 recycled-virgin PP fibre	0.819	0.75	0.071

As shown in Fig. 3.11, after the hot drawing process the virgin and recycled PP crystallise into the monoclinic α-form via diffractions at 2θ = 14.2°, 17° and 18.8°, associated with the (110), (040) and (130) planes, respectively (Huang et al., 2005). On these facets the diffraction peak positions have no change, but the intensities of the peaks increased drastically. The intensity of the diffraction peak reveals the crystallinity and orientation of materials. It indicates that the hot drawing process did not affect the α-form crystal type, but significantly improved the crystallisation and orientation of the PP fibres. It was interesting to note that these three peaks overlapped to some extent, indicating that both crystal and mesomorphic phases co-existed in the fibres. The (111) and (041) doublet peaks moved to the off-axis and disappeared from the equator after the hot drawing process. On contrary, new peaks at 2θ = 25.5°, 28.4° are visible, indicating the generation of new β-form crystals.

When 5% of HDPE was added into the virgin and recycled PP fibre, both their crystallinity were slightly decreased due to the heterogeneous structure. The crystallisation of HDPE restrained α- and β-crystallinity, as shown in Table 3.7.

Therefore, the HDPE decreased the Young's modulus of PP fibres, but increased the ductility of PP fibres as shown in Fig. 3.11. However, when 50% of virgin PP was mixed with the recycled PP, the α-crystallinity kept as high as the virgin PP fibre, but the β-crystallinity was limited to lower rate of 7.1% (in Table 3.7). Therefore, 50:50 Virgin-Recycled PP fibre obtained the highest Young's modulus in all the PP fibres.

3.6. Conclusions

1. The virgin PP fibre of high tensile strength (457 MPa) and high Young's modulus (7526 MPa) was successfully produced by the melt spinning and hot drawing process under factory conditions. However, the recycled PP fibre produced by the same method showed significantly lower tensile strength (342 MPa), but comparable Young's modulus (7115 MPa). Fibres made of virgin or recycled PP, modified with 5% HPDE showed higher ductility than the pure PP fibres. Fibres made from 50% virgin and 50% recycled PP showed similar tensile strength and higher Young's modulus compared to the virgin PP fibres.

2. From the FTIR tests, the recycled PP granules did not have obvious molecular orientations. However, after the melt spinning and hot drawing process, the crystal phase of the recycled PP fibre exhibited considerable molecular orientation, which leads to high crystallinity.

3. After the melting spinning and hot drawing process, the melting enthalpy and crystallinity of the virgin and recycled PP fibres were increased dramatically. Both α-form and β-form crystals were found in the PP fibres. The virgin PP fibre had high rate of stable α-form crystals, thus obtaining high mechanical properties. However, the recycled PP fibre was found to have a large amount of less stable β-form crystals, so it had lower tensile properties. 5% of HDPE was found to decrease the α-form crystallisation in the virgin PP fibre, while restrain the formation of β-form crystals in the recycled PP fibre. When 50% of virgin PP was mixed with 50% of recycled PP, the 50% of virgin PP not only retained high crystallinity and crystal structure, but effectively restrained the formation of β-form crystals in the recycled PP fibre.

4. From the WAXS measurements, the crystallinity of raw materials of virgin and recycled PP was measured as 47.2% and 51.2%, respectively. The melt spinning and hot drawing process significantly improved the crystallinity of virgin and recycled PP fibres to 82.7% and 81.7%. Therefore, the high tensile strength and Young's modulus were obtained due to the significantly improved crystallinity.

Chapter 4 Comparative Evaluation of 100% Recycled and Virgin PP Fibre Reinforced Concretes

Publication

S. Yin, R. Tuladhar, J. Riella, D. Chung, T. Collister, M. Combe, N. Sivakugan. Comparative evaluation of virgin and recycled polypropylene fibre reinforced concrete. Construction and Building Materials. 2015 (Under review).

Cement matrix is highly alkaline with pH value of around 13, thus durability of the plastic fibre in concrete alkaline environment is an important factor that needs proper consideration. This chapter assessed alkali resistance of 100% recycled PP fibre in four different alkaline solutions with pH value ranging from 12.3 to 13.5, and compared with virgin PP fibre.

Performance of the 100% recycled PP fibre was then studied in different grades of concrete and was compared with the virgin PP fibre. Two volume percentages of fibres were chosen to reinforce 40 MPa and 25 MPa concrete, which are the standard grades of concrete used in precast panels and concrete footpaths, respectively. Through crack mouth opening displacement (CMOD) test and round determinate panel test (RDPT), this chapter proved the industrial feasibility of using 100% recycled PP fibre to replace virgin PP fibre. After proving the feasibility of using 100% recycled PP fibre in different construction applications in this chapter, the reinforcement of newly developed various recycled PP fibres described in Chapter 3 will be studied in next chapter (Chapter 5).

4.1 Alkali Resistance of the 100% Recycled and Virgin PP Fibres

Alkali resistance test was conducted to study possible degradation of the 100% recycled and virgin PP fibres in alkaline environment. As shown in Fig. 4.1, the PP fibres were immersed into Lawrence solution (0.48 g/l $Ca(OH)_2$+3.45g/l KOH+0.88 g/l NaOH, pH=12.9), which is considered to simulate pore water composition of a fully hydrated cement paste (Silva et al., 2005). The PP fibres were also immersed in three other

alkaline solutions with pH value ranging from 12.3 to 13.5 to study degradation of the fibres in different pH ranges and types. Three alkaline solutions used were $Ca(OH)_2$ saturated solution (pH=12.3), 0.28 mol/l NaOH solution (pH=13.45), and 0.068 mol/l KOH solution (pH=12.83).

The PP fibres were immersed into these solutions for 28 days at ambient temperature. The alkaline environment is strong mainly in the fresh concrete when mixing the fibres. When concrete is cured and hardens, the movement of OH^- becomes minimal due to absence of water. Based on most of the standards, such as AS 1012.9:2014 (AS, 2014c), BS EN 14651-2005+A1-2007 (EN, 2005) and ASTM C1550-12 (ASTM, 2012), the hardened concrete is tested on the 28 days of curing. Therefore, the 28 days is chosen in this research to simulate the period of fresh and curing concrete. The tensile strength and Young's modulus of the fibre were measured before and after immersion, according to ASTM D3822-07 (ASTM, 2007c). 30 specimens were tested for each type of fibre and solution.

Fig. 4.1 Test setup for alkali resistance test

As can be seen from Fig. 4.2, all the curves representing fibre immersion in the alkaline solutions nearly overlap with the curve of fibre without immersion, indicating that the 100% recycled PP fibre has very good alkali resistance in the various alkaline environments. However, there still are some minor changes on the mechanical

properties after immersion. As shown in Table 4.1, NaOH solution slightly embrittles the recycled PP, thus decreasing the tensile strength and increasing Young's modulus of the fibre, due to the its high pH value. The KOH solution slightly decreases the tensile strength of the fibre. However, there is nearly no change after immersing the fibre in the Lawrence solution which simulates a fully hydrated cement paste. Overall, the recycled PP fibre shows good alkali resistance in all the alkaline environments tested.

As a comparison, the degradation behaviour of the virgin PP fibre was also studied. As shown in Fig. 4.3 and Table 4.2, the virgin PP fibre has a minimum degradation in all kinds of alkaline environments, which is consistent with the study of Brown et al. (2002) and EPC (2012).

It is worth to note that the mechanical properties of 100% recycled and virgin PP fibres used in this chapter and following chapters are much lower than those of 100% recycled and virgin PP fibres produced in the Chapter 3. The fibres produced in the Chapter 3 have smooth surface. Chapter 3 studied the molecular orientation, crystal structure and crystallinity of PP fibres, which are not affected by the surface pattern of PP fibres. Moreover, the WAXS test can be conducted only on the smooth surface. When using fibres to reinforce concrete, surface indentation on the fibres is needed to improve bonding with concrete. However, the surface indentation highly decreased mechanical properties of the PP fibres. In this Chapter and following Chapters, the fibres used for reinforcing concrete are all indented.

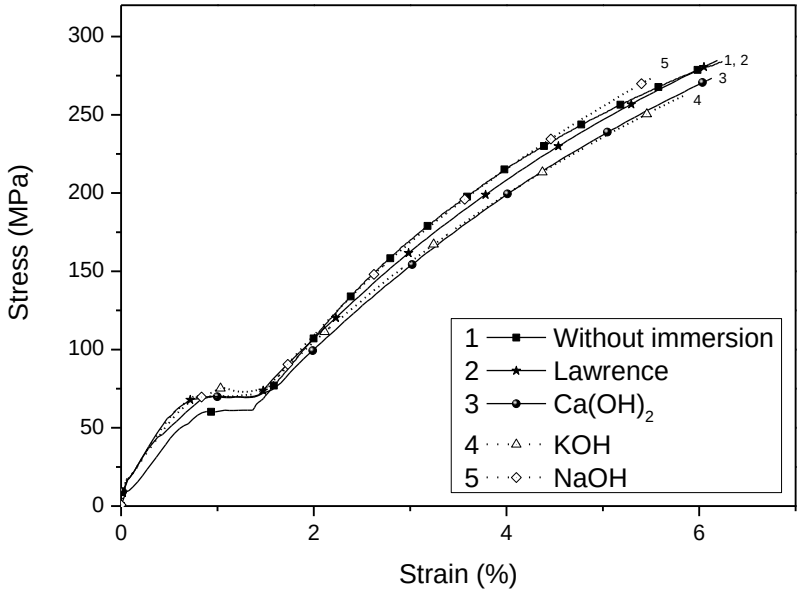

Fig. 4.2 Typical stress-strain curves of the 100% recycled PP fibre before and after immersing in the alkaline solutions for 28 days

Table 4.1 Mechanical properties of the 100% recycled PP fibre before and after immersing in the alkaline solutions for 28 days

	Tensile strength (MPa)		Young's Modulus (MPa)		Elongation at break (%)	
	Average	Standard deviation	Average	Standard deviation	Average	Standard deviation
Without immersion	284.1	33.7	4582	268.9	6.2	2.3
Lawrence solution	284.7	22.7	4592	153.4	6.2	0.9
$Ca(OH)_2$ solution	273.4	34.7	4482	380.2	6.1	1.7
KOH solution	261.9	17.4	4516	114.5	5.8	1.0
NaOH solution	273.1	14.2	4965	214.2	5.5	1.1

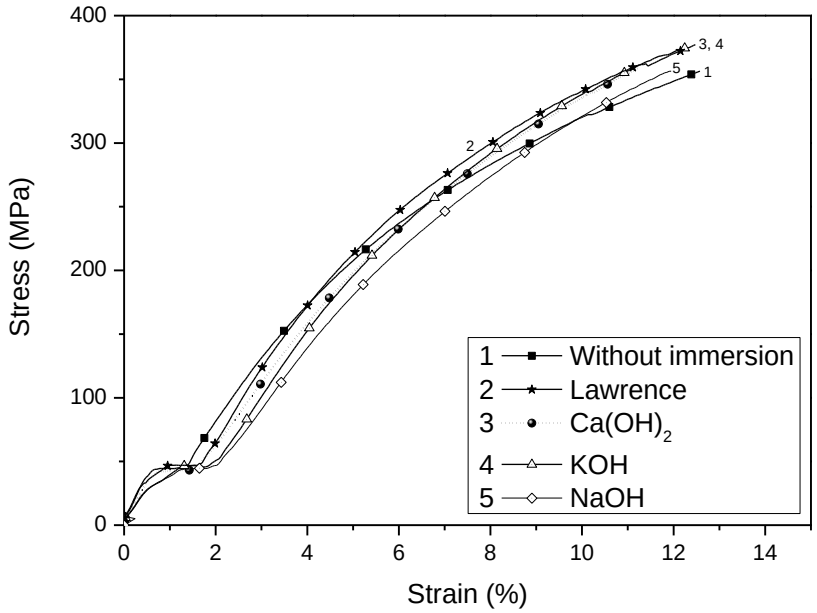

Fig. 4.3 Typical stress-strain curves of the virgin PP fibre before and after immersing in the alkaline solutions for 28 days

Table 4.2 Mechanical properties of the virgin PP fibre before and after immersing in the alkaline solutions for 28 days

	Tensile strength (MPa)		Young's modulus (MPa)		Elongation at break (%)	
	Average	Standard deviation	Average	Standard deviation	Average	Standard deviation
Without immersion	356.4	14.6	3129	589	12.6	0.5
Lawrence solution	372.3	12.5	3377	267	12.1	1.0
$Ca(OH)_2$ solution	358.6	27.3	3502	355	11.2	1.2
KOH solution	377.2	35.4	3318	313	12.5	1.4
NaOH solution	356.4	22.2	3295	612	11.9	0.6

4.2. Concrete Mix Design and Experimental Program

4.2.1. Concrete Mix Design

Based on industry practice, standard mix designs for 40 MPa and 25 MPa concrete were used in this study (as shown in Table 4.3). Two types of PP fibres used in this study were: 100% virgin PP fibres and 100% recycled PP fibres. For the 40 MPa concrete mix design, 6 kg/$m^3$of PP fibres were mixed with concrete. This mix design is normally used for precast panels. For the 25 MPa target strength concrete, 4 kg/m^3 of PP fibres were mixed. This design is commonly used for construction of concrete footpaths.

In this study, concrete was delivered from the batch plant (Holcim Australia Pty. Ltd.) in a standard concrete truck without plastic fibres. The average slump of 40 MPa concrete was 60 mm, while the 25 MPa concrete was 100 mm, based on AS 1012.3.1-2014 (AS, 2014a). Recycled and virgin PP fibres were then mixed separately with concrete in a drum mixer. Good dispersion of fibres could be achieved using this method as fibres were sprinkled in to avoid clumping. After casting, based on AS 1012.8.1:2014 (AS, 2014b), all the concrete cylinders, beams and round panels were allowed to stand for 24 hr in laboratory before demoulding. The specimens were cured in water at 23 ± 2 ℃ for 28 days.

Table 4.3 Concrete mix proportions

Material	40 MPa Concrete	25 MPa Concrete
0.6-4.75 mm Coarse sand (kg/m^3)	350	410
6.7-9.5 mm Concrete aggregate (kg/m^3)	950	260
0.3-5 mm Crusher dust (kg/m^3)	220	200
0.075-0.3 mm Fine sand (kg/m^3)	290	350
9.5-19 mm Concrete aggregate (kg/m^3)	-	690
Fly ash (kg/m^3)	130	134
Cement (kg/m^3)	256	186
Polyheed 8190 admixture (ml/ 100 kg cementitious materials)	337	281
Air entrapment admixture (ml/ 100 kg cementitious materials)	-	22
Water (l/m^3)	105	116
PP fibre (kg/m^3) (virgin or 100% recycled)	6	4

4.2.2. Compressive Strength of Concrete

Compressive strength tests were performed on the PP fibre reinforced concrete specimens according to AS 1012.9:2014 (AS, 2014c). Fibre concrete cylinders of 100 mm diameter by 200 mm height were tested at an age of 28 days. The diameter, height and mass of the cylinders were recorded before testing. The concrete specimen was placed in the test rig, ensuring the rubber cap had a snug fit, and the safety guard was closed. The axial load was incrementally applied at a rate of 20 ±2 MPa compressive stress per minute until specimen failure in the universal testing machine with a maximum load capacity of 2000 kN. The compressive strength results for concrete reinforced with each fibre type were based on an average value of four specimens.

The compressive strength ($f_c^{'}$) is calculated by dividing the ultimate load at failure (F, kN) by the cross sectional area of the specimen (A, mm^2), and then converted into Mega Pascals (MPa) as seen in Equation 7.

$$f_c^{'}(MPa) = \frac{F(N)}{A(mm^2)} \tag{7}$$

4.2.3. Residual Flexural Tensile Strength with CMOD

In this study post-cracking behaviour of the recycled PP fibre reinforced concrete was quantified and compared with that of virgin PP fibres through the Crack Mouth Opening Displacement (CMOD), according to BS EN 14651-2005+A1-2007 (EN, 2005). The CMOD test demonstrates the relationship between residual flexural strength and cracking behaviour, reflecting how the fibres control the cracks. The CMOD test can clearly assess the ability of the fibres to redistribute the stresses and bridge the cracks formed (Buratti et al., 2011).

As shown in Fig. 2.3.7, the flexural beams were of size of 150 mm x 150 mm x 600 mm. A notch of 2 mm wide and 25 mm depth were cut at mid-span of each beam. The notched beams were loaded using a 500 kN hydraulic testing machine on a three-point loading setup. The CMOD was measured using two clip gauges installed at the centre of the notch and averaged CMOD values were adopted. The clip gauges attached to knife edges glued to the bottom of the beam were connected to a data acquisition system and a Linear Variable Displacement Transformer (LVDT), as shown in Fig. 4.4. The tests were displacement controlled to achieve a constant rate of CMOD at 0.05 mm/min. The tests were carried out at K&H Geotechnical Services Pty Ltd, Australia. Three samples for each fibre and concrete type were tested. One plain concrete beam was tested as a control specimen.

The residual flexural tensile strength $f_{R,j}$ is given by the Equation 8:

$$f_{R,j} = \frac{3F_j l}{2bh_{sp}^2} \tag{8}$$

Where, $f_{R,j}$, is the residual flexural tensile strength corresponding with CMOD = $CMOD_j$ (j = 1,2,3,4), in Newton per square millimetre; F_j, is the load corresponding with CMOD = $CMOD_j$ (j = 1,2,3,4), in Newton; l, is the span length, in millimetres; b, is the width of the specimen, in millimetres; h_{sp}, is the distance between the tip of the notch and the top of the specimen, in millimetres.

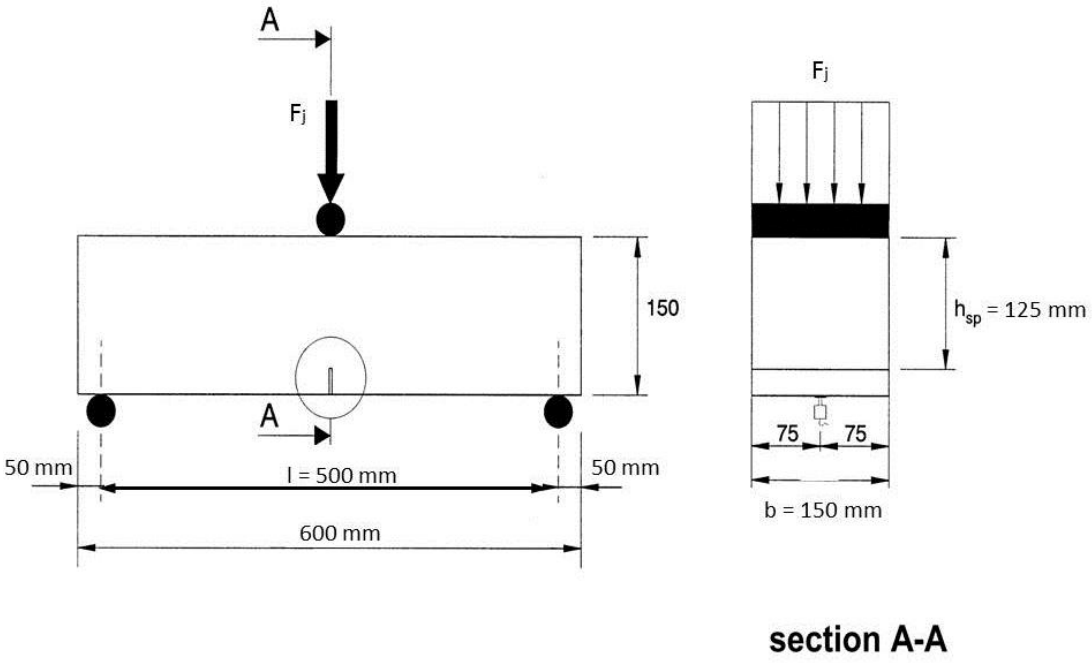

Fig. 4.4 Schematic diagram of the CMOD test

4.2.4. Round Determinate Panel Test

Round determinate panel test (RDPT) is another effective test that reflects the post-cracking behaviour of fibre reinforced concrete. The panel-based performance assessment is desirable, because panels fail through a combination of stress actions that reflect in-situ behaviour of concrete more closely than other mechanical tests in the laboratory (Cengiz and Turanli, 2004; Parmentier et al., 2008). This test has a significantly lower variability in the post-cracking performance than other tests. Energy absorption by the fibre reinforced concrete specimen is considered in RDPT, making it one of the most reliable test methods for post-cracking performance assessment (Bernard, 2002).

The RDPT specimens were tested in flexure according to ASTM C1550-12 (ASTM, 2012). Production of the round panels began with the circular metal ring forms, which were

mounted on a wood pallet. The forms had a diameter and height of 800 and 75 mm, respectively, per ASTM C1550 specifications (Fig. 4.5). The ring forms, and the wooden pallets on which they were mounted, were coated in form oil to allow easy extraction of the shotcrete panel. After casting, the panels were covered with plastic and left in the lab for a week. After that, the panels were sent to K&H Geotechnical Services Pty Ltd, Australia, and placed in their curing room. The temperature of the curing room was maintained around 21 ℃, with 95% relative humidity.

Fig. 4.5 Preparation of round panel

Before they were tested, the panels were removed from the curing room and placed in the testing apparatus with a hand-operated forklift. A panel was removed from the curing room only when it was time for the panel to be tested. As can be seen in Fig. 2.3.8, a central point load was applied on the round panel supported on three symmetrically arranged hinged supports. The three pivoted supports ensured that load distribution was always determinate in the round panel specimens. A hydraulic universal testing machine with a capacity of 250 kN was used for applying the load. As specified in the standard, the load piston advanced at a constant rate of 4.0 $\pm$ 1.0

mm/min up to a central displacement of at least 45.0 mm. The deflection was recorded by a Linear Variable Deflection Transducer (LVDT) placed under the centre of the specimen. The tests (Fig. 4.6) were carried out at K&H Geotechnical Services Pty Ltd, Australia.

Fig. 4.6 Test apparatus for the RDPT

Three panels for each type were produced for testing, two of which must test correctly. To test correctly, a panel must break into three pieces and be within certain size specifications. The data were plotted as a load-net deflection curve, with a maximum centre point deflection value of 40 mm. The area under the curve represented the energy absorption of a panel. Its value was entered into a formula and corrected to account for any deviation from ASTM C1550 specifications in thickness or diameter by using the following equation:

$$w = w' \cdot \left(\frac{t_0}{d_0}\right)^{\beta} \cdot \left(\frac{d_0}{d}\right) \qquad (9)$$

Where:

$$\beta = 2 - \left(\frac{\delta - 0.5}{80}\right)$$

w = the corrected energy absorption,

w' = the measured energy absorption,

δ = the specified central deflection at which the capacity to absorb energy is measured, mm,

t = the measured average thickness, mm,

t_0 = the nominal thickness of 75 mm,

d = the measured average diameter, mm, and

d_0 = the nominal diameter of 800 mm.

4.3. Mechanical Properties of the 100% Recycled and Virgin PP Fibres

As shown in Fig. 4.7, the 100% recycled and virgin PP fibres produced by same melt spinning and hot drawing process, have same geometry and dimensions (1.5 mm in width, 0.7 mm in thickness, and 47 mm in length).

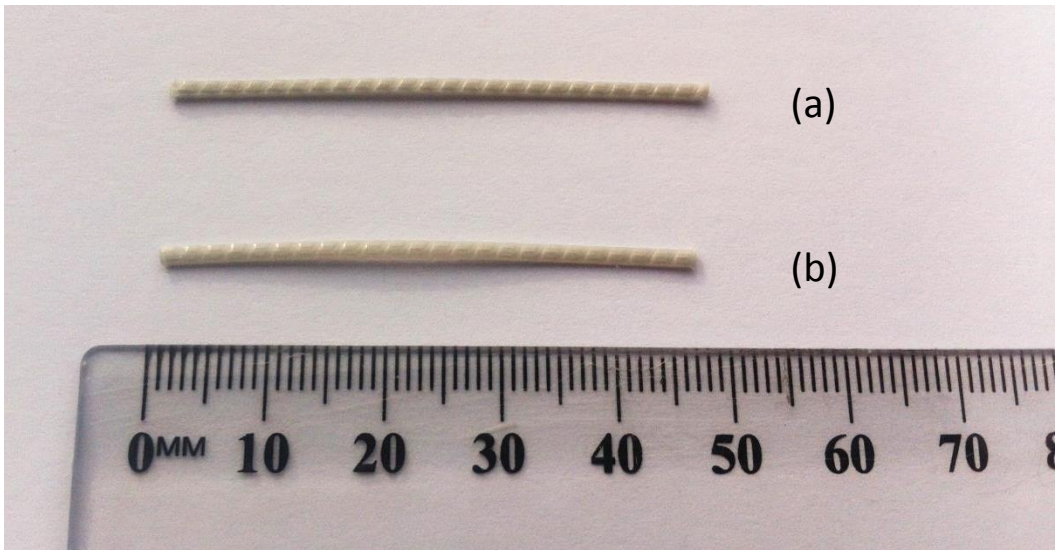

Fig. 4.7 (a) 100% recycled and (b) virgin PP fibres

A brittle mode of failure was seen in both fibres (Fig. 4.8), with a short elastic phase of steep slope and a progression of sharply rising stress until fracture. The averages of the tensile strength, Young's modulus based on 30 specimens for each fibre type are shown in Table 4.4 as well as the elongation at break and their standard deviation. As can be seen, the 100% recycled PP fibre shows lower tensile strength (284.1 MPa) but much higher Young's modulus (4582 MPa) than those of virgin PP fibre. According to

the research in Chapter 3, the 100% recycled PP fibre has lower molecular weight and shorter molecular chains than those of virgin PP fibre. The shorter molecular chains make the recycled PP fibre easier to be crystallised, thus producing higher Young's modulus. However, the shorter molecular chains have less molecular entanglement and hence, lower tensile strength.

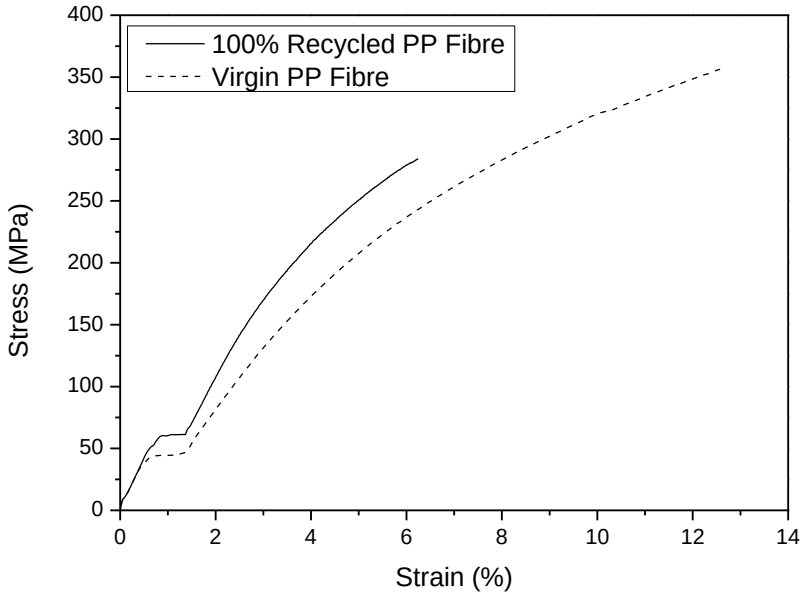

Fig. 4.8 Typical stress-strain curves of PP fibres

Table 4.4 Mechanical properties of PP fibres

	Tensile stress (MPa)		Young's Modulus (MPa)		Elongation at break (%)	
	Average	Standard deviation	Average	Standard deviation	Average	Standard deviation
Virgin PP Fibre	356.4	30.6	3129	564	12.6	2.8
100% Recycled PP Fibre	284.1	21.0	4582	1661	6.2	2.2

4.4. Compressive Strength of Concrete

100% recycled and virgin PP fibre reinforced concrete cylinder's compressive strength is shown in Fig. 4.9. This shows no significant effect on compressive strength through addition of fibres. This can be contributed to the concrete matrix containing fibres in quantities low enough (4 and 6 kg/m^3) to have no effect on compressive strength (Hasan et al., 2011). However, larger fibre doses (i.e. 13 to 18 kg/m^3) can lead to improper distribution resulting in balling of fibres and air pockets which adversely affect the compressive strength of concrete (Ochi et al., 2007). This correlates with the outcomes of many researchers (Choi and Yuan, 2005; Ochi et al., 2007; Soroushian et al., 2003; Wang et al., 1994), who have recorded no significant variation to compressive strength of concrete with PP fibre addition. Moreover, recycled fibre and virgin fibre reinforced concrete cylinders had comparable compressive strength results, as shown in Fig. 4.9. It should also be noted that during the compression tests PP fibre reinforced concrete cylinder failure was characterised by numerous minor surface cracks while plain concrete cylinders failed catastrophically, at peak load, with a large single crack, as shown in Fig. 4.10. In other words, the fibre samples displayed a more ductile mode of failure.

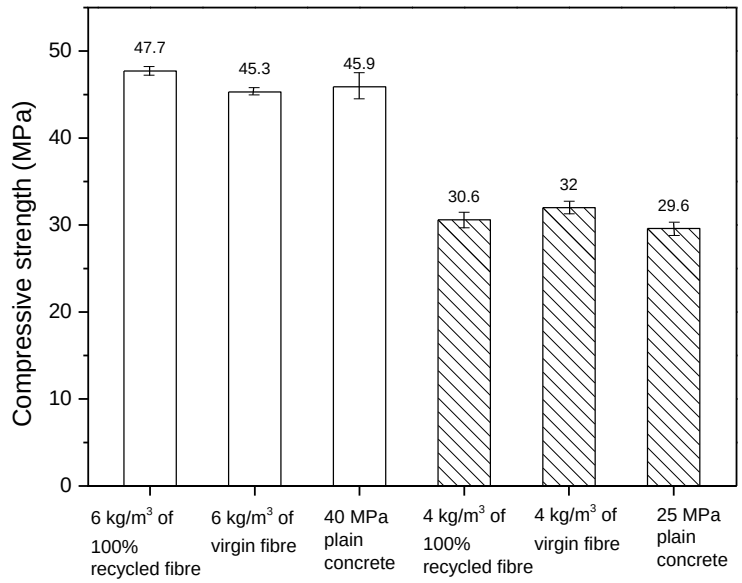

Fig. 4.9 Compressive strength of the PP fibre reinforced concrete cylinders

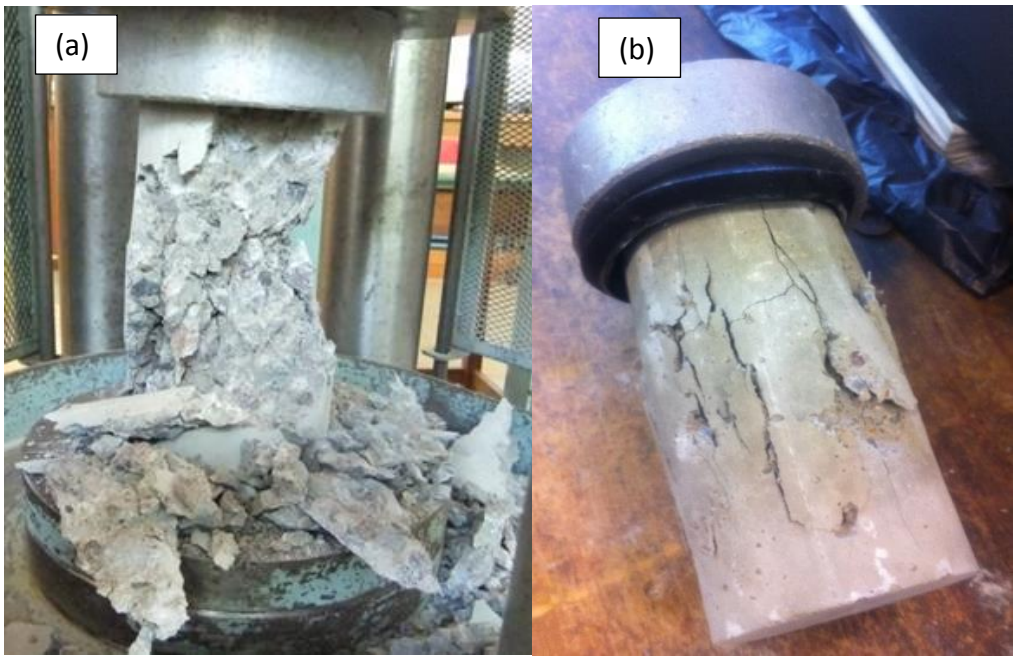

Fig. 4.10 Failure behaviour of (a) plain concrete and (b) fibre reinforced concrete in the compression test

4.5. Residual Flexural Tensile Strength with CMOD

Fig. 4.11.a shows load-CMOD curves of 6 kg/m^3 PP fibres reinforced concrete beams of 40 MPa compressive strength. Peaked loads reached for all the recycled and virgin PP fibre reinforced concrete beams were approximately 14 kN, this was then followed by a sharp drop associated with CMOD range of 0.05 mm to 0.5 mm. Further, CMOD from 0.5 mm to 3 mm was associated with increased loads, which then remained stable at 4-8 kN on further loading. However, the load dropped to zero for the plain concrete beam after the peak load was attained.

Fig. 4.11.b exhibits load-CMOD curves of 4 kg/m^3 PP fibre reinforced concrete beams of target strength 25 MPa. The peak loads for all the beams were approximately around 13 kN, before a sudden drop. Unlike the Fig. 4.11.a, the loads then just kept stable at 2-5 kN until failure. It shows inferior post-cracking performance than that of the fibres in 40 MPa concrete, due to lower compressive strength of concrete and lower amount of fibre. As expected, the load dropped to 0 kN soon after the peak load for the plain concrete beam. Fig. 4.11 confirms the outstanding post-cracking

performance of the 100% recycled and virgin PP fibre reinforced concrete beams, compared to the plain concrete.

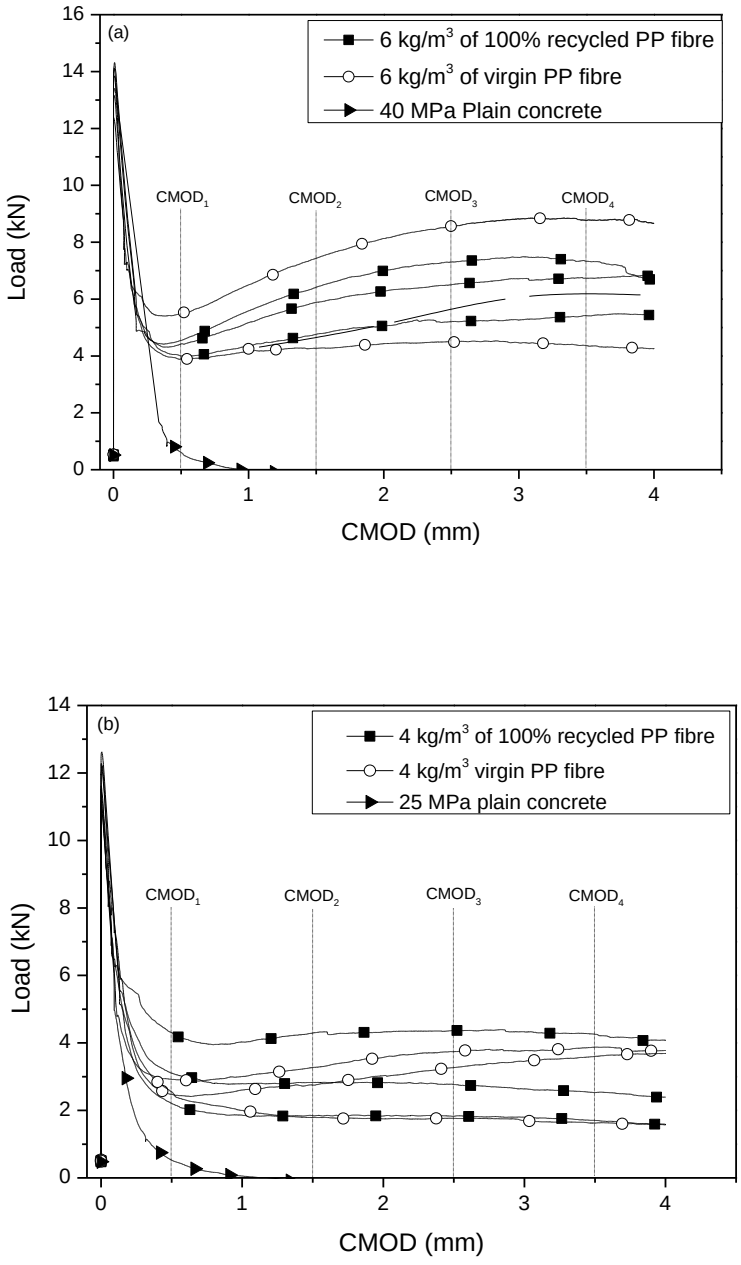

Fig. 4.11 Load-CMOD curves for (a) 6 kg/m^3 of PP fibre reinforced 40 MPa concrete, and (b) 4 kg/m^3 of PP fibre reinforced 25 MPa concrete

Fig. 4.12 compares residual flexural tensile strength at the peak load for the 100% recycled and virgin PP fibre reinforced concrete beams compared to the plain control concrete beams. As can be seen, for both 40 MPa and 25 MPa concrete beams, the

100% recycled PP fibre reinforced concrete beams have comparable residual flexural tensile strength to that of virgin PP fibre reinforced concrete. Compared to 40 MPa and 25 MPa plain concrete beams, there is no obvious change after adding the PP fibres.

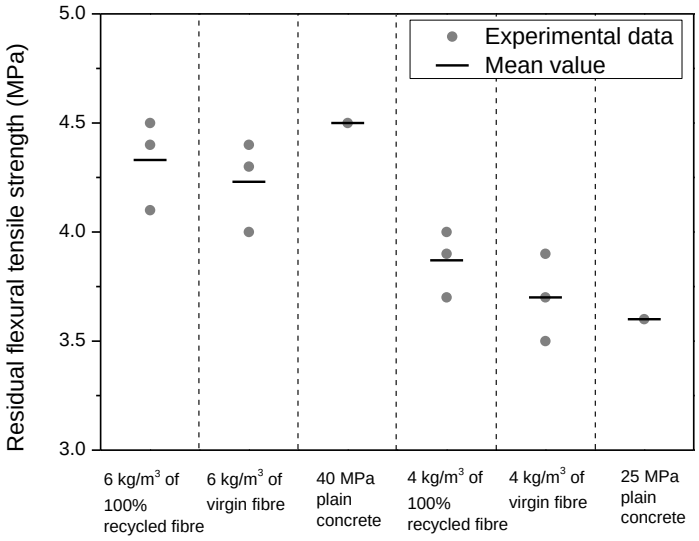

Fig. 4.12 Residual flexural tensile strengths at the peak load

Fig. 4.13 compares the residual flexural tensile strength of PP fibres reinforced concrete beams at $CMOD_1$, $CMOD_2$, $CMOD_3$ and $CMOD_4$. As can be seen, for the 40 MPa concrete, the 100% recycled PP fibre reinforced concretes show comparable or only slightly lower residual flexural strength than that reinforced by the virgin PP fibre. Moreover, from Fig. 4.13.a to Fig. 4.13.d, with the increase of CMOD, the residual flexural tensile strength of the fibre reinforced 40 MPa concrete beam increases from 1.5 MPa to 2.0 MPa. On the other hand, for the 4 kg/m^3 fibre reinforced 25 MPa concrete, the average residual flexural tensile strength of 100% recycled PP reinforced concretes is slightly higher that of virgin PP fibre reinforced concretes. Furthermore, the residual flexural tensile strength just keeps stable around 1.0 MPa from $CMOD_1$ to $CMOD_4$, instead of increasing.

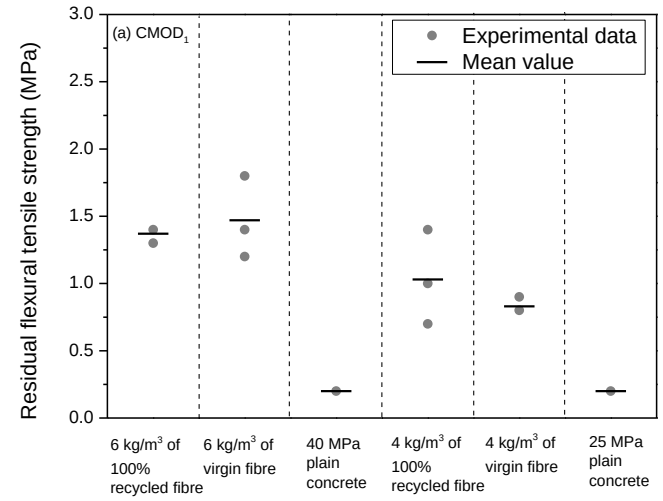
(a) CMOD1
Experimental data
Mean value
Residual flexural tensile strength (MPa)
3.0
2.5
2.0
1.5
1.0
0.5
0.0
6 kg/m3 of 100% recycled fibre
6 kg/m3 of virgin fibre
40 MPa plain concrete
4 kg/m3 of 100% recycled fibre
4 kg/m3 of virgin fibre
25 MPa plain concrete

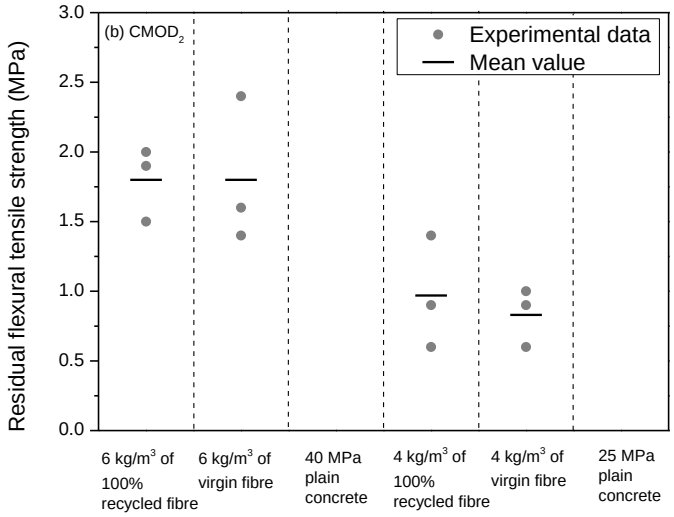
(b) CMOD2
Experimental data
Mean value
Residual flexural tensile strength (MPa)
3.0
2.5
2.0
1.5
1.0
0.5
0.0
6 kg/m3 of 100% recycled fibre
6 kg/m3 of virgin fibre
40 MPa plain concrete
4 kg/m3 of 100% recycled fibre
4 kg/m3 of virgin fibre
25 MPa plain concrete

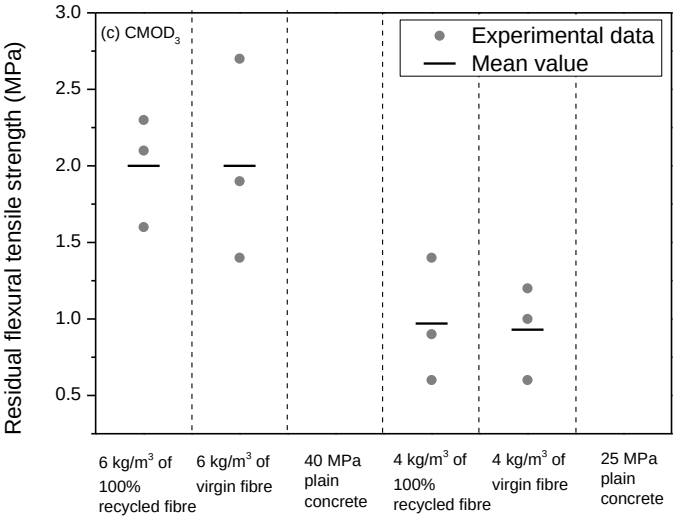
(c) CMOD3
Experimental data
Mean value
Residual flexural tensile strength (MPa)
3.0
2.5
2.0
1.5
1.0
0.5
6 kg/m3 of 100% recycled fibre
6 kg/m3 of virgin fibre
40 MPa plain concrete
4 kg/m3 of 100% recycled fibre
4 kg/m3 of virgin fibre
25 MPa plain concrete

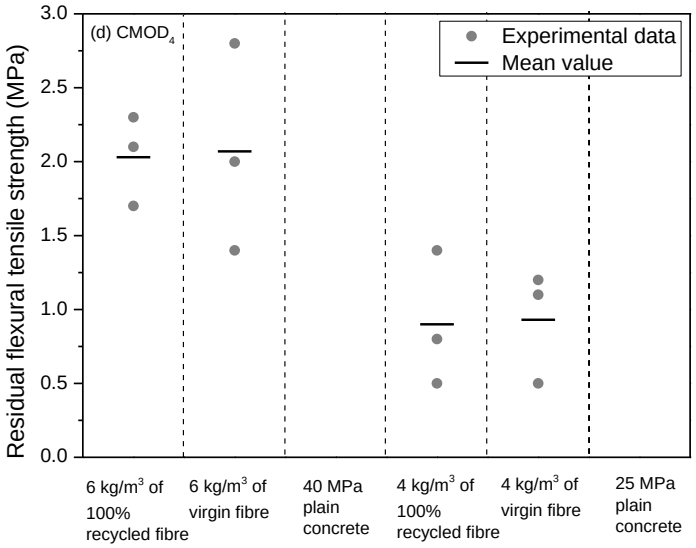

Fig. 4.13 Residual flexural tensile strength of PP fibres reinforced concrete beams at (a) $CMOD_1$, (b) $CMOD_2$, (c) $CMOD_3$ and (d) $CMOD_4$

Fig. 4.14 shows the fracture faces of the fibre reinforced concrete beams. Fig. 4.14.a and b represent the fracture faces of 100% recycled and virgin PP fibre reinforced 40 MPa concrete beams, respectively. As can be seen, fibre breakage was higher than fibre pull out, which indicates good bonding of fibres with a high-strength concrete matrix. Tensile capacity of the broken PP fibres was fully realised, thus producing good reinforcement. As the ultimate tensile capacity was reached in the broken fibres, the performance of the fibres depended on both their tensile strength and Young's modulus. From Table 4.4, it can be seen that the 100% recycled PP fibre had higher Young's modulus but lower tensile strength than the virgin PP fibre. Consequently, the 100% recycled PP fibre produced similar or slightly lower performance than the virgin PP fibre in the 40 MPa concrete beams. Moreover, the failure mechanism of 100% recycled and virgin PP fibre themselves are different. In the case of 100% recycled PP fibre concrete (Fig. 4.14.a), the fibres broke with relatively brittle mode of failure, while the broken virgin PP fibre was stretched into massive split micro fibres, showing a more ductile failure (Fig. 4.14.b). This is because the 100% recycled PP fibre has very low elongation at break (6.2%), while the virgin PP fibre is more ductile and has much higher elongation at break at 12.6%.

The fracture faces of 25 MPa concrete beams are different with those of 40 MPa concretes as shown in Fig. 4.14.c and d. In the low-strength concrete, nearly all the fibres were pulled out without being broken, indicating that the low-strength concrete has a poor bonding with the fibres. Because of this poor bonding, the majority of the fibres remained intact and their full tensile capacity was not realised. Therefore, Young's modulus of the fibres is more effective on their reinforcement than the tensile strength. Since the 100% recycled PP fibre has higher Young's modulus than that of virgin PP fibre, thus producing better reinforcement in the CMOD tests.

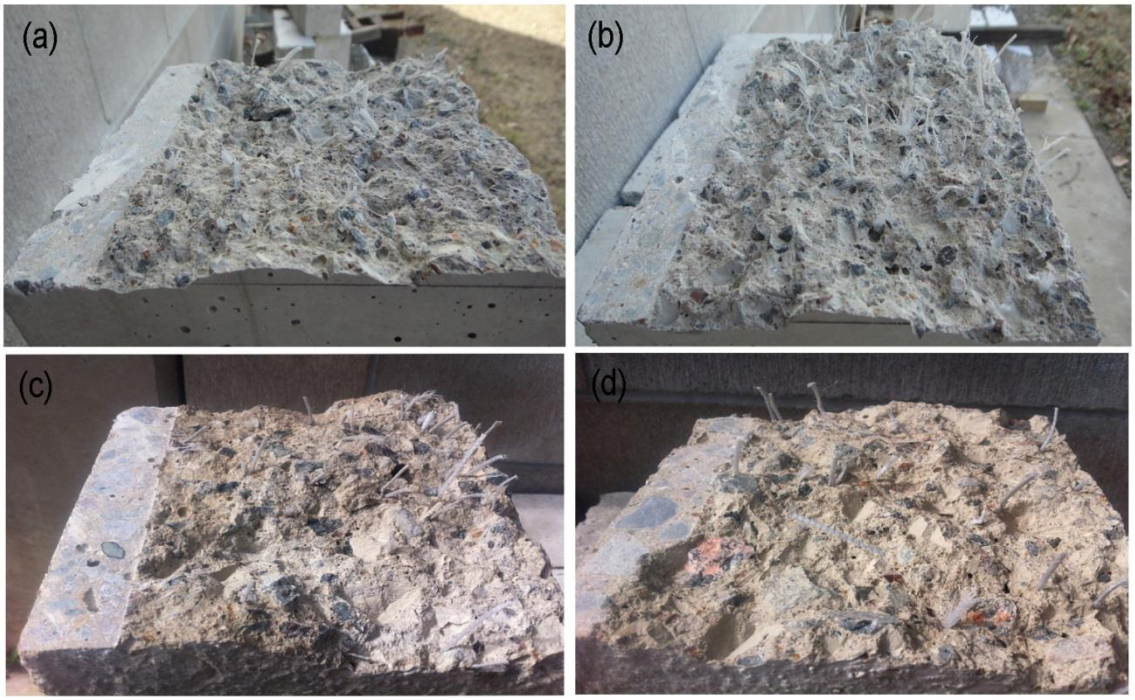

Fig. 4.14 Fracture surfaces of PP fibres reinforced concrete beams: (a) 6 kg/m^3 of 100% recycled PP fibre, (b) 6 kg/m^3 of virgin PP fibre, (c) 4 kg/m^3 of 100% recycled PP fibre, and (d) 4 kg/m^3 of virgin PP fibre

4.6. Flexural Strength and Toughness from RDPT

RDPT is another effective test that reflects the behaviour of fibre reinforced concrete. As can be seen from Fig. 4.15, all the fibre reinforced concrete panels reached a peak load at the deflection of 1 mm, before a sudden drop to 5-8 kN. The loads then kept flat until deflection at 10 mm, before a stable downward trend to about 1.5 kN.

The energy absorption is the area under the load curves, which also reflects the performance of fibre reinforcement in dissipating energy. As can be seen from Fig. 4.15.a, the 100% recycled PP fibre had slightly lower energy absorption than that of the virgin PP fibre, indicating that the 100% recycled PP fibre produced slightly lower post-cracking reinforcement than that of virgin PP fibre. This result is consistent with CMOD results. The reinforcement of the PP fibres in high-strength concrete depends on both their Young's modulus and tensile strength. Although the 100% recycled PP fibre had lower tensile strength, its higher Young's modulus improved its reinforcing effects. Consequently, a comparable reinforcement with virgin PP fibre was produced by the 100% recycled PP fibre in the 40 MPa concrete.

For the 25 MPa concrete, the 100% recycled PP fibre produced higher post-cracking reinforcement than that of virgin PP fibre (Fig. 4.15.b). As we discussed before, the PP fibres have a poor bonding with concrete matrix in the low-strength concrete, hence, the Young's modulus is more effective on the reinforcement. The 100% recycled PP fibre has higher Young's modulus, thus producing better reinforcement.

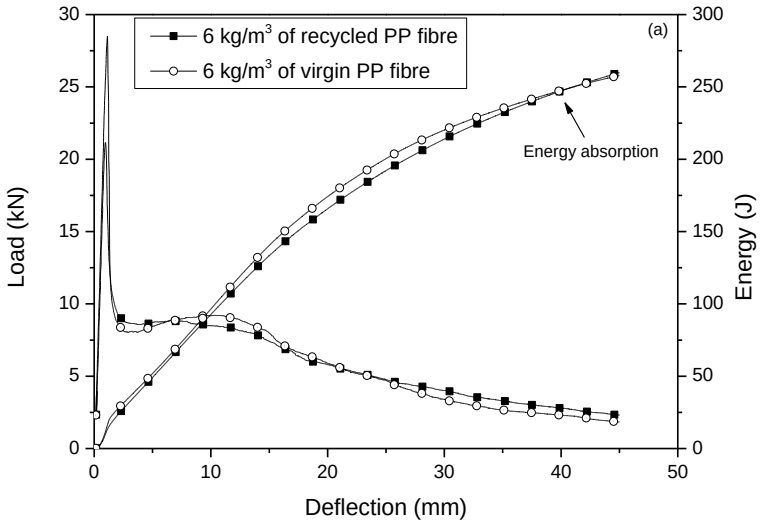

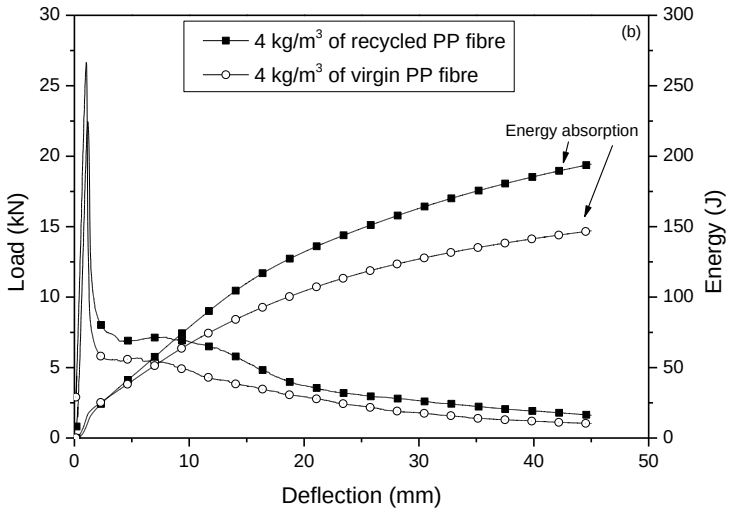

Fig. 4.15 Energy absorption and load curves from Round Determinate Panel Tests: (a) 6 kg/m^3 of PP fibre reinforced 40 MPa concrete, and (b) 4 kg/m^3 of PP fibre reinforced 25 MPa concrete

4.7. Conclusions

1. The virgin PP fibre had a minimum degradation in all kinds of alkaline environments. However, there were some minor changes on the mechanical properties of recycled PP fibre after immersion. NaOH solution slightly embrittled the recycled PP, thus decreasing the tensile strength and increasing Young's modulus of the fibre, due to its high pH value. The KOH solution slightly decreased the tensile strength of the fibre. However, there was nearly no change after immersing the fibre in the Lawrence solution which simulates a fully hydrated cement paste. Overall, the 100% recycled PP fibre showed good alkali resistance in all the alkaline environments tested.

2. Addition of the 100% recycled plastic fibre at low dose rate (4 and 6 kg/m^3) did not affect compressive strength of concrete, however, it significantly improved the residual flexural tensile strength of concrete.

3. CMOD tests on 40 MPa concrete beams with 6 kg/m^3 PP fibres (normally used for precast concrete elements) showed that most of the fibres were broken

instead of being pulled out at the failure load. This inferred good bonding of fibres with concrete, hence the performance of PP fibres were influenced by both Young's modulus and tensile strength of fibres. The 100% recycled fibre had higher Young's modulus but lower tensile strength than the virgin PP fibre. Consequently, the 100% recycled PP fibre had slightly lower performance than that of virgin plastic fibre in 40 MPa concrete. In 25 MPa concrete, majority of fibres were being pulled out instead of breaking. As the fibres did not reach ultimate tensile strength, its Young's modulus was more influential. The 100% recycled PP fibre had higher Young's modulus and hence, performed better than virgin plastic fibre in 25 MPa concrete.

4. RDPT also proved that the 100% recycled PP fibre produced comparable post-cracking performance to that of the virgin PP fibre in the 40 MPa concrete, and better performance than that of virgin PP fibre in the 25 MPa concrete. This proved that the post-cracking performance of 100% recycled PP fibre reinforced concrete is in par with the virgin PP fibre reinforced concrete. Therefore, the 100% recycled plastic fibre can be used to replace virgin plastic fibres in concrete footpaths and precast panels.

Chapter 5 Post-cracking Performance of Concrete Reinforced by Various Newly Developed Recycled PP Fibres

Publication

S. Yin, R. Tuladhar, T. Collister, M. Combe, N. Sivakugan, Z. Deng. Post-cracking performance of recycled polypropylene fibre in concrete. Construction and Building Materials. 2015, 101(1):1069-1077

In the previous chapter (Chapter 4), the reinforcement of 100% recycled PP fibre with line indentation was studied to ascertain the feasibility of using 100% recycled PP fibre in concrete. In this chapter, various newly developed recycled PP fibres described in Chapter 3 were used to reinforce concrete, and their performance in concrete was determined.

Target compressive strength of concrete used in the concrete footpaths, based on industrial practice, normally ranges from 25 to 40 MPa, and the standard fibre dosage is 4 kg/m^3. In the previous Chapter (Chapter 4), 4 kg/m^3 fibre reinforced 25 MPa concrete for the application of concrete footpaths has been assessed. In order to evaluate fibre's reinforcement in other concrete-footpath applications, 4 kg/m^3 newly developed recycled PP fibres were used to reinforce standard mix design of 40 MPa concrete in this chapter.

The effects of tensile strength and Young's modulus of these recycled PP fibres on their reinforcing effects in the concrete were studied. In order to enhance the fibre-concrete bonding, different types of surface indentations (line and diamond) were made on fibre surface, as shown in Fig. 5.1, and their ability to bond with concrete were also observed in the RDPT and CMOD tests. All the fibres have 0.9-1 mm^2 of cross section, 47 mm of length and 0.1-0.2 mm of indentation depth. Table 5.1 lists these newly developed recycled PP fibres. They were Virgin PP Fibre (Line), Recycled PP Fibre (Line), 50:50 Virgin-Recycled PP Fibre (Line), Recycled PP Fibre (Diamond), and 5:95 HDPE-Recycled PP Fibre (Diamond). Their details can be seen in Table 5.1.

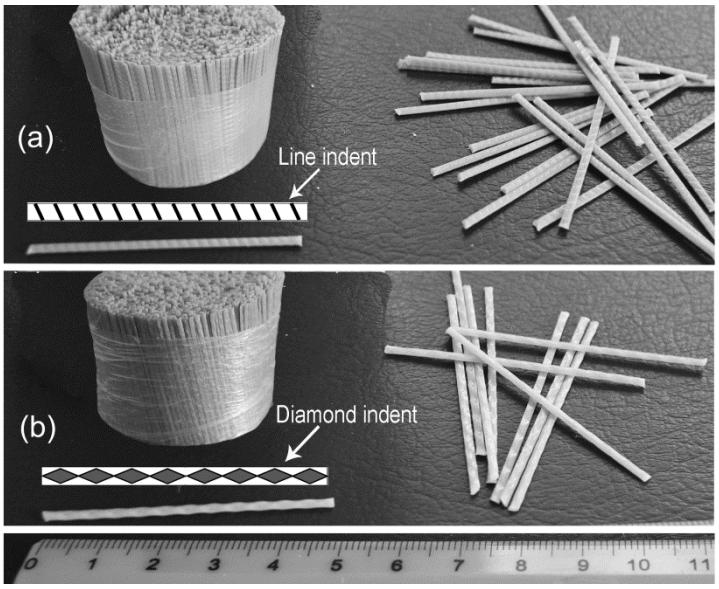

Fig. 5.1 (a) Line-indent PP fibre, and (b) diamond-indent PP fibre

Table 5.1 Details of PP fibres

Specimen	Indent type	Details
Virgin PP Fibre (Line)	Line	100% virgin PP
Recycled PP Fibre (Line)	Line	100% recycled PP
50:50 Virgin-Recycled PP Fibre (Line)	Line	mixture of 50% of virgin PP and 50% recycled PP
Recycled PP Fibre (Diamond)	Diamond	100% recycled PP
5:95 HDPE-Recycled PP Fibre (Diamond)	Diamond	mixture of 5% of HDPE and 95% recycled PP

As can be seen in Fig. 5.2, all the fibres show a brittle mode of failure, with a short elastic period of steep slope and a regime of sharply rising stress until fracturing occurred at strains between 5 and 14%. 30 specimens for each type of fibre were tested. Table 5.2 presents the averages of the tensile strength, Young's modulus and elongation at break of these fibres and their standard deviation. The Virgin PP Fibre (Line) showed high tensile strength (359.2 MPa) and elongation at break (14%), but lowest Young's modulus (only 3801 MPa). The Recycled PP Fibre (Line) showed much lower tensile strength (284.7 MPa), but much higher Young's modulus (6272 MPa) than those of The Virgin PP Fibre (Line). When 50% of the virgin PP was mixed with 50%

of the recycled PP, the Young's modulus of the 50:50 Virgin-Recycled PP Fibre (Line) increased to 7513 MPa, and the tensile strength was even higher than the virgin PP fibre at 392.9 MPa. When the surface indent of recycled PP fibre was changed to diamond indents, Young's modulus in the Recycled PP Fibre (Diamond) was considerably improved to 8727 MPa, with no obvious change in the tensile strength, compared to the Recycled PP Fibre (Line). This indicates that these two patterns of indents do not affect the tensile strength, but considerably affect Young's modulus of the fibres. HDPE brought ductility to the fibre, hence, 5:95 HDPE-Recycled PP Fibre (Diamond) showed lower Young's modulus and higher elongation at break than the Recycled PP Fibre (Diamond).

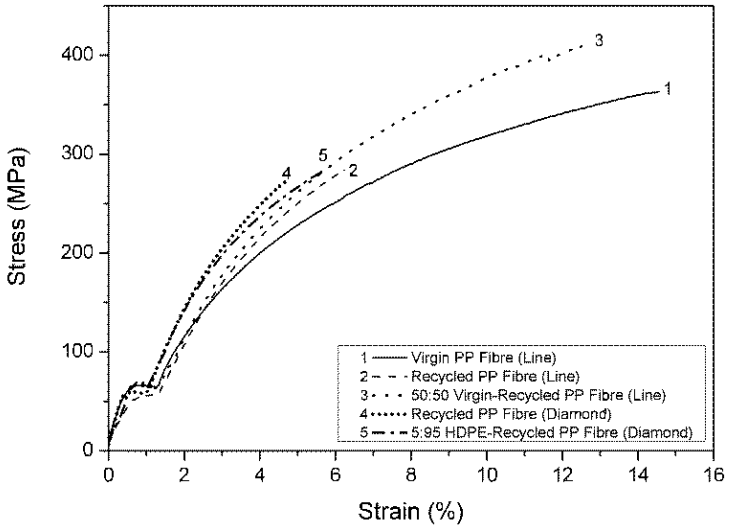

Fig. 5.2 Typical stress-strain curves of PP fibres

Table 5.2 Mechanical properties of PP fibres

PP fibre	Tensile stress (MPa)		Young's Modulus (MPa)		Elongation at break (%)	
	Average	Standard deviation	Average	Standard deviation	Average	Standard deviation
Virgin PP Fibre (Line)	359.2	30.6	3801	564	14.0	2.8
Recycled PP Fibre (Line)	284.7	21.0	6272	1661	7.4	2.2
50:50 Virgin-Recycled PP Fibre (Line)	392.9	18.2	7513	1460	12.5	1.4
Recycled PP Fibre (Diamond)	279.4	26.5	8727	1337	5.1	1.1
5:95 HDPE-Recycled PP Fibre (Diamond)	287.0	23.2	7294	1649	6.1	1.3

5.1. Compressive Strength of Concrete

Fig. 5.3 shows compressive strength of the PP fibre reinforced concrete cylinders. As can be seen, the addition of fibres does not have significant effects on the compressive strength. All the recycled fibre reinforced concrete cylinders have comparable compressive strength compared to the virgin fibre reinforced concrete. This is because the compressive strength of concrete was not influenced by the relatively low dosage of fibres (4 kg/m^3) according to the research of Hasan et al. (2011).

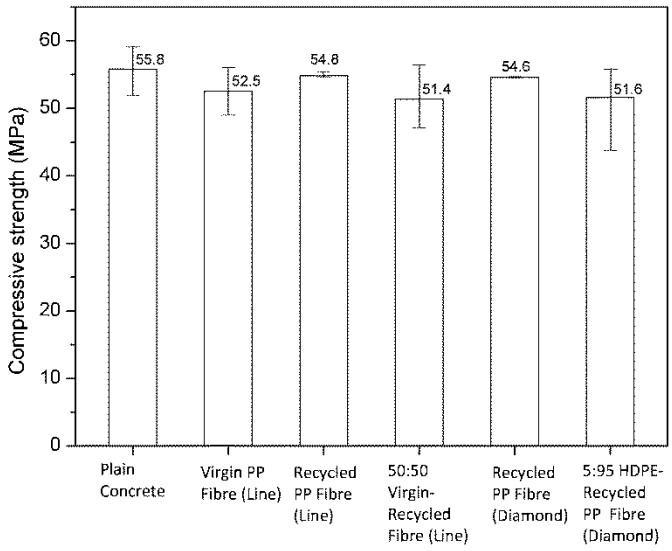

Fig. 5.3 Compressive strength of the PP fibre reinforced concrete cylinders

5.2. Residual Flexural Tensile Strength with CMOD

Fig. 5.4 shows load-CMOD curves of PP fibre reinforced concrete beams. Three samples for each fibre and concrete type were tested. One plain concrete beam was tested as a control specimen in this research. With increase of the CMOD, the loads of all the PP fibre reinforced concrete beams reached peak (around 20 kN) at the limit of proportionality (LOP), followed by a sudden drop in terms of the CMOD ranging from 0.05 mm to 0.5 mm. The loads then increased slightly with the increase of CMOD from 0.5 mm to 2 mm, and remained stable on further loading within the range of 1 to 5 kN. However, for the plain concrete beam, after the LOP, the load dramatically decreased to 0 kN. This indicated that all PP fibre reinforced concrete beams showed outstanding post-cracking behaviour.

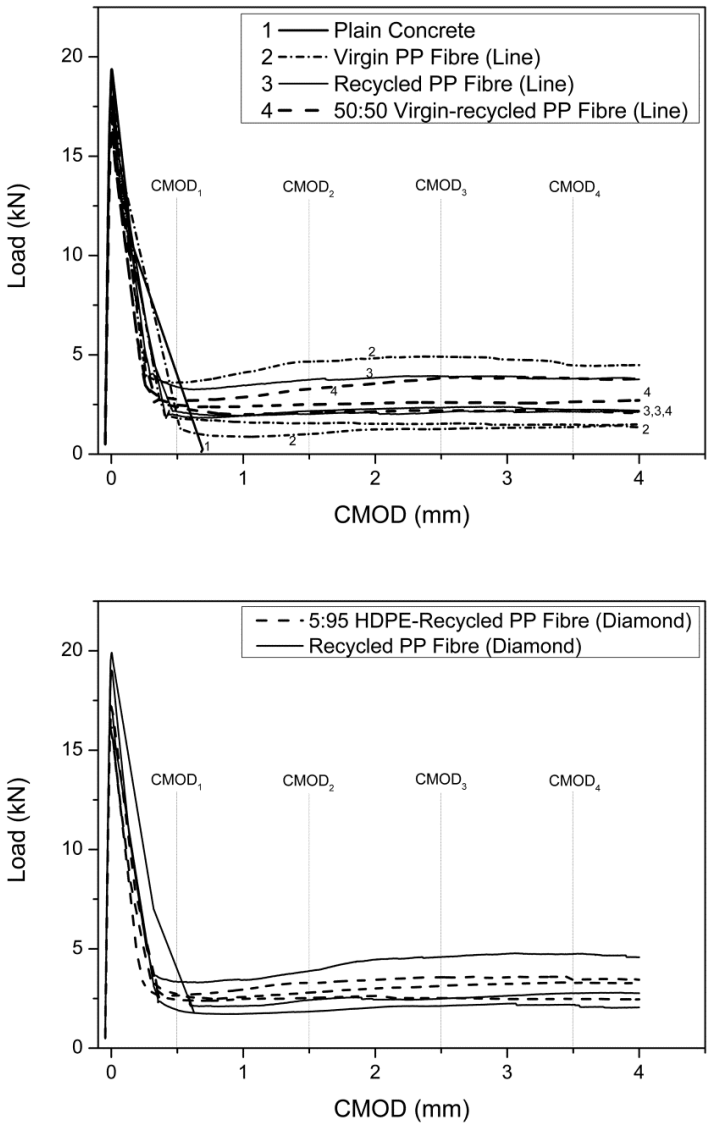

Fig. 5.4 Load-CMOD curves of PP fibres reinforced concrete beams

Fig. 5.5 shows residual flexural tensile strength at LOP for different fibre reinforced concrete beams compared to the plain concrete. Although all the fibre reinforced concretes have slightly lower residual flexural tensile strength at LOP, it should be noted that the PP fibres have not obvious effects on the residual flexural tensile strength at LOP. This is because the residual flexural tensile strength at LOP mainly depends on concrete properties rather than fibre properties. Moreover, since the CMOD test is for evaluating the post-cracking performance, only one plain concrete beam was tested as a control specimen, which may have led to some deviation in results.

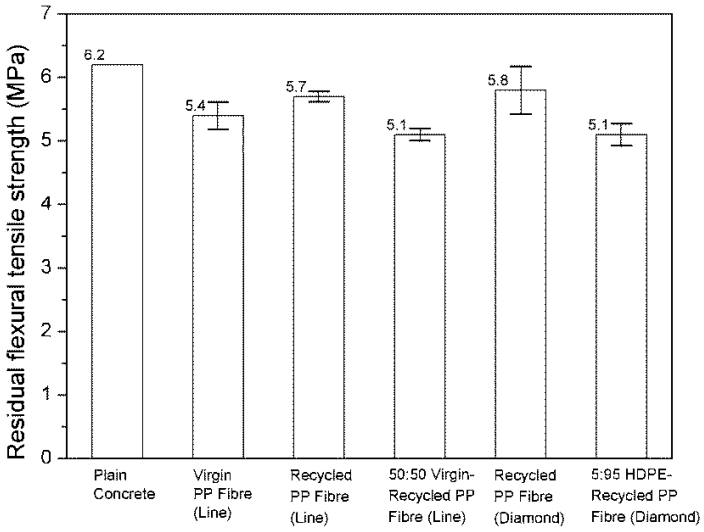

Fig. 5.5 Residual flexural tensile strength of PP fibres reinforced concrete beams at LOP

The Young's modulus of the fibre significantly affects the performance of the PP fibre in concrete. In the Fig. 5.6 the concrete beams reinforced by Recycled PP Fibre (Line) and 50:50 Virgin-Recycled PP Fibre (Line) showed higher residual flexural strength than that by the Virgin PP Fibre (Line), due to the higher Young's modulus of Recycled PP Fibre (Line) and 50:50 Virgin-Recycled PP Fibre (Line) than that of the Virgin PP Fibre (Line) (Table 5.2). From Table 5.2 it can be seen that the Virgin PP Fibre (Line) has much higher tensile strength than the Recycled PP Fibre (Line), while the Recycled PP Fibre (Line) reinforced concrete beams showed higher residual flexural strength than the Virgin PP Fibre (Line) reinforced concrete, indicating that for the line-indent PP fibres the Young's modulus of fibres are more effective on their reinforcement in the concrete than the tensile strength.

As can be seen in Fig. 5.6, the concrete reinforced by the diamond-indent PP fibres, namely Recycled PP Fibre (Diamond) and 5:95 HDPE-Recycled PP Fibre (Diamond), produced higher residual flexural strength than that by line-indent PP fibres. This indicates that the diamond-indent PP fibres produced better reinforcement than the line-indent PP fibres. Moreover, with the increase of CMOD, the residual flexural strength of concrete beams reinforced by Recycled PP Fibre (Diamond) and 5:95 HDPE-Recycled PP Fibre (Diamond) showed an upward trend at $CMOD_4$ (Fig. 5.6.d) and

$CMOD_3$ (Fig. 5.6.c) respectively, while the line-indent PP fibres just kept their flexural tensile strength constant from $CMOD_1$ to $CMOD_4$.

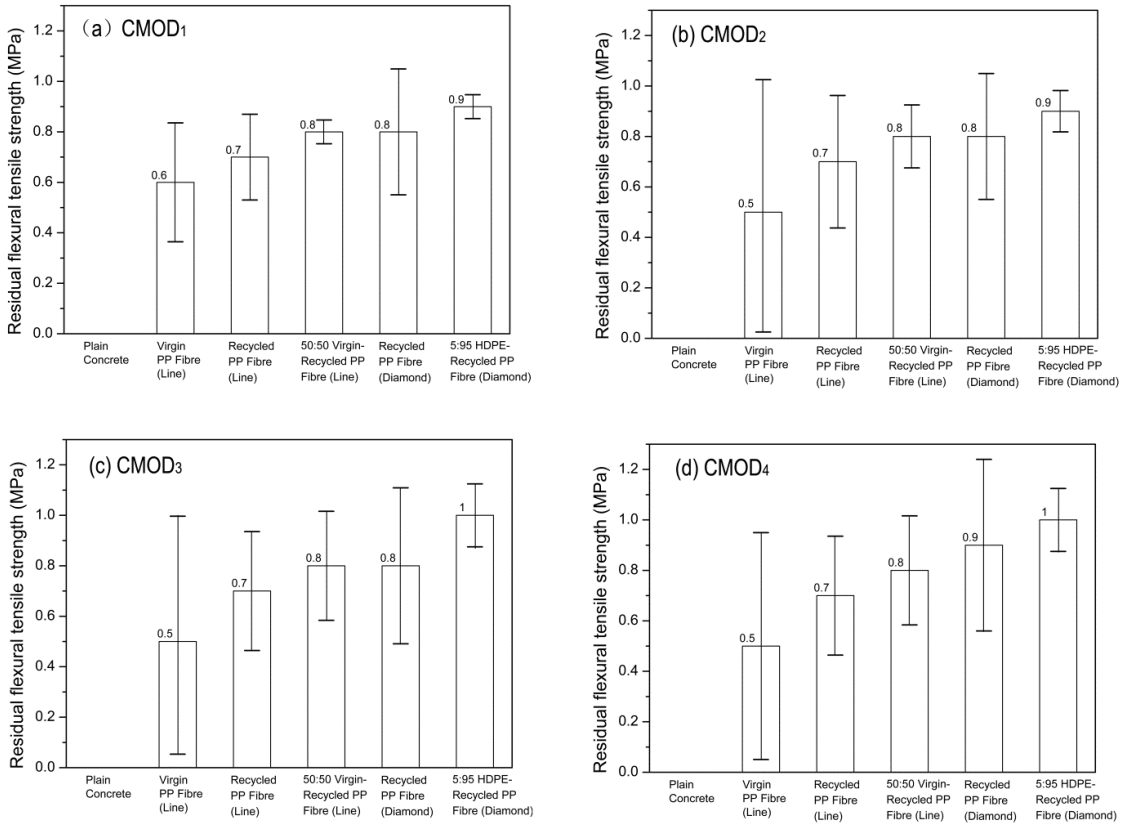

Fig. 5.6 Residual flexural tensile strength of PP fibres reinforced concrete beams at (a) $CMOD_1$, (b) $CMOD_2$, (c) $CMOD_3$, and (d) $CMOD_4$

Fig. 5.7 shows the fracture faces of the fibres reinforced concrete beams. Fig. 5.7.a represents the fracture faces of line-indent fibres reinforced concrete beams, including Virgin PP Fibre (Line), Recycled PP Fibre (Line), 50:50 Virgin-Recycled PP Fibre (Line). On the fracture faces of these three kinds of fibres reinforced concrete, nearly all of fibres were pulled out without being broken, indicating that the line indents have a poor bonding with the concrete. The fibres were pulled out and did not reach their ultimate tensile capacity, hence, the full tensile capacity of the fibres were not exploited. This explained why for the line-indent PP fibres the Young's modulus of fibres are more effective on their reinforcement than the tensile strength. Since the Virgin PP Fibre (Line) had lowest Young's modulus, hence it offered the concrete the lowest residential flexural tensile strength. Therefore, due to the poor bonding with

the concrete, the reinforcement of line-indent PP fibres mainly depends on their Young's modulus.

From Fig. 5.7.b, it can be seen that for the diamond-indent PP fibre reinforced concrete more fibres were broken than pulled out, indicating that the diamond indents had a better bonding with the concrete. The broken PP fibres fully exploited their tensile capacity, thus producing a better reinforcement than the line-indent PP fibres. Since more fibres reached their ultimate tensile capacity and were broken, the reinforcement of diamond-indent PP fibres depends on both their Young's modulus and tensile strength.

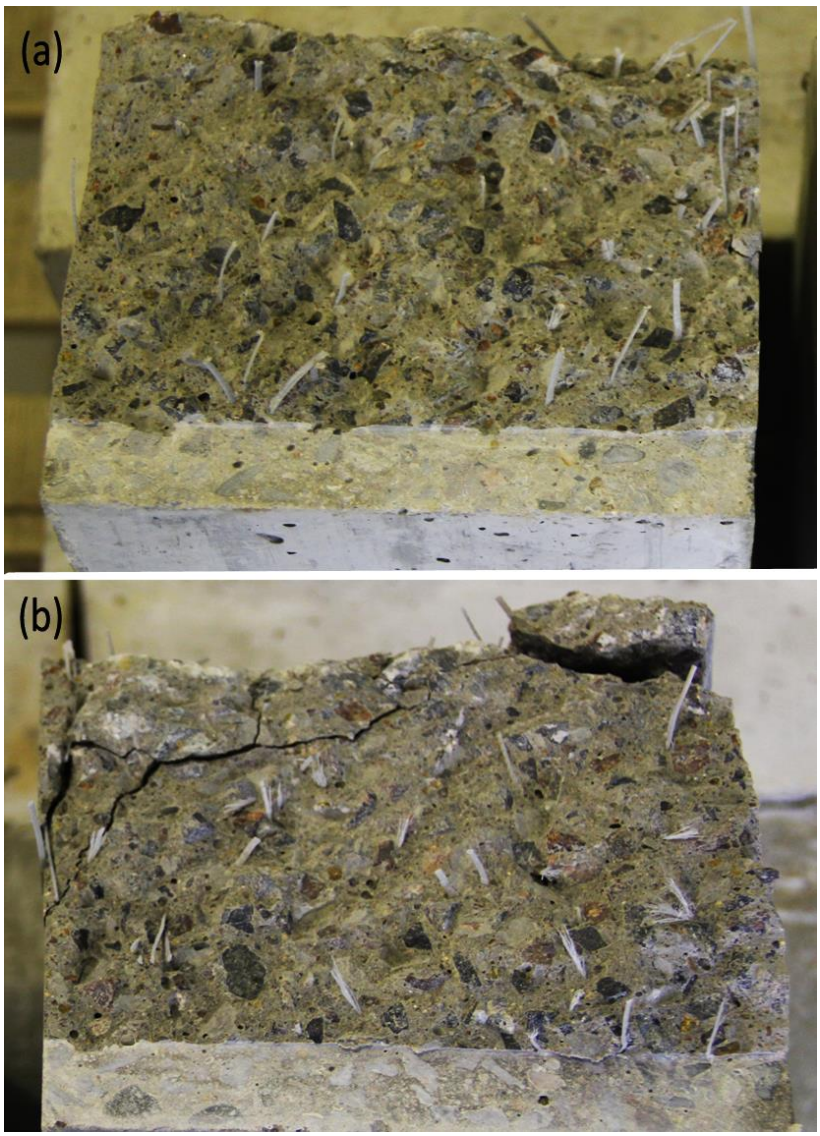

Fig. 5.7 Fracture faces of the PP fibres reinforced concrete beams: (a) line-indent PP fibre, and (b) diamond-indent PP fibre

5.3. Flexural Strength and Toughness from Round Determinate Panel tests

RDPT is an essential tool for assessment of post-cracking performance in fibre reinforced shotcrete within the underground construction and mining industries (Parmentier et al., 2008). The specimens can show a very low within-batch coefficient of variation in performance than any other test method for fibre reinforced concrete, mainly because of the large crack length experienced during testing (Bernard, 2002). Fig. 5.8 and Table 5.3 show the RDPT results of PP fibre reinforced concrete panels. As can be seen from Fig. 5.8, all of the curves attained a peak load at around 30 kN, followed by a sudden drop to 5-10 kN. The curves then kept flat or slightly increased until deflection at 10 mm, before a stable downward trend to about 1 kN.

From Table 5.3 it can be seen that the diamond-indent PP fibres, including Recycled PP Fibre (Diamond) and 5:95 HDPE-Recycled PP Fibre (Diamond), showed high post-cracking reinforcement, due to their high Young's modulus and good bonding with the concrete. The 50:50 Virgin-Recycled PP Fibre (Line) also showed high energy absorption due to its high Young's modulus and tensile strength. These three kinds of fibres all produced better reinforcement than the Virgin PP Fibre (Line). The Recycled PP Fibre (Line) produced lowest reinforcement due to its low tensile strength, Young's modulus, and poor bonding.

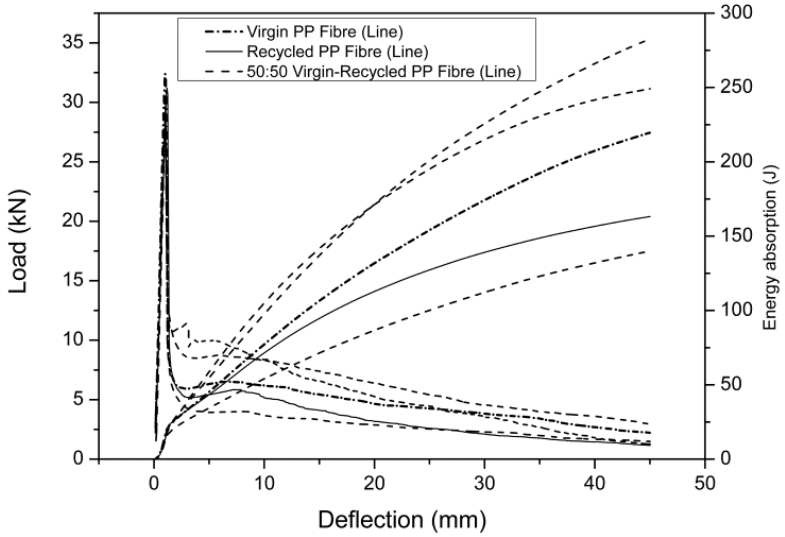

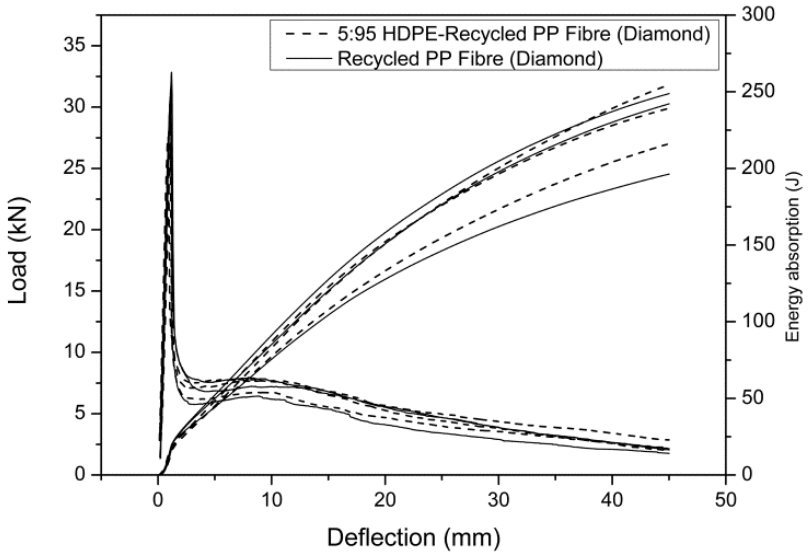

Fig. 5.8 Energy absorption and load curves from Round Determinate Panel Tests

Table 5.3 Energy absorption (Joules) of the Round Determinate Panel Tests

Deflection		5 mm	10 mm	20 mm	30 mm	40 mm
Virgin PP Fibre (Line)		44	74	126	166	198
Recycled PP Fibre (Line)		42	69	108	133	149
50:50 Virgin-Recycled PP Fibre (Line)	Median	56	99	160	201	225
	Standard deviation	10.0	20.9	36.8	47.7	54.2
Recycled PP Fibre (Diamond)	Median	48	80	141	184	213
	Standard deviation	3.7	6.5	12.3	17.1	20.5
5:95 HDPE-Recycled PP Fibre (Diamond)	Median	47	83	145	187	217
	Standard deviation	1.7	3.7	8.1	10.9	13.5

Fig. 5.9 shows fracture surfaces of the PP fibre reinforced concrete panels. As can be seen, for line-indent PP fibres (Fig. 5.9.a), including the Virgin PP fibre (Line) and 50:50 Virgin-Recycled PP Fibre (Line), nearly all the fibres were pulled out instead of breaking, owing to their high tensile strength and poor bonding with the concrete. For the diamond-indent PP fibres, namely, Recycled PP Fibre (Diamond), and 5:95 HDPE-

Recycled PP Fibre (Diamond), more fibres were broken than pulled out (Fig. 5.9.b). This shows that diamond indents are more effective than line indent to improve bonding of fibres with concrete. The broken fibres fully exploited their tensile capacity, thus producing better reinforcement than the Virgin PP fibre (Line).

Therefore, the reinforcement of the fibres in concrete is determined by tensile strength, Young's modulus and surface indents of fibres. The diamond-indent PP fibres, including Recycled PP Fibre (Diamond), and 5:95 HDPE-Recycled PP Fibre (Diamond), had a good balance of tensile strength, Young's modulus and surface indents. In the standard mix design of 40 MPa concrete for footpath applications, the diamond-indent PP fibres produced more brilliant post-cracking reinforcement than the commonly used Virgin PP Fibre (Line), proving their industrial feasibility.

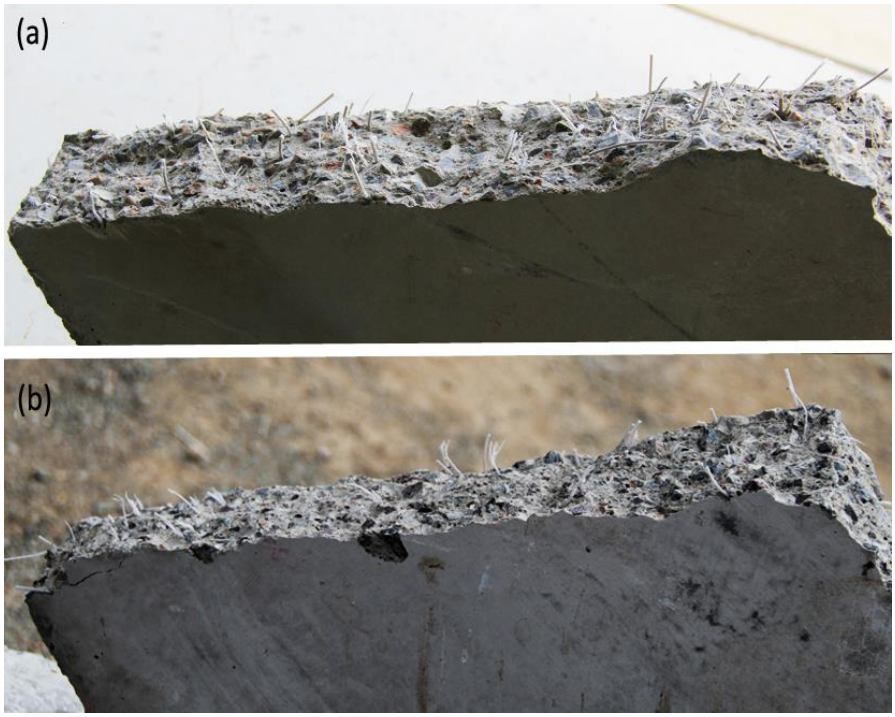

Fig. 5.9 Fracture faces of the PP fibres reinforced concrete round determinate panels: (a) line-indent PP fibre, and (b) diamond-indent PP fibre

5.4. Conclusions

1. Recycled PP fibres produced through an improved melt spinning and hot drawing process. The Recycled PP Fibre (Line) showed lower tensile strength but higher Young's modulus than the Virgin PP Fibre (Line), while the tensile strength of the recycled PP fibre could be significantly improved by mixing 50% virgin PP, as 50:50 Virgin-Recycled PP Fibre (Line).

2. The fibre with diamond indents, such as Recycled PP Fibre (diamond), had much higher Young's modulus than line-indent fibre, like Recycled PP Fibre (Line). HDPE could increase ductility of the recycled fibre, as seen in the results from 5:95 HDPE-Recycled PP Fibre (Diamond).

3. Due to the relatively low dosage of fibres (4 kg/m^3) in the concrete matrix, the compressive strength of concrete was not influenced by the presence of fibres. However, the PP fibre reinforced concrete cylinders failed with many minor cracks on the surface, showing a more ductile mode of failure.

4. In the CMOD and RDPT, the line-indent fibres were pulled out instead of being broken, indicating their poor bonding with the concrete. Since the fibres were not broken, the fibres did not reach their ultimate tensile capacity. The reinforcement of line-indent PP fibres mainly depends on their Young's modulus.

5. In the CMOD and RDPT, more diamond-indent fibres were broken than the fibres pulled out, indicating that the diamond indents had a better bonding with the concrete. The broken PP fibres fully exploited their tensile capacity, thus producing a better reinforcement than the line-indent PP fibres. The reinforcement of diamond-indent PP fibres depends on both their Young's modulus and tensile strength.

6. The diamond-indent fibres, including Recycled PP Fibre (Diamond) and 5:95 HDPE-Recycled PP Fibre (Diamond), had a good balance of tensile strength, Young's modulus and surface indents, thus showing brilliant post-cracking

reinforcement in the concrete. This shows that these recycled fibres have performance in par with the virgin plastic fibres and hence, can be used to replace steel mesh in concrete footpaths.

Chapter 6 Environmental Benefits of Using Recycled PP Fibre through a Life Cycle Assessment

Publication

S. Yin, R. Tuladhar, M. Sheehan, M. Combe, T. Collister. A life cycle assessment of recycled polypropylene fibre in concrete footpaths. Journal of Cleaner Production. 2016, 112(4): 2231-2242.

In order to help decision makers choose reinforcing material that causes the lowest environmental impact, it is very important to carry out a comparative impact analysis. There are a variety of general and industry specific assessment methods, such as GMP-RAM (Jesus et al., 2006), INOVA Systems (Jesus-Hitzschky, 2007), and fuzzy logic environmental impact assessment method (Afrinaldi and Zhang, 2014). However, life cycle assessment (LCA) is the most comprehensive among the available tools and has been widely used. The LCA methodology is generally considered the best environmental management tool for quantifying and comparing the eco-performance of alternative products.

Perugini et al. (2005) undertook LCA of recycled Italian household plastic packaging waste and compared environmental performance with conventional options. Their results confirmed that recycling scenarios were always preferable to those of non-recycling. Arena et al. (2003) studied the collection and mechanical recycling of post-consumer polyethylene (PE) and polyethylene terephthalate (PET) containers. They found that the recycled PET can reduce energy by between 29% and 45%, compared to virgin PET production. Similar reductions in energy use were observed for recycled PE compared to virgin PE. Shen et al. (2010) also assessed the environmental impact of PET bottle-to-fibre recycling, and LCA results showed that recycled PET fibres offered important environmental benefits over virgin PET fibre.

Although these studies show promise, the literature on LCA of recycling plastic waste are actually very limited, and are strongly influenced by final product types, plastic

sources, and by local characteristics of procedures for collecting and reprocessing plastic waste. Hence, these studies cannot be extrapolated to Australian conditions, where there is limited information on comparative LCA of recycling plastic waste. Moreover, recycling systems are typically multifunctional, which can constitute a challenge for LCA practitioners. LCAs of the same product can arrive at different conclusions when there are methodological differences or differences in life cycle inventory (LCI) data. It is therefore important to clearly define the scope, LCA methodology, inventory data sources, and functional unit (FU) involved. These issues are discussed in greater detail by Sandin et al. (2014).

This chapter focuses on the use of PP fibres in reinforcing footpaths where currently steel reinforcing mesh (SRM) is used. Chapter 4 and 5 clearly showed that the recycled PP fibre has sufficient strength to be used as a replacement for virgin PP fibre, which has already been used to replace SRM in footpath applications. The recycled PP fibre considered is sourced from industrial PP wastes, which are scrap off-cuts and off-specification items from the nappy manufacturing industry. An alternative source of recycled plastic fibre is domestic PP waste, consisting mostly of packaging materials from kerbside recycling collections. Recycled PP fibre from domestic waste has not been used in the footpath applications, mainly because of higher reprocessing cost and lower fibre strength. However, it is still worth considering the life cycle impact of using domestic recycled PP fibre in footpath applications.

The objective of this chapter is to quantify the life cycle environmental benefits brought about by using 100% recycled PP fibres from domestic and industrial waste as compared to using typical materials for reinforcing concrete footpaths. Alternative reinforcing materials assessed include virgin PP fibre and SRM. This study is based on Australian conditions and quantifies the environmental impacts in terms of material consumption, water use, and emissions to the environment. The scope of this study is limited to the first stage of the fibre or SRM reinforced footpaths, namely, the production of PP fibres and SRM. The primary audience for this study is intended to be local governments, city councils, solid waste planners, and industries, such as plastic waste recycling and plastic fibre reinforced concrete industries, who are interested in pursuing positive economic and environmental outcomes.

6.1. Life Cycle Assessment Process

6.1.1. Functional Unit and Scenario Formulations

Following the international standards, including ISO 14040: 2006 - Principles and framework (ISO14040, 2006), and ISO 14044: 2006 - Requirements and guidelines (ISO14044, 2006), LCA addresses the environmental aspects and potential environmental impacts throughout a product's life cycle from raw material acquisition through production, use, end-of-life treatment, recycling and final disposal.

The FU yields 40 kg of PP fibres and 364 kg of SRM, necessary to achieve the same degree of reinforcing in 100 mm thick concrete footpaths of area 10 m x 10 m. According to AS 3600-2009 (AS, 2009) for 100 m^2 of concrete footpath (100 mm thick) reinforced with Class L SRM, seven sheets of SL82 SRM (6 m × 2.4 m) are needed. The SL82 SRM consists of 7.6 mm steel bars at 200 mm spacing in both directions (Fig. 6.1.c). One SRM sheet weighs 52 kg. Alternatively, 4 kg/m^3 of PP fibres by volume (equivalent to 4 kg PP fibre per cubic meter of concrete) are found to be able to produce equivalent reinforcing effects to that of the SRM (Cengiz and Turanli, 2004). The PP fibres (Fig. 6.1.a and b) have a thickness of 0.7 mm, a width of 1.5 mm and a length of 47 mm.

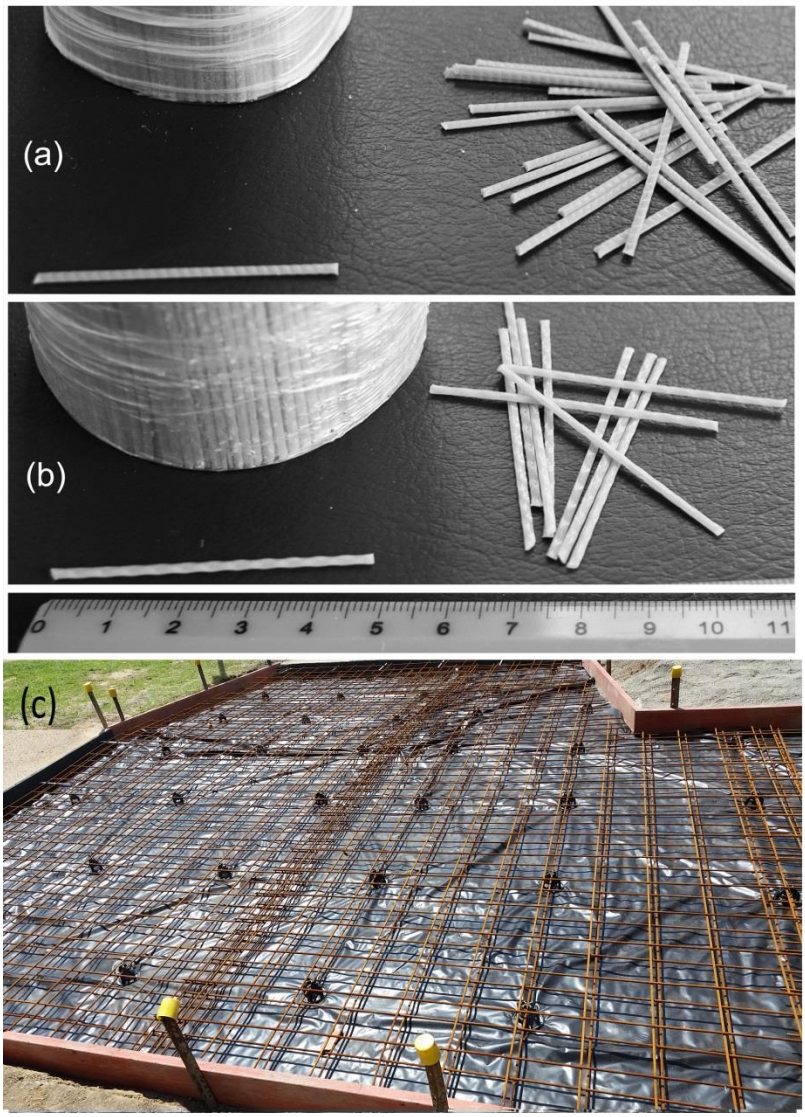

Fig. 6.1 Virgin PP fibre (a), 100% recycled PP fibre (b), and SL 82 SRM (c).

The study set out herein was carried out to compare four scenarios with equal reinforcing effects in 100 m^2 of concrete footpath:

Scenario a: Production of seven SL82 SRM (364 kg of total weight) using electric arc furnaces and basic oxygen furnace.

Scenario b: Virgin PP fibre production. 40 kg of virgin PP fibre produced from 42 kg of virgin raw materials using traditional extrusion process. 2 kg of waste produced during the fibre production is landfilled.

Scenario c: Industrial recycled PP fibre (100% recycled fibre), which refers to mechanically recycling industrial PP waste into recycled PP fibre. In order to get 40 kg

of recycled PP fibre, 46.5 kg of industrial PP waste is collected (taking into account manufacturing efficiency provided by Martogg Group and Danbar Plastic). During the processing of 46.5 kg of industrial waste, 6.5 kg of processing waste is landfilled.

Scenario d: Domestic recycled PP fibre (100% recycled fibre), which is produced from mechanically recycling domestic PP waste into PP fibre. Taking into account manufacturing efficiency according to the research of Chilton et al. (2010), Perugini et al. (2005), Arena et al. (2003), SimaPro 8.0 Australian LCA databases (Grant and Grant, 2011b, e) and on-site investigation, 68 kg of domestic plastic waste needs to be collected to obtain 40 kg of recycled PP fibre, 28 kg of waste produced during processing is considered to be landfilled.

6.1.2. System Boundaries

The scope of this cradle to gate LCA study is limited to the production of SRM, virgin fibre, and recycled fibres (industrial and domestic), and does not include environmental impact of end-of-life disposal of the concrete footpaths. The scope is limited to the first stages since it is assumed that the four scenarios have similar disposal procedures and lifespans in the Australian context.

For scenarios a and b (SRM and virgin PP fibre), system boundaries include all steps from the extraction and transportation of raw materials and fuels, followed by all conversion steps until the products are delivered at the factory gate. The system boundaries of scenarios b and c in this study begin with industrial and domestic PP waste products, and end at the point that they become fit for purpose recycled PP fibres. The upstream processes leading to the production of the PP waste are not included in order to avoid allocations. Labour and capital goods required in the process are not considered, because the analysis is focussed on environmental rather than economic impacts.

6.1.2.1. Steel Reinforcing Mesh

Fig. 6.2, taken from Australian Building Products LCI (BPIC, 2010), shows the production process of SRM and its system boundary. According to Strezov and

Herbertson (2006), around 93% of SRM is produced by electric arc furnaces (EAF) and the remaining is produced by basic oxygen furnaces (BOF). The EAF process produces 9% of slag and the BOF process produces 8% of slag, according to Australian building products LCI (BPIC, 2010). The iron obtained from EAF and BOF is continuously casted, milled and cold rolled into steel bars. At this stage 20% of steel scrap is reused in the BOF or EAF processes. The milled steel bars are then cut, bent and resistance welded into SRM (ZCBL, 2013). The cutting, bending and welding processes are mainly carried out by manual labour, and the electricity used in these processes is negligible compared to the BOF, EAF and casting processes. Hence the environmental impacts of these processes are not considered. GHG (such as CO_2), emissions causing eutrophication (such as NO_x), toxic gases (such as SO_2), particulate matter with 10 micrometers or less in diameter (PM10), and solid and liquid wastes are generated. The environmental impacts of BOF, EAF, casting and milling steel, and transportation are calculated using the SimaPro 8.0 databases (Associates and Sylvatica, 2004a, b; Grant and Grant, 2011a; Spielmann, 2012; Steiner, 2008).

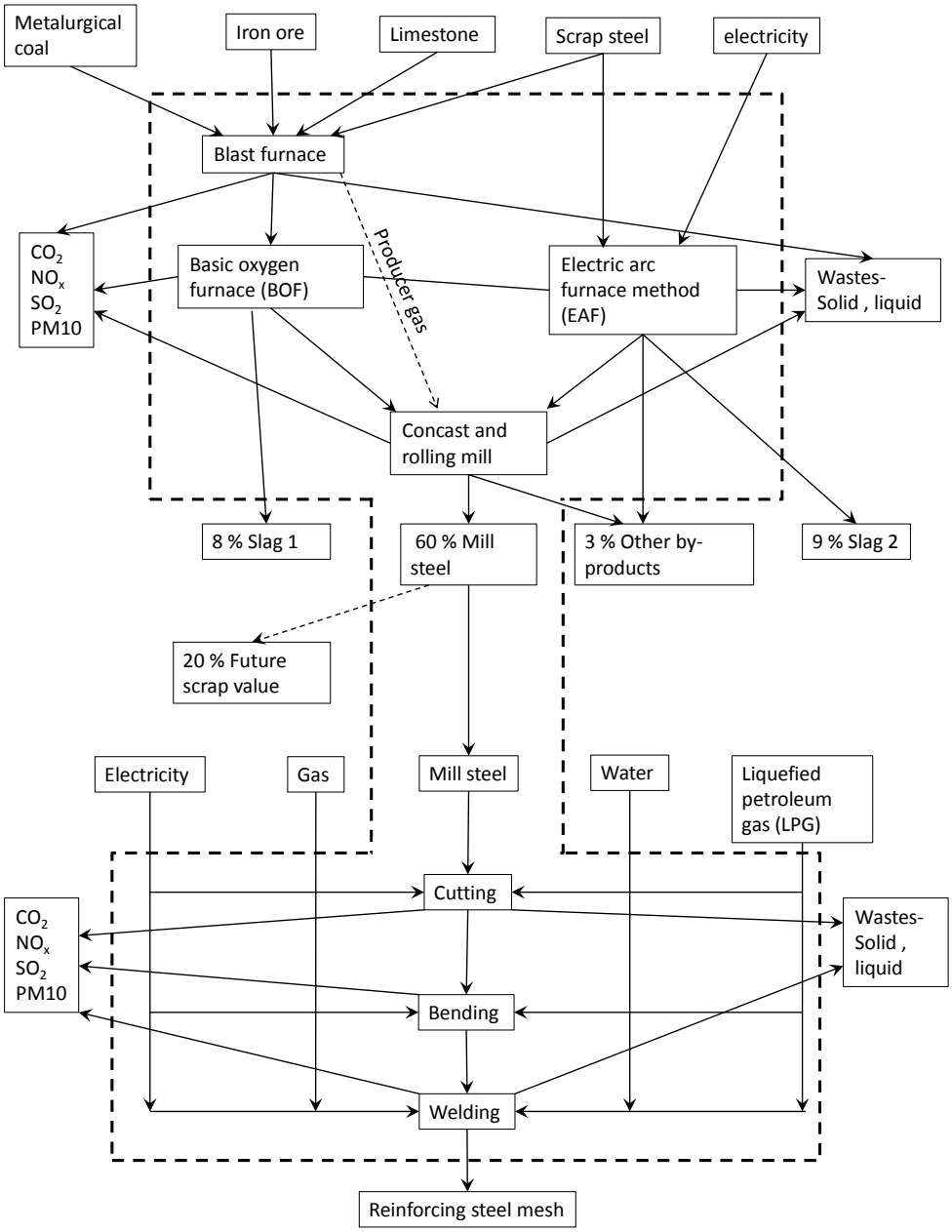

Fig. 6.2 Flow sheet of the production of SRM in traditional methods and the system boundary (BPIC, 2010).

6.1.2.2. Virgin PP Fibre

The virgin PP is produced commercially from olefin monomers (propylene). Two techniques (liquid propylene pool process and gas phase polymerisation) are normally used for the production of PP in Australia (LyondellBasell, 2012). Three main virgin PP granulate manufacturers (Kemcor Resins, Montell Clyde and Montell Geelong) form the basis of the Australasian Unit Process LCI data available in the SimaPro 8.0

database (Grant and Grant, 2011d). As shown in Fig. 6.3, Kemcor Resins extracts propylene from gasoil, while Montell Clyde extracts propylene through catalytic cracking from naphtha. Montell Geelong extrudes propylene from both gasoil and naphtha. The mass allocation splitting PP production across these three plants is 19%, 44% and 37%, respectively. The virgin fibre production process from virgin PP granulates is assumed to be the same as the production of recycled PP fibres.

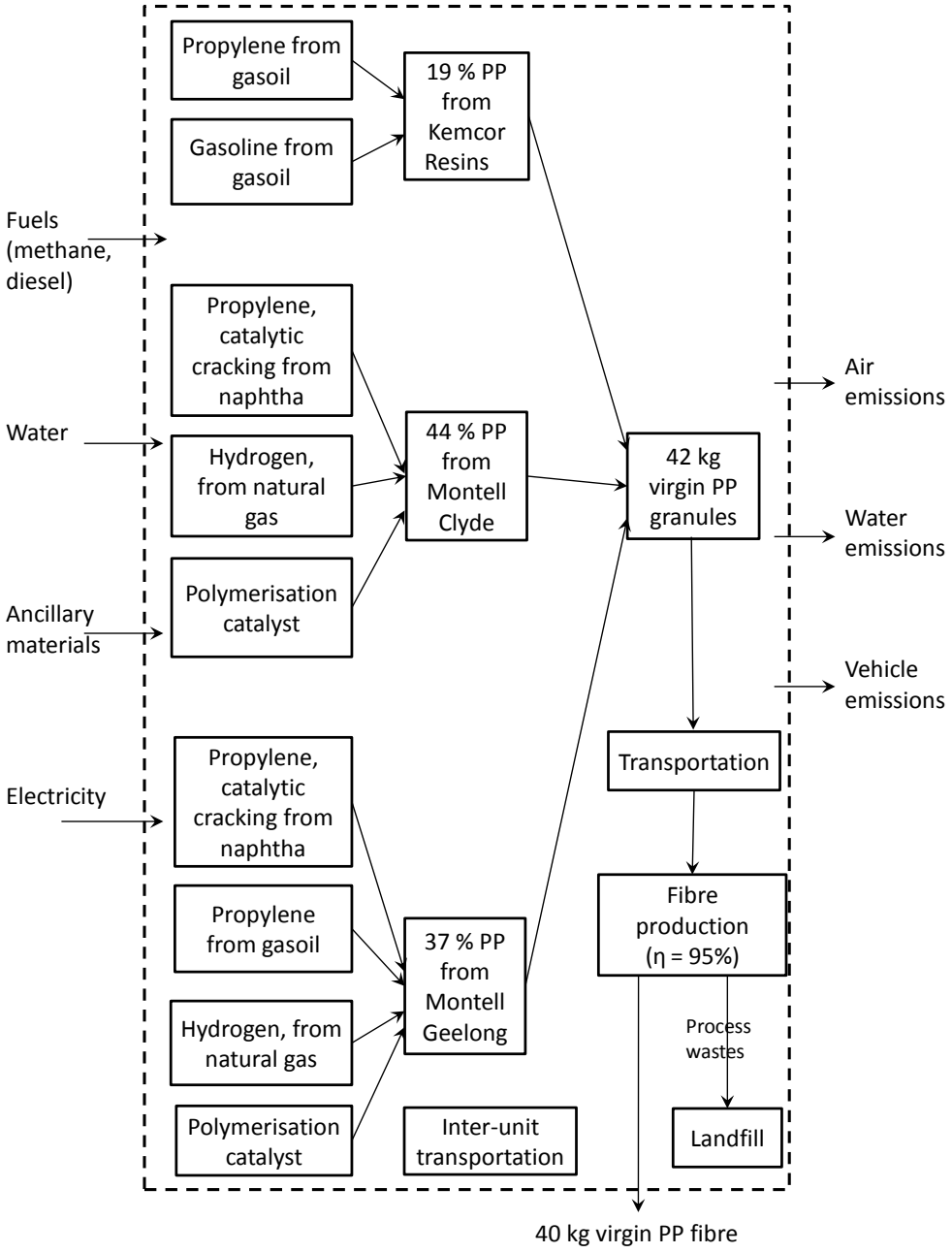

Fig. 6.3 Flow sheet of the production of virgin PP fibre in traditional methods and the system boundary.

6.1.2.3. Industrial Recycled PP Fibre

A diagram of the processes required in the production of industrial recycled PP fibre is shown in Fig. 6.4. The industrial PP waste are first compacted and then transported to a PP reprocessing plant by rigid trucks. The transport distance is on average 75 km. The collected industrial PP waste are shredded and recompounded in the PP reprocessing plant. The efficiency of both shredding and recompounding processes, as obtained directly from the reprocessing plant, is around 95%. The machine generates about 800 kg of the recycled material per hour, and the energy consumption on the reclaim line is roughly 280 kWh. The processed PP granulates are then transported about 55 km to a collection centre, and finally transported a further 100 km to a fibre production plant. The processing and transportation data were collected from the manager of the PP reprocessing plant (Martogg Group, Australia).

For the plastic fibre manufacturing process, an on-site investigation was carried out. The manufacturing process considered in this study includes PP granulates extrusion, PP fibre drawing and stabilisation, and fibre cutting and packing. In this process, the plastic granulates are vacuumed into an extruder, and then stretched and stabilised in ovens at 110-170 ^{o}C. The fibres are then cut into a length of 30-70 mm and packed. The majority of waste is generated during the cutting process (approximately 5%). The electricity consumption in the PP fibre manufacturing process is obtained through actual electricity bills from the plastic processing plant data. According to the data, 1445 kWh are used to produce one tonne of PP fibres. Fig. 6.4 also shows the system boundary of the LCA study for the recycled PP fibre. Information was collected from on-site investigation of Danbar Plastic, and communication with the managers of Martogg Group and Danbar Plastic. The environmental impacts of production of industrial recycled PP fibre were obtained by including this collected data within SimaPro 8.0 (LCS, 2014). The calculations are based on Australian databases (Grant, 2011a, b, 2012; Grant and Grant, 2011c) and Australian Indicator Set V3.00 method (SimaPro, 2010).

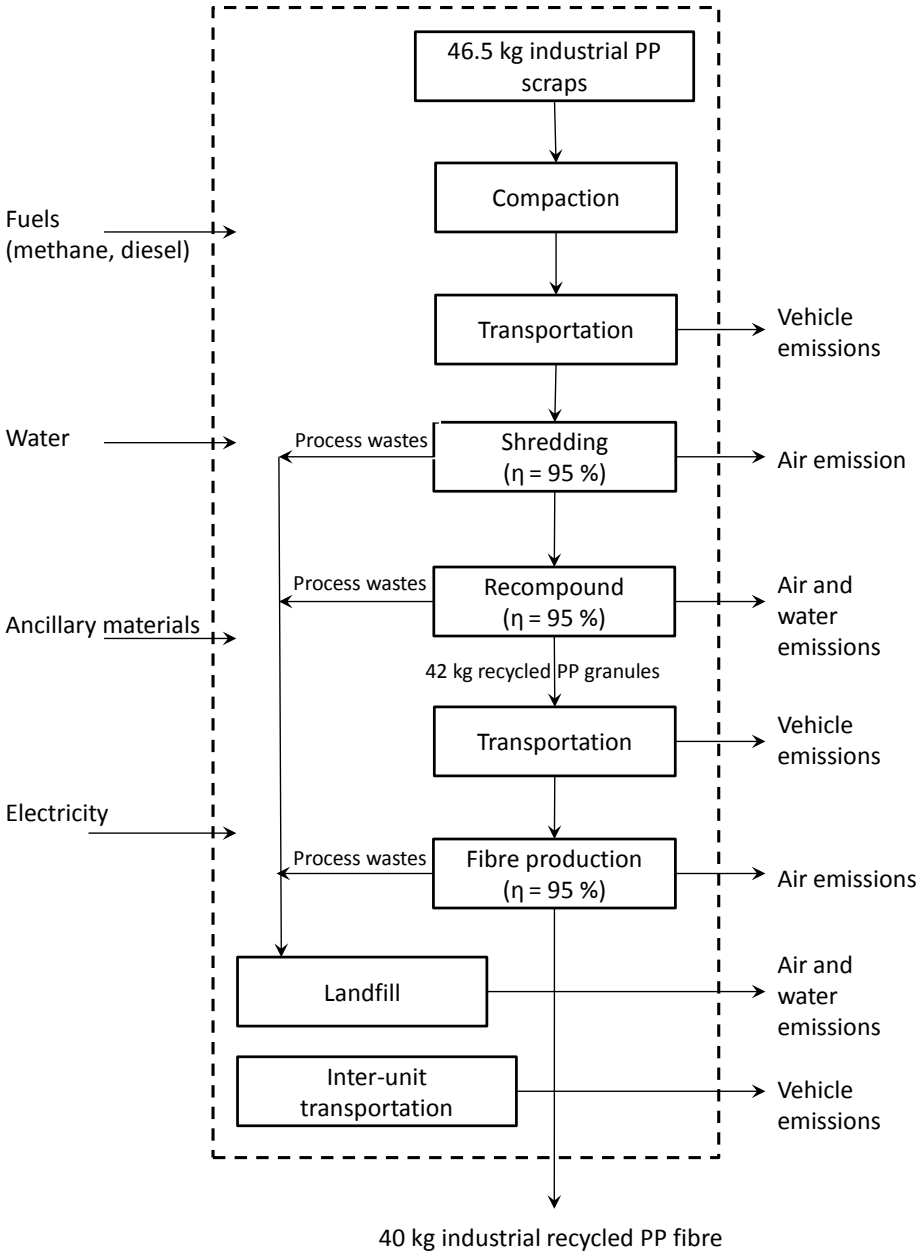

Fig. 6.4 Flow sheet of the production of recycled PP fibre from pre-consumer industrial PP wastes and the system boundary.

6.1.2.4. Domestic Recycled PP Fibre

Fig. 6.5 shows the flow of production of recycled PP fibre from domestic PP waste and its system boundary. The domestic recyclables are collected from kerbside bins every fortnight by local materials recovery facility (MRF) workers. Mixed recyclables are sorted in the MRF. The sorted plastic wastes are sent to plastic reprocessing plants, where manual and mechanical sorting is undertaken to separate out plastic bottles.

Plastics are then shredded and milled into flakes, before being washed in sodium hydroxide solution at 60 ℃. The PP fragments are then separated from other plastics (e.g. PET) based on density differences in a water tank. After centrifugation and drying, the PP fragments are extruded and recompounded into small granulates for future fibre production. The processing steps described here for domestic plastic waste are taken from the SimaPro databases for Australian PP reprocessing and recycling (Grant and Grant, 2011b, e), and relevant scientific publications (Arena et al., 2003; Shen et al., 2010). The MRF sorting efficiency is taken as 70%, based on a Townsville MRF plant and Perugini et al. (2005). The PP reprocessing efficiency is based on Perugini et al. (2005). The transportation and fibre production process are assumed to be same as those used for industrial recycled PP fibre.

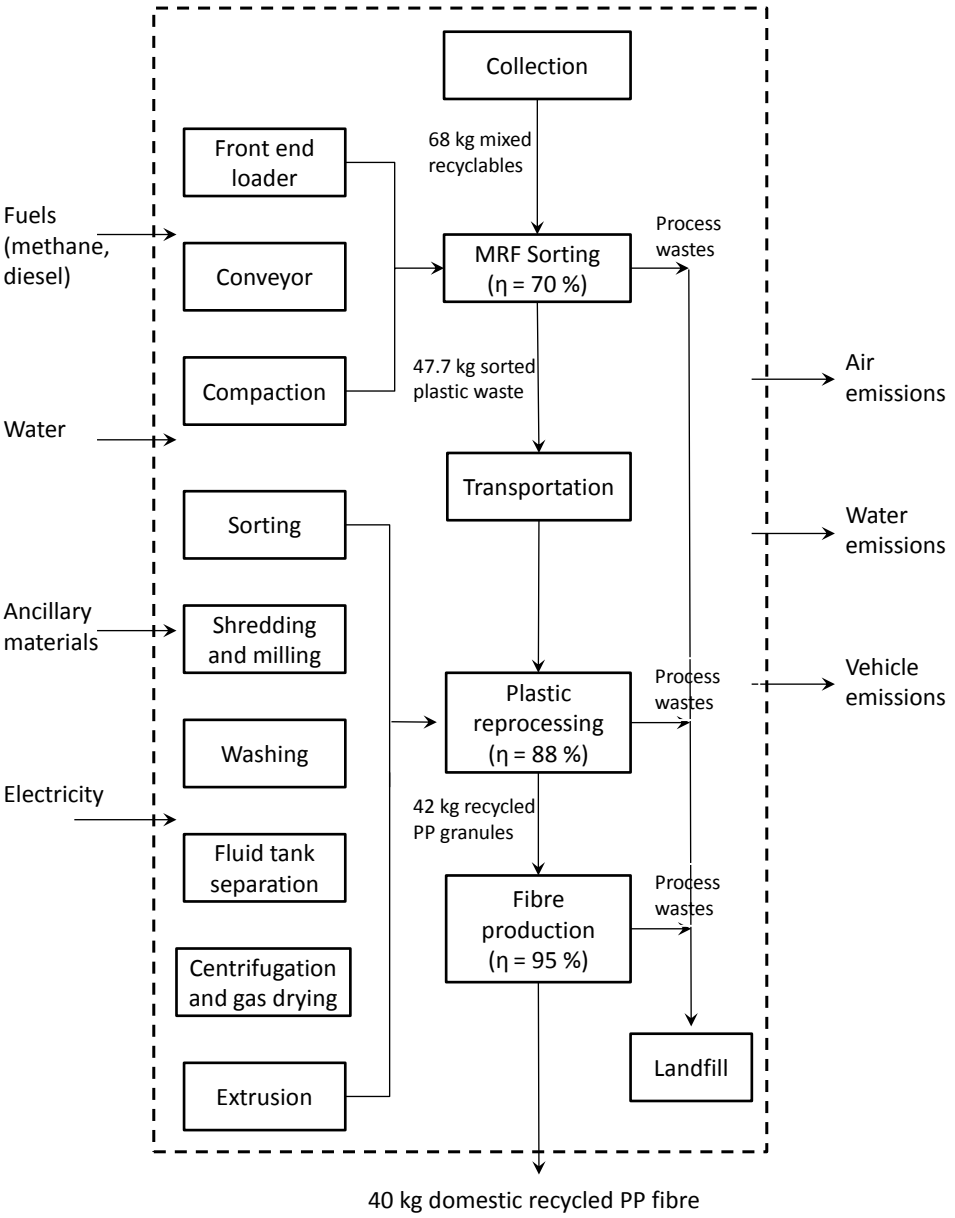

Fig. 6.5 Flow sheet of the production of recycled PP fibre from municipal PP wastes and the system boundary.

6.1.3. Life Cycle Inventory

The LCI data used in this study was obtained through cooperation with many companies, including Materials Recovery Facility, plastic waste reprocessing plants, the fibre production factory, and inventory databases such as SimaPro 8.0 Australian LCA databases (Associates and Sylvatica, 2004a, b; Grant, 2011a, b, 2012; Grant and Grant, 2011a, b, c, d, e; Spielmann, 2012; Steiner, 2008), Building Products LCI databases

(BPIC, 2010) and scientific publications (Arena et al., 2003; Chilton et al., 2010; Perugini et al., 2005; Shen et al., 2010; Strezov and Herbertson, 2006). These details are specifically outlined in Table 6.1.

Table 6.1 Summary of data sources used for the LCI phase

Data	Sources
Domestic PP waste collection	• On-site investigation and communication with a manager in Visy recycling-Townsville MRF (2012) • Scientific publications: Chilton et al. (2010) • Simapro 8.0 database, Australasian Unit Process LCI Library, Kerbside Collection of Mixed Recyclables (Grant and Grant, 2011b)
Domestic PP waste reprocessing	• Scientific publications: Perugini et al. (2005) and Arena et al. (2003) • Simapro 8.0 database, Australasian Unit Process LCI Library, Reprocessing PP from MRF's for Use in as Recycled Granulate (Grant and Grant, 2011e)
Industrial PP reprocessing	• Communication with a manager of Martogg Group (2013) • Simapro 8.0 database, AusLCI unit process library, Low voltage electricity (Grant, 2012)
Virgin PP granulates production	• Simapro 8.0 database, Australasian Unit Process LCI Library, Polypropylene Production Australian Average (Grant and Grant, 2011d)
PP granulates transportation	• Scientific publications: Shen et al. (2010) • Communication with the manager of Martogg Group to get actual transportation distances and vehicle types (2013) • Simapro 8.0 database, Australasian Unit Process LCI Library, Rigid Truck Transport in Australia (Grant, 2011b), Articulated Truck Transport (Grant, 2011a)
PP fibre production	• On-site investigation, checking real electricity bills to get electricity consumption, and communication with a manager in Danbar Plastic (2013) • Simapro 8.0 database, AusLCI Unit Process Library, Low Voltage Electricity (Grant, 2012)
Plastic waste landfilling	• Scientific publications: Perugini et al. (2005) and Arena et al. (2003) • Simapro 8.0 database, Australasian Unit Process LCI Library, LCI of 1000kg Plastic in Landfill (Grant and Grant, 2011c)
Steel production	• Communication with an executive director of Steel Reinforcement Institution of Australia (SRIA) • Scientific publications: Strezov and Herbertson (2006) • Building Products LCI from Australian Building Products

	Innovation Council, SRM (BPIC, 2010) • LCA databases Simapro 8.0 database, Franklin USA 98 library, Steel from Basic Oxygen Furnace (Associates and Sylvatica, 2004b), Cold-rolled steel sheet from Electric Arc Furnace (Associates and Sylvatica, 2004a)
Concast and rolling mill	• Communication with an executive director of SRIA • Building Products LCI form Australian Building Products Innovation Council, SRM (BPIC, 2010) • Simapro 8.0 database, Ecoinvent Unit Processes Library, Milling Steel (Steiner, 2008)
Mill steel transportation	• Communication with an executive director of SRIA • Scientific publications: Strezov and Herbertson (2006) • Building Products LCI form Australian Building Products Innovation Council, SRM (BPIC, 2010) • LCA databases Simapro 8.0 database, Australasian Unit Process LCI Library, Domestic Shipping in Australia (Grant and Grant, 2011a); AusLCI Unit Process Library, Lorry >32t (Spielmann, 2012)
SRM production	• Communication with an executive director of SRIA • Building Products LCI form Australian Building Products Innovation Council, SRM (BPIC, 2010)

6.1.4. Life Cycle Impact Assessment

The software SimaPro 8.0 has been used for the LCIA. All the LCIA data of the four scenarios, including all emissions released and all raw material requirements, are converted into environmental impact categories based on the Australian Indicator Set V3.00 (SimaPro, 2010). Impacts categories examined include CO_2 equivalent, PO_4 equivalent, water use and oil equivalent.

The processes of iron production, steel continuous casting and milling, virgin PP production, plastic waste collecting and recycling, and fibre production consume large amounts of primary energy and electricity. In Australia, the predominant primary energy sources for these processes are coal, oil and diesel, which lead to CO_2 emissions and associated global warming potential (GWP). Carbon dioxide equivalent (kg CO_2 eq) is a standard unit for measuring GWP, and the consumption of fossil fuels is used to assess the depletion of limited natural resources. Water use and water-based pollution are important issues in Australia, because of their scarcity. Water-based impacts can be significant in both steel production and also in domestic

recycling, where washing is an important processing step. In this study both quantity and pollution are assessed. Eutrophication pollution impacts are aggregated into PO_4 equivalent. Water-based toxicity is not assessed because of a scarcity of data in this area.

The CO_2 equivalent (kg) was calculated based on the database of 100-year greenhouse impacts reported by 2009 Intergovernmental Panel on Climate Change method and data (IPCC, 2009). PO_4 equivalent (kg) is based on the model of 2009 Climate Modelling Laboratory impact assessment (Mera, 2009). The consumption of fossil fuels (oil equivalent in kg) are based on 2008 Recipe database (Recipe, 2008).

6.1.5. Uncertainty Analysis

Uncertainty due to methodological choices (e.g. when defining the system boundaries, allocation vs. system expansion) has not been addressed in this study, because it is considered to be beyond the scope. However, the uncertainty in the estimation of environmental impacts associated with LCI raw input data variances was assessed.

In the SimaPro LCI databases, the quantities of required raw materials are stated for each basic process. Paired with each data entry is an estimate of the standard deviation in these raw material quantities. These standard deviations are used to define the range of uncertainty in each quantity. Monte-Carlo simulation, which is a function built into SimaPro 8.0 (LCS, 2014), is used to propagate data base value uncertainty to overall uncertainty across each environmental impact category. In the Monte-Carlo approach, 10,000 runs using random LCI data, generated within 95% confidence interval for each raw material input quantity, are calculated. Uncertainty distributions for each overall impact category are derived from these results. The uncertainty analysis performed is just a first approximation to a more robust analysis (i.e. using primary data) that would more substantially improve the assessment reliability. However, preliminary analysis demonstrates that the uncertainty in the comparative assessment is negligible.

6.2. Results

Fig. 6.6 shows the aggregated environmental impact comparison between recycled and virgin PP fibres across all impact categories. Because the fibre-based scenarios all have similar impact magnitudes, we cluster all fibre-based scenarios together in Fig. 6.6. Since there are orders of magnitude differences between use of any fibre and steel, we have selected the best performing fibre to compare to SRM in Fig. 6.7. As can be seen in Fig. 6.6, the production of industrial recycled PP fibre has minimum impacts on the environment under all categories considered. Generally, virgin PP fibre has higher environmental impacts than either of the recycled fibres, especially in terms of resource consumption.

To produce 40 kg of PP fibres, the industrial recycled fibre life cycle produces 81.7 kg of CO_2 equivalent. As explained in Fig. 6.5, processing of domestic PP waste into fibre needs more complex and energy intensive processes, such as PP waste collection and sorting, PP reprocessing, and fibre production. Hence, the production of domestic PP fibre consumes more energy and produces more CO_2 equivalent (109 kg). For the virgin PP fibre, 137 kg of CO_2 equivalent is predominately associated with the production of PP granulates and PP fibre, and also with propylene production (as Fig. 6.3).

The process used to produce the industrial recycled PP fibre contributes only minor eutrophication impact (0.033 kg of PO_4 equivalent). However, for the domestic recycled PP fibre, the waste washing process emits more significant PO_4 equivalent (0.069 kg of PO_4 equivalent), and leads to higher eutrophication impacts in comparison to industrial recycled PP. It is also interesting to note that despite the comparatively high total volume of water used in producing domestic recycled PP, the eutrophication impact of the waste water is low compared to virgin PP production. For example, the catalytic cracking unit used for virgin propylene production has substantial eutrophication impact in comparison. Overall, the virgin PP fibre production process causes the highest eutrophication impact (0.085 kg of PO_4 equivalent).

When it comes to water consumption, manufacturing domestic recycled PP fibre consumes much more water (0.99 m^3) than producing either industrial recycled PP fibre or virgin PP fibre, which explains the differences in eutrophication impacts between domestic and industrial recycled PP. High water consumption occurs when reprocessing domestic PP waste, because the shredded PP fragments are washed in large volumes of sodium hydroxide solution. After washing, effluent is neutralised, then discharged to domestic sewage. Substantial environmental benefits, including reduced water use and reduced eutrophication impact, could be made, if the effluent was treated and recycled back to the washing process.

In terms of natural resource consumption (in this case fossil fuel), virgin PP fibre production consumes three times more fossil fuel (91.3 kg) than the production of either recycled PP fibres. As well as oil/coal consumed for electricity production, the propylene monomer is extracted through the catalytic cracking of crude oil.

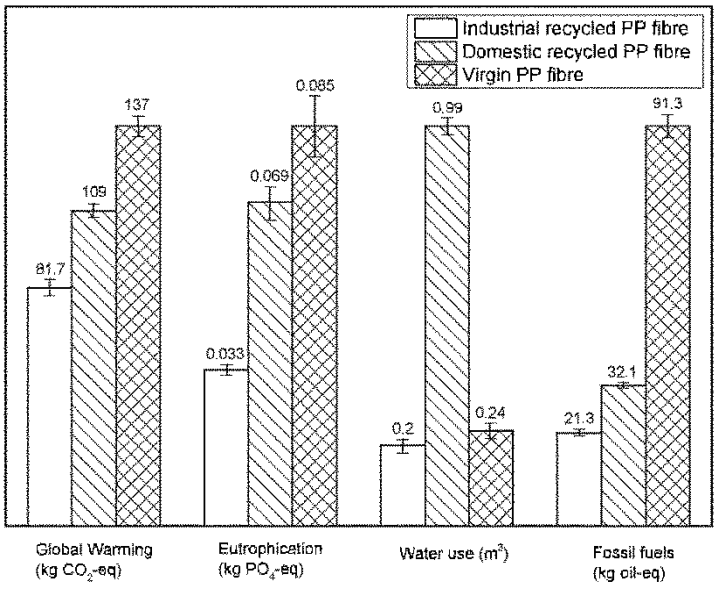

Fig. 6.6 LCIA results from the three scenarios producing 40 kg of PP fibre.

In Fig. 6.7 we compare the environmental impacts of industrial recycled PP fibre with SRM. Across all categories the environmental impacts of producing the industrial recycled PP fibre is negligible in comparison. As shown in Fig. 6.7, the production of 364 kg of SRM emits 15 times the CO_2 equivalent than production of 40 kg of industrial recycled PP fibre. The eutrophication impact of the SRM production is 33 times higher

than that of industrial recycled PP fibre. 20.9 m^3 of water is needed for the production of 364 kg SRM, which is consistent with American government survey results for water use in steel production (Walling and Otts, 1967). The water consumption is 20 times higher than that of even domestic recycled PP fibre. 245 kg of oil equivalent is also needed, which is 11.5 times more than that of industrial recycled PP fibre. Although any PP substitution leads to reduced impacts, comparing the best performing PP fibre process to the SRM, the production of industrial recycled PP fibre can save 93% of CO_2 equivalent, 97% of PO_4 equivalent, 99% of water and 91% of oil equivalent.

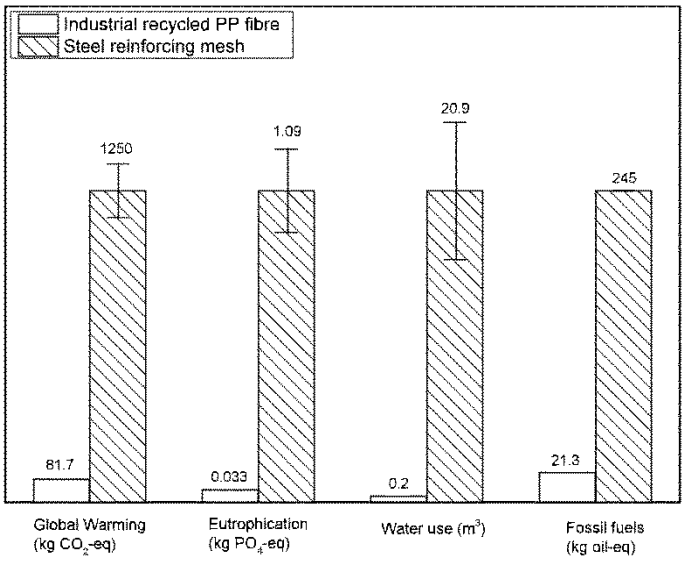

Fig. 6.7 LCIA results of the industrial recycled PP scenario (40 kg of PP fibre) vs. the reinforcing steel scenario (364 kg of SRM).

Uncertainty is an inherent feature of LCA, and it can be caused by multiple reasons: missing inventory data or inventory data inaccuracy; model uncertainty; uncertainty due to choices of allocation rules; impact factors and system boundaries; spatial and temporal variabilities; and epistemological uncertainty. In Figs. 6.6 and 6.7 the uncertainty range per impact category is shown, and expresses the 95% confidence interval. Across all categories except fossil fuel use, SRM shows much greater uncertainties than all other product alternatives, primarily as a result of the larger raw material quantities associated with SRM. This is particularly evident in water use, where uncertainty is very large. For global warming potential and water use, the

recycled and virgin PP fibres show similar degrees of uncertainty. For eutrophication potential, only industrial recycled PP fibre shows a small level of uncertainty, whilst the other fibres are subject to greater uncertainty. This may be the result of limited data describing the variance in input raw materials and output flows associated with industrial recycled PP processing inventory data. However, the impact of uncertainty on the project conclusions is negligible. For the comparative assessment, the impacts of industrial recycled PP fibre are clearly smaller than all other scenarios considered, particularly in comparison to SRM.

Fig. 6.8 shows contribution of major sub-stages to the overall impacts, for each PP production pathway. As can be seen, in the industrial recycled PP fibre production processes, the global warming potential, eutrophication impact, water use and fossil fuel consumption are dominated by the fibre production process. Reprocessing industrial PP waste into recycled PP granulates also gives rise to a substantial proportion of the burdens to environment. For the domestic recycled PP fibre processes, the fibre production process is again the dominant source of impact. However, the domestic waste collection, sorting and reprocessing stages are also significant, and emit considerable CO_2 equivalent and PO_4 equivalent, as well as consuming substantial fossil fuels. Most notably, large amounts of water are needed to wash and separate plastic wastes. Improvements in processing and water recycling at this stage can make domestic recycling more competitive with industrial PP recycling in terms of environmental impacts. For the virgin PP fibre, the production of virgin PP granulates emits considerable CO_2 equivalent and PO_4 equivalent, and consumes significant water. Obviously, substantial fossil fuels are also needed in this sub-stage because crude oil is used as raw material for production of virgin PP granulates. As shown in Fig. 6.8.d, 83% of crude oil use is for monomer production and the remaining 17% is consumed for energy.

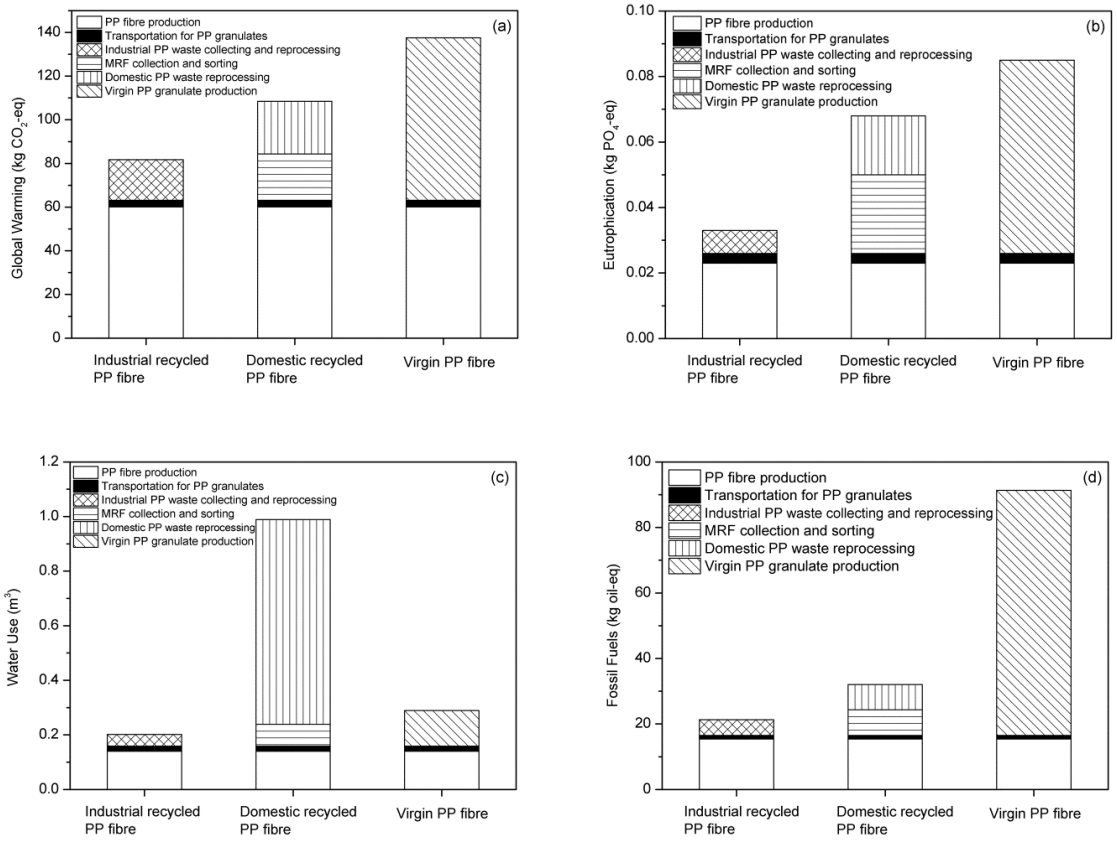

Fig. 6.8 Contribution of major sub-stages for three PP fibre scenarios to the overall impacts within each impact category.

In the production of SRM, the EAF is the main process used to produce iron. In Fig. 6.9, which compares the SRM scenario impacts to the industrial recycled PP scenario, the EAF is energy intensive and emits substantial amounts of CO_2 equivalent and PO_4 equivalent, and also consumes considerable quantity of fossil fuels. Whether iron is produced by EAF or BOF processes, the iron will be continuously casted and roll milled, which also emits significant CO_2 equivalent and PO_4 equivalent. 40% of the total CO_2 equivalent contribution is from EAF, while 52% of the total is from continuous cast and rolling mill processes. 46% of the total eutrophication impact originates during the EAF process and 49% from the continuous cast and rolling mill. Casting and roll milling also require orders of magnitude larger amounts of water. Regarding the use of the fossil fuels, 9% of total consumption is for producing heat in the BOF process, while 89% of total consumption is within the EAF process.

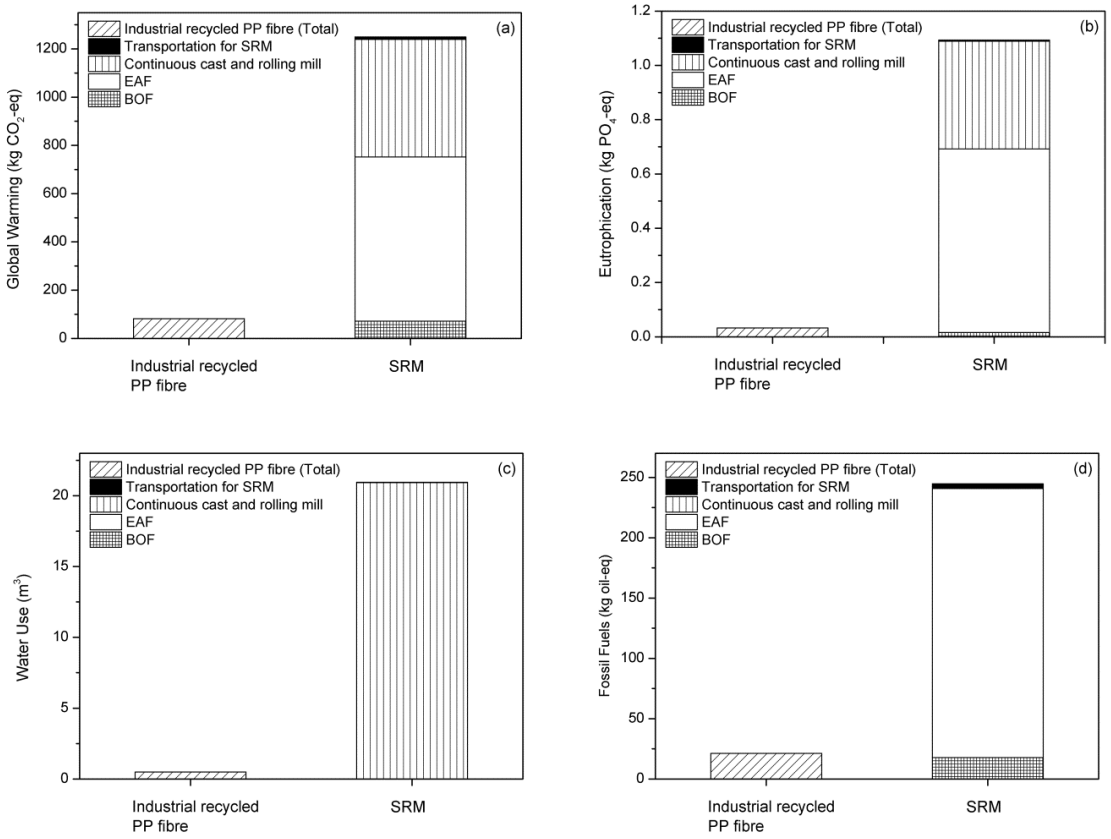

Fig. 6.9 Contribution of major sub-stages for the SRM scenario within each impact category, compared to the total impacts for the industrial recycled PP scenario.

6.3. Discussion

In common with other LCA's of plastic recycling processes, the boundaries of this LCA excluded the end-of-life impacts of the four products. These exclusions include disposal, landfilling, further recycling and reuse, which could provide a longer term view of the impacts. It is well known that in comparison to PP, steel has a lower impact in the disposal stage because of its easy recyclability (Guo et al., 2014). Thus it is reasonable to assume that if end-of-life options were considered, the conclusions of this study could be different. However in Australian context, we do not believe that including end-of-life impacts would alter the final conclusions. Firstly, based on a study of the long term durability of plastic fibres in alkaline environments (EPC, 2012; Roque et al., 2009), all four scenarios would require the same level of maintenance and have equal life spans. Furthermore, despite being easily recycled, end-of-life

concrete footpaths in Australia are almost always landfilled, as sorting and recycling for the small volumes is considered uneconomical. In essence, the processes that would lead to different end-of-life impacts are, in practice, unlikely to occur. We would also argue that the extent of these end-of-life impacts would not be sufficient to make up for the substantial differences that arise during production. Furthermore, because the use of fibres in footpaths is a relatively new application, end-of-life impacts are not well defined. Including these estimates would introduce more uncertainty, and may not be useful for decision makers. However, we would recommend that the potential for water based pollution (i.e. toxicity) associated with PP leaching during the use phase, be more carefully considered.

From a pragmatic point of view, the main objective of this research is to provide decision makers with accurate information on environmental impacts from plastic waste collection stage to the production of recycled PP fibre. This LCA study only considers the environmental impacts of the four products, and it is worth noting that other factors such as costs, markets for recovered products and national and international policy and regulations are not taken into account. Uncertainties regarding the quantities of required raw materials were considered in this study. However, uncertainty accuracy of data and data inventory has not been considered here, thus a more thorough uncertainty analysis using primary data is recommended for future studies.

Since this study is based on the Australian context and Australian inventory data, it is interesting to compare this work with the LCA by Shen et al. (2010), who assessed the impacts of recycled and virgin plastic fibres (PET) in a Western European context. Both studies used the same system boundaries, namely, starting from the point the plastic products become a waste and ending at the point that they become recycled plastic fibres. Although it was not clear if the PET fibres in Shen et al. (2010) were able to be used directly in concrete reinforcing, according to our judgement, the PET fibres would not require additional processing to be fit for purpose. Thus the comparative impacts remain valid and relevant to our study. Collection, sorting, washing, reprocessing, transportation and fibre production were included, but end-of-life impacts were not considered. The results in both studies are very similar, which gives us confidence in

our methodology and sampled data. In comparison, the production of 40 kg domestic recycled plastic fibre in Australia has more global warming impact (109 kg CO_2 eq) and eutrophication impact (0.069 kg PO_4 eq) than those in Western Europe (81 kg CO_2 eq and 0.044 kg PO_4 eq). For the production of 40 kg virgin fibre, the two regions have a similar global warming impact (around 161 kg CO_2 eq), while Australian eutrophication impact (0.095 kg PO_4 eq) is much higher than in Western Europe (0.048 kg PO_4 eq), likely the result of more sophisticated water treatment and recycling initiatives in Western Europe. However, across all impact categories the comparisons between virgin and recycled fibres follow similar trends, and differences in absolute values arise because of local variations. These include differences in collection methods and frequency, transportation infrastructure and distances, as well as differences in the maturity of sorting, reprocessing and fibre production methods. Moreover, the different plastic types considered in these studies also contribute to differences in the calculated impacts.

6.4. Conclusions

1. The LCA results show that the industrial recycled PP fibre offers substantial environmental benefits over all other reinforcing options.

2. The industrial recycled PP fibre can reduce CO_2 equivalent emission by 50%, PO_4 equivalent by 65%, use 29% less water and use 78% less oil equivalent natural resources compared to the virgin PP fibre.

3. The domestic recycled PP fibre offers 32% reduced CO_2 equivalent emissions, 27% reduced PO_4 equivalent emissions, and 67% reduction in oil equivalent resource consumption compared to virgin PP fibre. However, the production of domestic recycled PP fibre consumes 3.5 times more water than the virgin PP fibre due to washing. Improvements in water use can make domestic recycling a more attractive option for sourcing PP fibre.

4. Compared to SRM, the production of industrial recycled PP fibre can save 93% of CO_2 equivalent, 97% of PO_4 equivalent, 99% of water use and 91% of oil equivalent resource use.

5. Across all categories PP fibres show reduced impacts when compared to the use of SRM in concrete footpath applications.

Chapter 7 Applications of 100% Recycled PP Fibre Reinforced Concretes

To showcase the industrial application of 100% recycled PP fibre produced in this research, the fibre performance was tested in various real-life applications which included concrete footpaths and precast concrete pits. This Chapter described the complete process of using recycled PP fibre to replace steel mesh in a concrete footpath, showing the efficiency of using recycled PP fibre. The drying shrinkage cracks in this real application were also assessed. The feasibility of using recycled PP fibre to replace steel mesh in the precast concrete drainage pits was also studied.

7.1 Concrete Footpaths

A footpath is a type of thoroughfare that is intended for use mainly by pedestrians and cyclists. Footpaths usually include alleys, lanes, steps, bridleways, byways, towpaths and green lanes. Steel reinforcing mesh is typically used to reinforce concrete footpaths (Ibrahim, 2011; Shannag and Bin Ziyyad, 2007). Steel reinforcing mesh is a prefabricated steel grid consisting of a series of parallel longitudinal wires welded to cross wires at the required spacing (AS, 2009; ASTM, 2007a, b). Steel mesh improves post-cracking performance of concrete and helps to control plastic and dry shrinkage cracks in concrete footpaths. According to AS 3600-2009 (AS, 2009) concrete footpath are typically reinforced with Class L steel mesh, such as SL82 steel sheets which normally come in 6 m × 2.4 m size. SL82 steel mesh consists of 7.6 mm steel bars at 200 mm spacing in both directions (Fig. 7.1).

Fig. 7.1 Steel reinforcing mesh for concrete footpath

To demonstrate the application of 100% recycled diamond-indent PP fibre in concrete footpath, a footpath with a size of 100 m long and 1.5 m wide was casted in James Cook University in 5th May 2015. The concrete used was of 32 MPa target strength, and the fibre dosage was 4 kg/m^3. Fig. 7.2 shows the processes of casing the concrete footpath. A road roller was used to compact the soil base, before a form work of the footpath was built (Fig. 7.2.a). 4 kg/m^3 of 100% recycled diamond-indent PP fibre was mixed with concrete directly in a concrete truck and delivered to the field. The ready-mixed concrete was poured into the form work directly (Fig. 7.2.b). As shown in Fig. 7.2.c, the PP fibres were evenly dispersed in the concrete. The footpath surface was smoothed as Fig. 7.2.d. The edge of footpath was then smoothed, and the footpath was dummy jointed every 2.5 meters to prevent drying shrinkage cracks (Fig. 7.2.e). Fig. 7.2.f shows the finished footpath in the fresh stage. Standard curing procedure using water spraying was carried out to prevent plastic shrinkage cracks (Fig. 7.2.g). The footpath was ready to use on the third day of casting (Fig. 7.2.h). There were not any challenges in the concrete casting and finishing. Plastic shrinkage cracks did not appear after casting. The footpath has been used for half a year, and there are not any drying shrinkage cracks as well.

(a) Footpath form work and a road roller compacting the soil base

(b) Ready-mixed concrete pouring into the form work

(c) 100% recycled PP fibre dispersing in the fresh concrete

(d) Smoothing the surface of footpath

(e) Edge smoothing and dummy joint

(f) Finished footpath in the fresh stage

(g) Water spraying for curing fresh concrete footpath

(h) Footpath ready to use

Fig. 7.2 Processes of casing concrete footpath

7.2 Precast Concrete Drainage Pits

This section focuses on the successful applications of 100% recycled PP fibres produced in this research in the precast concrete pit project. Due to the intellectual property rights, the names of the industries are omitted.

7.2.1. Materials and Specimens

The testing program was carried out on 6th October 2014. A set of concrete pits with fibres was cast for load testing and another set of current pit designs without fibres was cast as control. This testing program involved load testing a concrete drainage pit base with a riser and a lid in vertical orientation to determine the maximum load capacity. In total four tests were conducted: two fibre reinforced drainage pits and two control steel reinforced drainage pits, as shown in Table 7.1. In this project, 6 kg/m^3 of 100% recycled PP fibre with diamond indents were used. Concrete used was of 50 MPa target strength. Average compressive strength of concrete cylinders measured on the test date was 65 MPa. The tests were conducted at Structural Laboratory in James Cook University, Townsville. The test equipment consisted of a load testing frame, a rubber mat, a hydraulic cylinder, a load cell, and a wood block.

Table 7.1 Details of testing specimens

Specimen name	Date tested	Load orientation	Reinforcement type
Control Pit 1	17/09/2014	Vertical load test	Standard steel reinforcement
Control Pit 2	18/09/2014	Vertical load test	Standard steel reinforcement
Fibre Pit 1	17/09/2014	Vertical load test	6 kg/m^3 recycled PP fibre
Fibre Pit 2	24/09/2014	Vertical load test	6 kg/m^3 recycled PP fibre

7.2.2. Pit Test Setup

The procedure was based on the test procedures used for access chambers (AS 4198 Appendix C and EN 1917 B.4.1 (AS4198, 1994)). The pit base with a 300 mm riser and lid were mounted on the loading frame as shown in Fig. 7.3. The load cell and hydraulic jack were positioned on the centre of lid. Load was applied on a hard wood block of 240 x 240 x 100 mm. A rubber mat of 10 mm to 25 mm thickness was placed on the bottom of the pit base as Fig. 7.3. The load was increased at a rate 1-3 kN per second until it reaches first crack, 80 kN (proof load) and 210 kN (ultimate load) as prescribed by the code. This test was conducted twice for each product design.

Fig. 7.3 Vertical load test assembly

7.2.3. Results and Discussion

Since there was an initial crack already present in the Fibre Pit 1 before testing, the first crack of the pit happened on a lower load of 17 kN at the bottom of pit base, as shown in Table 7.2. The riser did not have initial cracks, so the first crack happened at a higher load of 67.5 kN. For the Fibre Pit 2, the first crack of both base and riser happened on 41.1 kN. The riser had two long cracks at the 41.1 kN, while the base only had a short crack at the top right corner. For Control Pit 1 with steel reinforcement, the first crack of base happened on 26 kN and the riser first cracked on 43 kN, which are similar with the first cracks of both the Fibre Pits. The first crack of the base of Control Pit 2, however, happened at very high load of 120 kN, and the riser first cracked at 152 kN. At the proof load (80 kN), ultimate load (210 kN) and maximum load (330 kN), the steel reinforced pits showed slightly higher displacements at the loading point than those of fibre reinforced pits.

Table 7.2 Vertical load testing results of Fibre and Control Pits

			Displacement of the loading point		
	First crack of base (kN)	First crack of riser (kN)	Displacement at 80 kN (mm)	Displacement at 210 kN (mm)	Displacement at 330 kN (mm)
Fibre Pit 1	17	67.5	6.93	9.84	13.47
Fibre Pit 2	41.1	41.1	7.14	10.73	14.11
Control Pit 1	26	43	9.4	12.51	15
Control Pit 2	120	152	7.87	11.32	13.79

As shown in Fig. 7.4, all the pits have similar load-displacement curves. Due to limited load cell capacity (400 kN), the pits were not crushed to obtain an ultimate load capacity. The pits were loaded up to a maximum load of 330 kN. According to AS 4198 (AS4198, 1994), the ultimate strength requirement for the pits is 210 kN. Therefore, all the pits met the minimum strength requirement, indicating that the recycled PP fibre can be used to replace steel bars in the precast concrete pits.

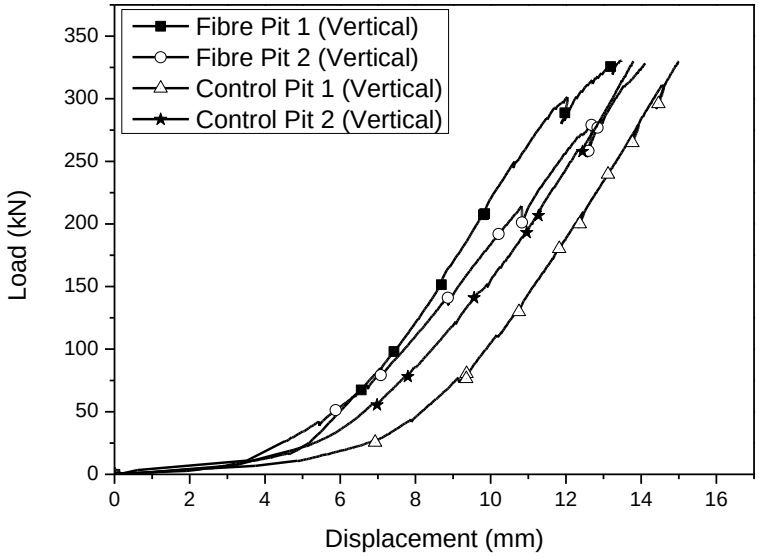

Fig. 7.4 Vertical load testing results of Fibre and Control Pits

Fig. 7.5 showed the crack distributions of the pits after the loading tests. As can been seen, the Fibre Pits exhibited a comparable crack distributions and amounts with those of the Control Pits. The maximum crack width was then measured by inserting the tip of feeler gauge along the crack. The maximum crack width of both fibre and steel mesh reinforced concrete pits was less than 0.05 mm. Except for the minor cracks, no residual deflection, dents, bulges, chips and spalls were found on all the specimens.

Fig 7.5 Crack distributions of (a) Fibre Pit 1, (b) Fibre Pit 2, (c) Control Pit 1 and (d) Control Pit 2 at 330kN vertical load

7.3. Conclusions

1. To demonstrate the application of 100% recycled PP fibre in concrete footpath, a footpath with a size of 100 m long and 1.5 m wide was casted in James Cook University. 4 kg/m^3 of 100% recycled PP fibre was used to fully replace traditionally used steel reinforcing mesh. Since the fibre was directly mixed with the concrete in a concrete truck, the labour work of laying, cutting and tying steel mesh was not required, thus significantly reducing labour work and cost. There were not any challenges in the concrete casting and finishing. Plastic shrinkage cracks did not appear after casting. The footpath has been used for half a year, and there are not any drying shrinkage cracks as well.

2. This research explored the feasibility of using 100% recycled PP fibres in concrete drainage pits to replace steel mesh. The 100% recycled PP fibre reinforced pits showed comparable testing results with the steel mesh reinforced pits in the vertical loading tests. All the pits reached to 330 kN without failing, which is significantly higher than the strength requirement (210 kN), according to AS 4198. The maximum crack width was then measured by inserting the tip of feeler gauge along the crack. The maximum crack width of

both fibre and steel mesh reinforced concrete pits was less than 0.05 mm. Except for the minor cracks, no residual deflection, dents, bulges, chips and spalls were found on all the specimens.

Chapter 8 Conclusions and Recommendations

8.1 Conclusions

In recent years, macro plastic fibres have been widely used to replace traditional steel reinforcement in construction industry due to ease of construction, reduced labour and lower cost. They can effectively improve the performance of concrete such as reducing drying shrinkage and improving post-cracking behaviour of concrete elements. Recycled PP fibres offer significant environmental benefits over virgin PP fibre or steel reinforcement. However, the recycled PP fibres have not yet been widely adopted by construction industry due to limited research and understanding of their mechanical properties, alkali resistance, and performance in concrete. Therefore, this PhD project investigated the production and use of recycled PP fibre to reinforce concrete, and the following important conclusions can be drawn from this research.

1. A melt spinning and hot drawing technique was developed in an industrial scale to produce 100% recycled PP fibre. The 100% recycled PP fibre produced through this technique has slightly lower tensile strength (342 MPa), but much higher Young's modulus (7115 MPa) than those of commercial virgin PP fibre. The results show that the 100% recycled PP fibre can be produced in the industrial scale and has enough capacity to be used in concrete.

2. Durability of the 100% recycled PP fibre in concrete was studied through an alkali resistance test. The results confirmed that the recycled PP fibre has minimum degradation in the concrete alkaline environment and is suitable for application in concrete elements.

3. Performance of the 100% recycled PP fibre in different grades of concrete was studied and compared with the commercial virgin PP fibre. The CMOD and RDPT tests on 40 MPa concrete with 6 kg/m^3 PP fibres (normally used for precast concrete elements) showed that most of the fibres were broken instead of being pulled out at the failure load. This inferred good bonding of fibres with concrete, hence the performance of PP fibres were influenced by

both Young's modulus and tensile strength of fibres. The 100% recycled fibre had higher Young's modulus but lower tensile strength than the virgin PP fibre. Consequently, the 100% recycled PP fibre had slightly lower performance than that of virgin plastic fibre in 40 MPa concrete.

4. In 25 MPa concrete with 4 kg/m^3 of line-indent PP fibres (normally designed for concrete footpaths), majority of fibres were being pulled out instead of breaking in the CMOD and RDPT tests. As the fibres did not reach ultimate tensile strength, its Young's modulus was more influential. The 100% recycled PP fibre had higher Young's modulus and hence, performed better than virgin plastic fibre in 25 MPa concrete. Therefore, the 100% recycled PP fibre can be used to replace commercial virgin PP fibre in the applications of precast concrete elements and concrete footpaths.

5. Performance of different types of recycled PP fibres was then assessed in the 40 MPa concrete. Fibre dosage used for all of the fibre types was 4 kg/m^3, which was based on standard mix design for industrial practice of footpaths. In order to further improve fibre bonding with concrete, a new indentation of diamond shape was made on the fibre surface and compared with the commonly used line indentation. In the CMOD and RDPT tests, diamond-indent 100% recycled PP fibres were mostly broken than line-indent 100% recycled PP fibres, indicating that the diamond indents had a better bonding with the concrete. The broken PP fibres fully exploited their tensile capacity, thus producing a better reinforcement. Therefore, the diamond-indent 100% recycled PP fibre showed more brilliant post-cracking reinforcement in the concrete than that of line-indent 100% recycled PP fibre and virgin PP fibre and hence, can be used to replace SRM in concrete footpaths.

6. The environmental impacts of using 100% recycled PP fibres from domestic and industrial waste to reinforce 100 m^2 of concrete footpath were assessed using a LCA methodology based on Australian context. The impacts were compared to other methods of reinforcing, including the use of virgin PP fibre and SRM. The LCA results show that the industrial recycled PP fibre offers substantial

environmental benefits over all other reinforcing options. The industrial recycled PP fibre can reduce CO_2 equivalent emission by 50%, PO_4 equivalent by 65%, 29% less water and 78% less oil equivalent natural resources compared to the virgin PP fibre. Compared to SRM, the production of industrial recycled PP fibre can save 93% of CO_2 equivalent, 97% of PO_4 equivalent, 99% of water and 91% of oil equivalent.

7. To showcase the industrial application of diamond-indented 100% recycled PP fibre produced in this research, the fibre performance was tested in various real-life applications which included precast concrete pits and concrete footpaths. 6 kg/m^3 of 100% recycled PP fibre reinforced pits showed comparable testing results with the steel mesh reinforced pits in the vertical loading tests. Fibre reinforced sustained 210 kN as required by AS 4198. Furthermore, a 100m long and 1.5m wide concrete footpath was casted in James Cook University. 4 kg/m^3 of diamond-indent 100% recycled PP fibre was used to fully replace traditionally used SRM. Concrete casting and finishing was completed without any difficulty. Plastic shrinkage cracks did not appear after casting. The footpath has been used for half a year, and there are no drying shrinkage cracks as well.

In summary, this research has developed a methodology of producing recycled PP fibres with optimum mechanical properties for reinforcing concrete. The great potential of using these fibres in various concrete applications such as footpaths and precast concrete elements has been shown. This will not only help reduce consumption of virgin materials like steel or plastic but also provides attractive avenue of recycling plastic waste.

8.2 Recommendations

Based on the findings of this study, the following recommendations for further research can be made:

- Investigate creep behaviour of recycled PP fibre in concrete.
- Explore chemical modification of the surface of recycled PP fibre to further improve fibre bonding with concrete.
- Carry out economic life cycle assessment on the recycled PP fibre and compare with traditionally used virgin PP fibre and SRM.
- Explore more applications of recycled PP fibre in other precast concrete elements, and shotcrete mine tunnels.
- Explore the use of other types of recycled plastic fibres such as PET fibres in concrete.

References

544, A.C., 1988. Measurements of properties of fiber reinforced concrete. Aci Mater J 85, 583-593.
A'Vard, D., Allan, P., 2014. 2013-14 National plastics recycling survey. National Packaging Covenant Industry Association, Sustainable Resource Use Pty Ltd, R03-03-A11013. .
Abas, F.M., Gilbert, R.I., Foster, S.J., Bradford, M.A., 2013. Strength and serviceability of continuous composite slabs with deep trapezoidal steel decking and steel fibre reinforced concrete. Eng Struct 49, 866-875.
Abd Aziz, F.N.A., Bida, S.M., Nasir, N.A.M., Jaafar, M.S., 2014. Mechanical properties of lightweight mortar modified with oil palm fruit fibre and tire crumb. Constr Build Mater 73, 544-550.
Achilias, D.S., Antonakou, E., Roupakias, C., Megalokonomos, P., Lappas, A., 2008. Recycling techniques of polyolefins from plastic wastes. Global Nest J 10, 114-122.
Achilleos, C., Hadjimitsis, D., Neocleous, K., Pilakoutas, K., Neophytou, P.O., Kallis, S., 2011. Proportioning of Steel Fibre Reinforced Concrete Mixes for Pavement Construction and Their Impact on Environment and Cost. Sustainability-Basel 3, 965-983.
Afrinaldi, F., Zhang, H.C., 2014. A fuzzy logic based aggregation method for life cycle impact assessment. J Clean Prod 67, 159-172.
Akchurin, M.S., Zakalyukin, R.M., 2013. On the role of twinning in solid-state reactions. Crystallogr Rep+ 58, 458-461.
Al-Mattarneh, H., 2014. Electromagnetic quality control of steel fiber concrete. Constr Build Mater 73, 350-356.
Al-Salem, S.M., Lettieri, P., Baeyens, J., 2009. Recycling and recovery routes of plastic solid waste (PSW): A review. Waste Manage 29, 2625-2643.
Alani, A.M., Beckett, D., 2013. Mechanical properties of a large scale synthetic fibre reinforced concrete ground slab. Constr Build Mater 41, 335-344.
Alavez-Ramirez, R., Montes-Garcia, P., Martinez-Reyes, J., Altamirano-Juarez, D.C., Gochi-Ponce, Y., 2012. The use of sugarcane bagasse ash and lime to improve the durability and mechanical properties of compacted soil blocks. Constr Build Mater 34, 296-305.
Alberti, M.G., Enfedaque, A., Galvez, J.C., 2014. On the mechanical properties and fracture behavior of polyolefin fiber-reinforced self-compacting concrete. Constr Build Mater 55, 274-288.
Ali, M., Chouw, N., 2013. Experimental investigations on coconut-fibre rope tensile strength and pullout from coconut fibre reinforced concrete. Constr Build Mater 41, 681-690.
Andricic, B., Kovacic, T., Klaric, I., 2008. Properties of recycled material containing poly(vinyl chloride), polypropylene, and calcium carbonate nanofiller. Polym Eng Sci 48, 572-577.
Arena, U., Mastellone, M.L., Perugini, F., 2003. Life cycle assessment of a plastic packaging recycling system. Int J Life Cycle Ass 8, 92-98.
AS1012.3.9, 1993. AS 1012.3.9 Workability of Fresh Concrete through Slump Testing. standard Australia.

AS1012.10, 2000. AS 1012.10: Determination of Indirect Tensile Strength of Concrete Cylinders ('Brazil' or Splitting Test). Standard Australia.
AS1012.11, 2000. AS 1012.11. Methods of Testing Concrete: Determination of the Modulus of Rupture. Australian standard.
AS4198, 1994. Precast concrete access chambers for sewerage applications. Standard Australia.
AS, 2009. AS 3600-2009 Concrete Structures. Standard Australia.
AS, 2014a. AS 1012.3.1:2014 Methods of testing concrete - Determination of properties related to the consistency of concrete - Slump test. Standard Australia.
AS, 2014b. AS 1012.8.1:2014 Methods of testing concrete - Method for making and curing concrete - Compression and indirect tensile test specimens. standard Australia.
AS, 2014c. AS 1012.9:2014 Methods of testing concrete - Compressive strength tests - Concrete, mortar and grout specimens. Standard Australia.
Aslani, F., Bastami, M., 2015. Relationship between Deflection and Crack Mouth Opening Displacement of Self-Compacting Concrete Beams with and without Fibers. Mech Adv Mater Struc 22, 956-967.
Associates, F., Sylvatica, 2004a. Cold-rolled steel sheet from Electric Arc Furnace SimaPro 8.0 Database: Franklin USA 98.
Associates, F., Sylvatica, 2004b. Steel from Basic Oxygen Furnace SimaPro 8.0 Database: Franklin USA 98.
ASTM, 1997. ASTM C 1018 Standard test method for flexural strength toughness and first crack strength of fiber reinforced concrete. American Society for Testing and Materials. Book of ASTM Standards.
ASTM, 2007a. ASTM A185/A185M-07 Standard Specification for Steel Welded Wire Reinforcement, Plain, for Concrete. Book of ASTM Standards. Philadelphia; 2007.
ASTM, 2007b. ASTM A497/A497M-07 Standard Specification for Steel Welded Wire Reinforcement, Deformed, for Concrete. Book of ASTM Standards. Philadelphia; 2007.
ASTM, 2007c. ASTM D3822. Standard Test Method for Tensile Properties of Single Textile Fibers. Book of ASTM Standards. Philadelphia.
ASTM, 2008a. ASTM C157 Length Change of Hardened Hydraulic-Cement Mortar and Concrete. American Society for Testing and Materials. Book of ASTM Standards.
ASTM, 2008b. ASTM E1290. Crack-Tip Opening Displacement (CTOD) Fracture Toughness Measurement. American Society for Testing and Materials. Book of ASTM Standards. .
ASTM, 2011a. ASTM C1399 Standard Test Method for Obtaining Average Residual-Strength of Fiber-Reinforced Concrete. Book of ASTM Standards.
ASTM, 2011b. ASTM C1609 Standard Test Method for Flexural Performance of Fiber-Reinforced Concrete (Using Beam With Third-Point Loading). Book of ASTM Standards.
ASTM, 2012. ASTM C1550 - 12a Standard Test Method for Flexural Toughness of Fiber Reinforced Concrete (Using Centrally Loaded Round Panel). American Society for Testing and Materials. Book of ASTM Standards.
Auchey, F.L., 1998. The use of recycled polymer fibres as secondary reinforcement in concrete structures. Journal of Construction Education 3, 131-140.
Aurrekoetxea, J., Sarrionandia, M.A., Urrutibeascoa, I., Maspoch, M.L., 2001. Effects of recycling on the microstructure and the mechanical properties of isotactic polypropylene. J Mater Sci 36, 2607-2613.

Bahlouli, N., Pessey, D., Ahzi, S., Remond, Y., 2006. Mechanical behavior of composite based polypropylene: Recycling and strain rate effects. J Phys Iv 134, 1319-1323.
Banthia, M., Dubey, A., 2000. Measurement of flexural toughness of fiber-reinforced concrete using a novel technique - Part 2: Performance of various composites. Aci Mater J 97, 3-11.
Banthia, N., Dubey, A., 1999. Measurement of flexural toughness of fiber-reinforced concrete using a novel technique - Part 1: Assessment and calibration. Aci Mater J 96, 651-656.
Banthia, N., Gupta, R., 2006. Influence of polypropylene fiber geometry on plastic shrinkage cracking in concrete. Cement Concrete Res 36, 1263-1267.
Banthia, N., Mindess, S., 2004. Toughness characterization of fiber-reinforced concrete: Which standard to use? J Test Eval 32, 138-142.
Banthia, N., Trottier, J.F., 1995. Test Methods for Flexural Toughness Characterization of Fiber-Reinforced Concrete - Some Concerns and a Proposition. Aci Mater J 92, 48-57.
Barr, B., Gettu, R., AlOraimi, S.K.A., Bryars, L.S., 1996. Toughness measurement - The need to think again. Cement Concrete Comp 18, 281-297.
Beglarigale, A., Yazici, H., 2015. Pull-out behavior of steel fiber embedded in flowable RPC and ordinary mortar. Constr Build Mater 75, 255-265.
Bernard, E.S., 2002. Correlations in the behaviour of fibre reinforced shotcrete beam and panel specimens. Mater Struct 35, 156-164.
Berndt, M.L., 2009. Properties of sustainable concrete containing fly ash, slag and recycled concrete aggregate. Constr Build Mater 23, 2606-2613.
Bordelon, A., Cervantes, V., Roesler, J.R., 2009. Fracture properties of concrete containing recycled concrete aggregates. Mag Concrete Res 61, 665-670.
BPIC, 2010. Building Products Life Cycle Inventory www.bpic.asn.au/LCI (assessed by 10/11/2014).
Brachet, P., Hoydal, L.T., Hinrichsen, E.L., Melum, F., 2008. Modification of mechanical properties of recycled polypropylene from post-consumer containers. Waste Manage 28, 2456-2464.
Brandt, A.M., 2008. Fibre reinforced cement-based (FRC) composites after over 40 years of development in building and civil engineering. Compos Struct 86, 3-9.
Brems, A., Baeyens, J., Dewil, R., 2012. Recycling and Recovery of Post-Consumer Plastic Solid Waste in a European Context. Therm Sci 16, 669-685.
Brown, R., Shukla, A., Natarajan, K.R., 2002. Fiber reinforcement of concrete structures. URITC PROJECT NO. 536101.
BSI, 2007. BS EN 14651:2005 +A1:2007. Test method for metallic fibre concrete - Measuring the flexural tensile strength (limit of proportionality (LOP), residual). British Standards Institution.
Buratti, N., Ferracuti, B., Savoia, M., 2013. Concrete crack reduction in tunnel linings by steel fibre-reinforced concretes. Constr Build Mater 44, 249-259.
Buratti, N., Mazzotti, C., Savoia, M., 2011. Post-cracking behaviour of steel and macro-synthetic fibre-reinforced concretes. Constr Build Mater 25, 2713-2722.
Campione, G., 2006. Influence of FRP wrapping techniques on the compressive behavior of concrete prisms. Cement Concrete Comp 28, 497-505.
Cao, M.L., Zhang, C., Lv, H.F., 2014. Mechanical response and shrinkage performance of cementitious composites with a new fiber hybridization. Constr Build Mater 57, 45-52.

Carvalho, A., Mimoso, A.F., Mendes, A.N., Matos, H.A., 2014. From a literature review to a framework for environmental process impact assessment index. J Clean Prod 64, 36-62.
Carvalho, M.T., Ferreira, C., Santos, L.R., Paiva, M.C., 2012. Optimization of froth flotation procedure for poly(ethylene terephthalate) recycling industry. Polym Eng Sci 52, 157-164.
Castro, A.C.M., Carvalho, J.P., Ribeiro, M.C.S., Meixedo, J.P., Silva, F.J.G., Fiuza, A., Dinis, M.L., 2014. An integrated recycling approach for GFRP pultrusion wastes: recycling and reuse assessment into new composite materials using Fuzzy Boolean Nets. J Clean Prod 66, 420-430.
Cengiz, O., Turanli, L., 2004. Comparative evaluation of steel mesh, steel fibre and high-performance polypropylene fibre reinforced shotcrete in panel test. Cement Concrete Res 34, 1357-1364.
Cerqueira, D.A., Rodrigues, G., Assuncao, R.M.N., 2006. A new value for the heat of fusion of a perfect crystal of cellulose acetate. Polym Bull 56, 475-484.
Chaves, L.P., Cunha, J., 2014. Design of carbon fiber reinforcement of concrete slabs using topology optimization. Constr Build Mater 73, 688-698.
Chavooshi, A., Madhoushi, M., 2013. Mechanical and physical properties of aluminum powder/MDF dust/polypropylene composites. Constr Build Mater 44, 214-220.
Chen, H.B., Karger-Kocsis, J., Wu, J.S., Varga, J., 2002. Fracture toughness of alpha- and beta-phase polypropylene homopolymers and random- and block-copolymers. Polymer 43, 6505-6514.
Chilton, T., Burnley, S., Nesaratnam, S., 2010. A life cycle assessment of the closed-loop recycling and thermal recovery of post-consumer PET. Resour Conserv Recy 54, 1241-1249.
Choi, Y., Yuan, R.L., 2005. Experimental relationship between splitting tensile strength and compressive strength of GFRC and PFRC. Cement Concrete Res 35, 1587-1591.
Clemons, C., 2010. Elastomer modified polypropylene-polyethylene blends as matrices for wood flour-plastic composites. Compos Part a-Appl S 41, 1559-1569.
da Costa, H.M., Ramos, V.D., de Oliveira, M.G., 2007. Degradation of polypropylene (PP) during multiple extrusions: Thermal analysis, mechanical properties and analysis of variance. Polym Test 26, 676-684.
da Costa, H.M., Ramos, V.D., Rocha, M.C.G., 2005. Rheological properties of polypropylene during multiple extrusion. Polym Test 24, 86-93.
Dai, Q.L., Wang, Z.G., Hasan, M.R.M., 2013. Investigation of induction healing effects on electrically conductive asphalt mastic and asphalt concrete beams through fracture-healing tests. Constr Build Mater 49, 729-737.
Daniel, J.I., Gopalaratnam, V.S., Galinat, M.A., 2002. State-of-the-art Report on Fiber Reinforced Concrete, ACI Committee 544, Report 544, 1R-96, American Concrete Institute, Detroit, USA.
de Montaignac, R., Massicotte, B., Charron, J.P., Nour, A., 2012. Design of SFRC structural elements: post-cracking tensile strength measurement. Mater Struct 45, 609-622.
de Oliveira, L.A.P., Castro-Gomes, J.P., 2011. Physical and mechanical behaviour of recycled PET fibre reinforced mortar. Constr Build Mater 25, 1712-1717.

Decker, J., Madsen, P., Gall, V., O'Brien, T., 2012. Use of Synthetic, Fiber-Reinforced, Initial Shotcrete Lining at Devil's Slide Tunnel Project in California. Transp Res Record, 147-154.
Demirel, B., Daver, F., 2013. Experimental study of preform reheat temperature in two-stage injection stretch blow molding. Polym Eng Sci 53, 868-873.
Ding, Y.N., 2011. Investigations into the relationship between deflection and crack mouth opening displacement of SFRC beam. Constr Build Mater 25, 2432-2440.
Dodbiba, G., Furuyama, T., Takahashi, K., Sadaki, J., Fujita1), T., 2007. Life Cycle Assessment: A Tool for Evaluating and Comparing Different Treatment Options for Plastic Wastes from Old Television Sets. Data Science Journal 6, S39-S50.
Dodbiba, G., Takahashi, K., Sadaki, J., Fujita, T., 2008. The recycling of plastic wastes from discarded TV sets: comparing energy recovery with mechanical recycling in the context of life cycle assessment. J Clean Prod 16, 458-470.
Dormer, A., Finn, D.P., Ward, P., Cullen, J., 2013. Carbon footprint analysis in plastics manufacturing. J Clean Prod 51, 133-141.
Duval, D., MacLean, H.L., 2007. The role of product information in automotive plastics recycling: a financial and life cycle assessment. J Clean Prod 15, 1158-1168.
El-Ashkar, N.H., Kurtis, K.E., 2006. A new, simple, practical method to characterize toughness of fiber-reinforced cement-based composites. Aci Mater J 103, 33-44.
Elias, M.B., Machado, R., Canevarolo, S.V., 2000. Thermal and dynamic-mechanical characterization of uni- and biaxially oriented polypropylene films. J Therm Anal Calorim 59, 143-155.
EN, B., 2005. BS EN 14651:2005+A1:2007 Test method for metallic fibre concrete. Measuring the flexural tensile strength (limit of proportionality (LOP), residual).
EPC, 2012. Advanced alkalinity testing. Elasto Plastic Concrete. www.elastoplastic.com (assessed by 10/11/2014).
Eriksson, O., Reich, M.C., Frostell, B., Bjorklund, A., Assefa, G., Sundqvist, J.O., Granath, J., Baky, A., Thyselius, L., 2005. Municipal solid waste management from a systems perspective. J Clean Prod 13, 241-252.
Fibercon, 2015. www.fibercon.com.au. (accessed by 25/04/2015).
Foti, D., 2011. Preliminary analysis of concrete reinforced with waste bottles PET fibers. Constr Build Mater 25, 1906-1915.
Foti, D., 2013. Use of recycled waste pet bottles fibers for the reinforcement of concrete. Compos Struct 96, 396-404.
Fraternali, F., Ciancia, V., Chechile, R., Rizzano, G., Feo, L., Incarnato, L., 2011. Experimental study of the thermo-mechanical properties of recycled PET fiber-reinforced concrete. Compos Struct 93, 2368-2374.
Fraternali, F., Farina, I., Polzone, C., Pagliuca, E., Feo, L., 2013. On the use of R-PET strips for the reinforcement of cement mortars. Compos Part B-Eng 46, 207-210.
Fraternali, F., Spadea, S., Berardi, V.P., 2014. Effects of recycled PET fibres on the mechanical properties and seawater curing of Portland cement-based concretes. Constr Build Mater 61, 293-302.
Fuente, A.d.l., Escariz, R.C., Figueiredo, A.D.d., Aguado, A., 2013. Design of macro-synthetic fibre reinforced concrete pipes. Constr Build Mater 43, 523-532.
Gabel, K., Forsberg, P., Tillman, A.M., 2004. The design and building of a life cycle-based process model for simulating environmental performance, product performance and cost in cement manufacturing. J Clean Prod 12, 77-93.

Gallardo, A., Carlos, M., Bovea, M.D., Colomer, F.J., Albarran, F., 2014. Analysis of refuse-derived fuel from the municipal solid waste reject fraction and its compliance with quality standards. J Clean Prod 83, 118-125.
Gonzalez-Gonzalez, V.A., Neira-Velazquez, G., Angulo-Sanchez, J.L., 1998. Polypropylene chain scissions and molecular weight changes in multiple extrusion. Polym Degrad Stabil 60, 33-42.
Gopalaratnam, V.S., Shah, S.P., Batson, G.B., Criswell, M.E., Ramakrishnan, V., Wecharatana, M., 1991. Fracture-Toughness of Fiber Reinforced-Concrete. Aci Mater J 88, 339-353.
Grant, T., 2011a. Articulated Truck Transport SimaPro 8.0 Database: Australasian Unit Process LCI.
Grant, T., 2011b. Rigid Truck Transport in Australia. SimaPro 8.0 Database: Australasian Unit Process LCI.
Grant, T., 2012. Electricity LV. SimaPro 8.0 Database: AusLCI unit process.
Grant, T., Grant, M., 2011a. Domestic Shipping in Australia. SimaPro 8.0 Database: Australasian Unit Process LCI.
Grant, T., Grant, M., 2011b. Kerbside collection of mixed recyclables. SimaPro 8.0 Database: Australasian Unit Process LCI.
Grant, T., Grant, M., 2011c. LCI of 1000kg Plastic in Landfill. SimaPro 8.0 Database: Australasian Unit Process LCI.
Grant, T., Grant, M., 2011d. Polypropene Production Australian Average. SimaPro 8.0 Database: Australasian Unit Process LCI.
Grant, T., Grant, M., 2011e. Reprocessing PP from MRF's for use in as Recycled Granulate. SimaPro 8.0 Database: Australasian Unit Process LCI.
Gregor-Svetec, D., Sluga, F., 2005. High modulus polypropylene fibers. I. Mechanical properties. J Appl Polym Sci 98, 1-8.
Guneyisi, E., Gesoglu, M., Mohamadameen, A., Alzeebaree, R., Algin, Z., Mermerdas, K., 2014. Enhancement of shrinkage behavior of lightweight aggregate concretes by shrinkage reducing admixture and fiber reinforcement. Constr Build Mater 54, 91-98.
Guo, X.Y., Xiang, D., Duan, G.H., Mou, P., 2010. A review of mechanochemistry applications in waste management. Waste Manage 30, 4-10.
Guo, Y.C., Zhang, J.H., Chen, G.M., Xie, Z.H., 2014. Compressive behaviour of concrete structures incorporating recycled concrete aggregates, rubber crumb and reinforced with steel fibre, subjected to elevated temperatures. J Clean Prod 72, 193-203.
Ha, K.H., Kim, M.S., 2012. Application to refrigerator plastics by mechanical recycling from polypropylene in waste-appliances. Mater Design 34, 252-257.
Habib, A., Begum, R., Alam, M.M., 2013. Mechanical properties of synthetic fibers reinforced mortars. International Journal of Scientific & Engineering Research 4.
Haktanir, T., Ari, K., Altun, F., Karahan, O., 2007. A comparative experimental investigation of concrete, reinforced-concrete and steel-fibre concrete pipes under three-edge-bearing test. Constr Build Mater 21, 1702-1708.
Hasan, M., Afroz, M., Mahmud, H., 2011. An experimental investigation on mechanical behavior of macro synthetic fibre reinforced concrete. International Journal of Civil & Environmental Engineering IJCEE-IJENS 11, 18-23.
Hasanah, T.I.T.N., Wijeyesekera, D.C., Lim, A.J.M.S., Ismail, B., 2014. Recycled PP/HDPE Blends: A Thermal Degradation and Mechanical Properties Study. 4th Mechanical and Manufacturing Engineering, Pts 1 and 2 465-466, 932-936.

Hinsken, H., Moss, S., Pauquet, J.R., Zweifel, H., 1991. Degradation of Polyolefins during Melt Processing. Polym Degrad Stabil 34, 279-293.
Hirose, M., Yamamoto, T., Naiki, M., 2000. Crystal structures of the alpha and beta forms of isotactic polypropylene: a Monte Carlo simulation. Comput Theor Polym S 10, 345-353.
Horvath, Z., Menyhard, A., Doshev, P., Gahleitner, M., Tranninger, C., Kheirandish, S., Varga, J., Pukanszky, B., 2013. Effect of molecular architecture on the crystalline structure and stiffness of iPP homopolymers: Modeling based on annealing experiments. J Appl Polym Sci 130, 3365-3373.
Hsie, M., Tu, C., Song, P.S., 2008. Mechanical properties of polypropylene hybrid fiber-reinforced concrete. Mat Sci Eng a-Struct 494, 153-157.
Huang, Y.P., Chen, G.M., Yao, Z., Li, H.W., Wu, Y., 2005. Non-isothermal crystallization behavior of polypropylene with nucleating agents and nano-calcium carbonate. Eur Polym J 41, 2753-2760.
Huo, H., Jiang, S.C., An, L.J., 2005. Oscillation effects on the crystallization behavior of iPP. Polymer 46, 11112-11116.
Ibrahim, H.M., 2011. Experimental investigation of ultimate capacity of wired mesh-reinforced cementitious slabs. Constr Build Mater 25, 251-259.
Ingrao, C., Lo Giudice, A., Tricase, C., Mbohwa, C., Rana, R., 2014. The use of basalt aggregates in the production of concrete for the prefabrication industry: Environmental impact assessment, interpretation and improvement. J Clean Prod 75, 195-204.
IPCC, 2009. Intergovernmental Panel on Climate Change, www.ipcc.ch (assessed by 10/11/2014).
Iribarren, D., Marvuglia, A., Hild, P., Guiton, M., Popovici, E., Benetto, E., 2015. Life cycle assessment and data envelopment analysis approach for the selection of building components according to their environmental impact efficiency: a case study for external walls. J Clean Prod 87, 707-716.
ISO14040, 2006. Environmental Management - Life Cycle Assessment - Principles and Framework. . London, UK: British Standards Institution.
ISO14044, 2006. Environmental Management - Life Cycle Assessment - Requirements and guidelines. London, UK: British Standards Institution.
Jafarifar, N., Pilakoutas, K., Bennett, T., 2014. Moisture transport and drying shrinkage properties of steel-fibre-reinforced-concrete. Constr Build Mater 73, 41-50.
Jesus-Hitzschky, K.R.E.d., 2007. Impact Assessment System for Technological Innovation: INOVA-tec System. Journal of Technology Management & Innovation 2, 67-82.
Jesus, K.R.E.d., Lanna, A.C., Vieira, F.D., Abreu, A.L.d., Lima, D.U.d., 2006. A Proposed Risk Assessment Method for Genetically Modified Plants Applied Biosafety 11, 127-137.
JSCE, 2005a. JSCE-G 551 1999. Test method for compressive strength and compressive toughness of steel fiber reinforced concrete. Test Methods and Specifications, 362.
JSCE, 2005b. JSCE-G 552-1999. Test Method for Bending Strength and Bending Toughness of Steel Fiber Reinforced Concrete. Standard Specification for Concrete Structures, Test Methods and Specifications.
Kabamba, E.T., Rodrigue, D., 2008. The effect of recycling on LDPE foamability: Elongational rheology. Polym Eng Sci 48, 11-18.

Kaufmann, J., Frech, K., Schuetz, P., Munch, B., 2013. Rebound and orientation of fibers in wet sprayed concrete applications. Constr Build Mater 49, 15-22.
Kaupp, G., 2009. Mechanochemistry: the varied applications of mechanical bond-breaking. Crystengcomm 11, 388-403.
Khan, Z.A., Kamaruddin, S., Siddiquee, A.N., 2010. Feasibility study of use of recycled High Density Polyethylene and multi response optimization of injection moulding parameters using combined grey relational and principal component analyses. Mater Design 31, 2925-2931.
Kim, J.H.J., Park, C.G., Lee, S.W., Lee, S.W., Won, J.P., 2008. Effects of the geometry of recycled PET fiber reinforcement on shrinkage cracking of cement-based composites. Compos Part B-Eng 39, 442-450.
Kim, S.B., Yi, N.H., Kim, H.Y., Kim, J.H.J., Song, Y.C., 2010. Material and structural performance evaluation of recycled PET fiber reinforced concrete. Cement Concrete Comp 32, 232-240.
Koo, B.M., Kim, J.H.J., Kim, S.B., Mun, S., 2014. Material and Structural Performance Evaluations of Hwangtoh Admixtures and Recycled PET Fiber-Added Eco-Friendly Concrete for CO2 Emission Reduction. Materials 7, 5959-5981.
La Vedrine, M.A.G., Sheahan, D.A., Gioia, R., Rowles, B., Kroeger, S., Phillips, C., Kirby, M.F., 2015. Substitution of hazardous offshore chemicals in UK waters: an evaluation of their use and discharge from 2000 to 2012. J Clean Prod 87, 675-682.
Lasvaux, S., Schiopu, N., Habert, G., Chevalier, J., Peuportier, B., 2014. Influence of simplification of life cycle inventories on the accuracy of impact assessment: application to construction products. J Clean Prod 79, 142-151.
LCS, 2014. LCS (Life cycle strategies), www.lifecycles.com.au (assessed by 10/11/2014).
Lebovitz, A.H., Khait, K., Torkelson, J.M., 2003. Sub-micron dispersed-phase particle size in polymer blends: overcoming the Taylor limit via solid-state shear pulverization. Polymer 44, 199-206.
Li, J., Li, H.L., Meng, L.P., Li, X.Y., Chen, L., Chen, W., Zhou, W.M., Qi, Z.M., Li, L.B., 2014. In-situ MR imaging on the plastic deformation of iPP thin films. Polymer 55, 1103-1107.
Liu, C.P., Wang, M.K., Xie, J.C., Zhang, W.X., Tong, Q.S., 2013. Mechanochemical degradation of the crosslinked and foamed EVA multicomponent and multiphase waste material for resource application. Polym Degrad Stabil 98, 1963-1971.
Liu, Y., Yang, W.M., Hao, M.F., 2010. Research on mechanical performance of roof tiles made of tire powder and waste plastic. Advanced Polymer Processing 87-88, 329-332.
LyondellBasell, 2012. Polypropylene. Environmental Information Document Australian Manufacture.
LyondellBasell, 2013. LyondellBasell Polymers. polymers.lyondellbasell.com/ (accessed by 05/06/2013).
Mahmud, G.H., Yang, Z.J., Hassan, A.M.T., 2013. Experimental and numerical studies of size effects of Ultra High Performance Steel Fibre Reinforced Concrete (UHPFRC) beams. Constr Build Mater 48, 1027-1034.
Martogg, 2013. www.martogg.com.au/www/home/(accessed by 05/06/2013).
Mazaheripour, H., Ghanbarpour, S., Mirmoradi, S.H., Hosseinpour, I., 2011. The effect of polypropylene fibers on the properties of fresh and hardened lightweight self-compacting concrete. Constr Build Mater 25, 351-358.

Mbarek, S., Jaziri, M., Carrot, C., 2006. Recycling poly(ethylene terephtalate) wastes: Properties of poly(ethylene terephtalate)/polycarbonate blends and the effect of a transesterification catalyst. Polym Eng Sci 46, 1378-1386.
Meddah, M.S., Bencheikh, M., 2009. Properties of concrete reinforced with different kinds of industrial waste fibre materials. Constr Build Mater 23, 3196-3205.
Mengeloglu, F., Karakus, K., 2008. Thermal degradation, mechanical properties and morphology of wheat straw flour filled recycled thermoplastic composites. Sensors-Basel 8, 500-519.
Mera, R.J., 2009. Climate Modeling Laboratory climlab02.meas.ncsu.edu (accessed by 10/11/2014).
Meran, C., Ozturk, O., Yuksel, M., 2008. Examination of the possibility of recycling and utilizing recycled polyethylene and polypropylene. Mater Design 29, 701-705.
Mindess, S., Chen, L., Morgan, D.R., 1994. Determination of the 1st-Crack Strength and Flexural Toughness of Steel Fiber-Reinforced Concrete. Adv Cem Based Mater 1, 201-208.
Myllari, V., Ruoko, T.P., Syrjala, S., 2015. A comparison of rheology and FTIR in the study of polypropylene and polystyrene photodegradation. J Appl Polym Sci 132.
Najm, H., Balaguru, P., 2002. Effect of large-diameter polymeric fibers on shrinkage cracking of cement composites. Aci Mater J 99, 345-351.
Nili, M., Afroughsabet, V., 2010. The effects of silica fume and polypropylene fibers on the impact resistance and mechanical properties of concrete. Constr Build Mater 24, 927-933.
Ochi, T., Okubo, S., Fukui, K., 2007. Development of recycled PET fiber and its application as concrete-reinforcing fiber. Cement Concrete Comp 29, 448-455.
Oh, B.H., Kim, J.C., Choi, Y.C., 2007. Fracture behavior of concrete members reinforced with structural synthetic fibers. Eng Fract Mech 74, 243-257.
OneSteel, 2015. OneSteel Reinforcing. www.reinforcing.com.au [accessed 25.04.15].
Ozger, O.B., Girardi, F., Giannuzzi, G.M., Salomoni, V.A., Majorana, C.E., Fambri, L., Baldassino, N., Di Maggio, R., 2013. Effect of nylon fibres on mechanical and thermal properties of hardened concrete for energy storage systems. Mater Design 51, 989-997.
Pacheco-Torgal, F., Jalali, S., 2011. Cementitious building materials reinforced with vegetable fibres: A review. Constr Build Mater 25, 575-581.
Park, S.S., 2011. Unconfined compressive strength and ductility of fiber-reinforced cemented sand. Constr Build Mater 25, 1134-1138.
Parmentier, B., De Grove, E., Vandewalle, L., Van Rickstal, F., 2008. Dispersion of the mechanical properties of FRC investigated by different bending tests. Tailor Made Concrete Structures: New Solutions for Our Society, 123-123.
Parthasarthy, G., Sevegney, M., Kannan, R.M., 2002. Rheooptical Fourier transform infrared spectroscopy of the deformation behavior in quenched and slow-cooled isotactic polypropylene films. J Polym Sci Pol Phys 40, 2539-2551.
Peche, R., Rodriguez, E., 2009. Environmental impact assessment procedure: A new approach based on fuzzy logic. Environ Impact Asses 29, 275-283.
Pelisser, F., Neto, A.B.D.S., La Rovere, H.L., Pinto, R.C.D., 2010. Effect of the addition of synthetic fibers to concrete thin slabs on plastic shrinkage cracking. Constr Build Mater 24, 2171-2176.

Pereira-De-Oliveira, L.A., Castro-Gomes, J.P., Nepomuceno, M.C.S., 2012. Effect of acrylic fibres geometry on physical, mechanical and durability properties of cement mortars. Constr Build Mater 27, 189-196.
Perugini, F., Mastellone, M.L., Arena, U., 2005. Life cycle assessment of mechanical and feedstock recycling options for management of plastic packaging wastes. Environ Prog 24, 137-154.
Peyvandi, A., Soroushian, P., Jahangirnejad, S., 2013. Enhancement of the structural efficiency and performance of concrete pipes through fiber reinforcement. Constr Build Mater 45, 36-44.
PlasticsEurope, 2015. Plastics - the Facts 2014/2015. An analysis of European plastics production, demand and waste data www.plasticseurope.org (assesed by 09/03/2015).
PTTPM, 2013. PTT Polymer Marketing. www.pttpm.com/product_hdpe.aspx (assess by 05/6/2013).
Pujadas, P., Blanco, A., Cavalaro, S., Aguado, A., 2014a. Plastic fibres as the only reinforcement for flat suspended slabs: Experimental investigation and numerical simulation. Constr Build Mater 57, 92-104.
Pujadas, P., Blanco, A., Cavalaro, S., de la Fuente, A., Aguado, A., 2014b. Fibre distribution in macro-plastic fibre reinforced concrete slab-panels. Constr Build Mater 64, 496-503.
Ramezanianpour, A.A., Esmaeili, M., Ghahari, S.A., Najafi, M.H., 2013. Laboratory study on the effect of polypropylene fiber on durability, and physical and mechanical characteristic of concrete for application in sleepers. Constr Build Mater 44, 411-418.
Recipe, 2008. Recipe database. . www.lcia-recipe.net (assessed by 10/11/2014).
RILEM, 2002. RILEM TC 162-TDF. Test and Design Methods for Steel Fibre Reinforced Concrete: Bending Test. RILEM J of Materials and Structures 35, 579-582.
Roque, P., Kim, N., Kim, B., Lopp, G., 2009. Durability of fiber-reinforced concrete in Florida environments. Technical report submitted to Florida department of transportation, Florida, the USA.
Sanchez, C., Hortal, M., Aliaga, C., Devis, A., Cloquell-Ballester, V.A., 2014. Recyclability assessment of nano-reinforced plastic packaging. Waste Manage 34, 2647-2655.
Sandin, G., Peters, G.M., Svanstrom, M., 2014. Life cycle assessment of construction materials: the influence of assumptions in end-of-life modelling. Int J Life Cycle Ass 19, 723-731.
Sanjuan, M.A., Moragues, A., 1997. Polypropylene-fibre-reinforced mortar mixes: Optimization to control plastic shrinkage. Compos Sci Technol 57, 655-660.
Santos, A.S.F., Teixeira, B.A.N., Agnelli, J.A.M., Manrich, S., 2005. Characterization of effluents through a typical plastic recycling process: An evaluation of cleaning performance and environmental pollution. Resour Conserv Recy 45, 159-171.
Sayyar, M., Soroushian, P., Sadiq, M.M., Balachandra, A., Lu, J., 2013. Low-cost glass fiber composites with enhanced alkali resistance tailored towards concrete reinforcement. Constr Build Mater 44, 458-463.
Shaheen, E., Shrive, N.G., 2007. Cyclic loading and fracture mechanics of Ductal (R) concrete. Int J Fracture 148, 251-260.
Shannag, M.J., Bin Ziyyad, T., 2007. Flexural response of ferrocement with fibrous cementitious matrices. Constr Build Mater 21, 1198-1205.
Shen, L., Worrell, E., Patel, M.K., 2010. Open-loop recycling: A LCA case study of PET bottle-to-fibre recycling. Resour Conserv Recy 55, 34-52.

Siddique, R., Khatib, J., Kaur, I., 2008. Use of recycled plastic in concrete: A review. Waste Manage 28, 1835-1852.
Silva, D.A., Betioli, A.M., Gleize, P.J.P., Roman, H.R., Gomez, L.A., Ribeiro, J.L.D., 2005. Degradation of recycled PET fibers in Portland cement-based materials. Cement Concrete Res 35, 1741-1746.
Silva, F.D., Toledo, R.D., Melo, J.D., Fairbairn, E.D.R., 2010. Physical and mechanical properties of durable sisal fiber-cement composites. Constr Build Mater 24, 777-785.
Silvestre, J.D., de Brito, J., Pinheiro, M.D., 2014. Environmental impacts and benefits of the end-of-life of building materials - calculation rules, results and contribution to a "cradle to cradle" life cycle. J Clean Prod 66, 37-45.
SimaPro, 2010. Australian Indicator Set V3.00 Australasian unit process LCI. SimaPro 8.0 Database: Methods Library.
Singh, S., Shukla, A., Brown, R., 2004. Pullout behavior of polypropylene fibers from cementitious matrix. Cement Concrete Res 34, 1919-1925.
Snelson, D.G., Kinuthia, J.M., 2010. Resistance of mortar containing unprocessed pulverised fuel ash (PFA) to sulphate attack. Cement Concrete Comp 32, 523-531.
Somani, R.H., Yang, L., Zhu, L., Hsiao, B.S., 2005. Flow-induced shish-kebab precursor structures in entangled polymer melts. Polymer 46, 8587-8623.
Song, P.S., Hwang, S., Sheu, B.C., 2005. Strength properties of nylon- and polypropylene-fiber-reinforced concretes. Cement Concrete Res 35, 1546-1550.
Soroushian, P., Plasencia, J., Revanbakhsh, S., 2003. Assessment of reinforcing effects of recycled plastic and paper in concrete. Aci Mater J 100, 203-207.
Soutsos, M.N., Le, T.T., Lampropoulos, A.P., 2012. Flexural performance of fibre reinforced concrete made with steel and synthetic fibres. Constr Build Mater 36, 704-710.
Soylev, T.A., Ozturan, T., 2014. Durability, physical and mechanical properties of fiber-reinforced concretes at low-volume fraction. Constr Build Mater 73, 67-75.
Spadea, S., Farina, I., Carrafiello, A., Fraternali, F., 2015. Recycled nylon fibers as cement mortar reinforcement. Constr Build Mater 80, 200-209.
Spielmann, M., 2012. Transport lorry >32t. SimaPro 8.0 Database Manual: AusLCI unit process.
Steiner, R., 2008. Milling steel. Simapro 8.0 database: Ecoinvent unit processes.
Strapasson, R., Amico, S.C., Pereira, M.F.R., Syclenstricker, T.H.D., 2005. Tensile and impact behavior of polypropylene/low density polyethylene blends. Polym Test 24, 468-473.
Streletskii, A.N., Kolbanev, I.V., Teselkin, V.A., Leonov, A.V., Mudretsova, S.N., Sivak, M.V., Dolgoborodov, A.Y., 2015. Defective structure, plastic properties, and reactivity of mechanically activated magnesium. Russ J Phys Chem B+ 9, 148-156.
Strezov, L., Herbertson, J., 2006. A Life Cycle Perspective on Steel Building Materials. Principals of the Crucible Group Pty Ltd
Stynoski, P., Mondal, P., Marsh, C., 2015. Effects of silica additives on fracture properties of carbon nanotube and carbon fiber reinforced Portland cement mortar. Cement Concrete Comp 55, 232-240.
Sukontasukkul, P., Pomchiengpin, W., Songpiriyakij, S., 2010. Post-crack (or post-peak) flexural response and toughness of fiber reinforced concrete after exposure to high temperature. Constr Build Mater 24, 1967-1974.

Tabatabaei, S.H., Carreau, P.J., Aji, A., 2009. Structure and properties of MDO stretched polypropylene. Polymer 50, 3981-3989.
Tassew, S.T., Lubell, A.S., 2014. Mechanical properties of glass fiber reinforced ceramic concrete. Constr Build Mater 51, 215-224.
Taylor, M., Lydon, F.D., Barr, B.I.G., 1997. Toughness measurements on steel fibre-reinforced high strength concrete. Cement Concrete Comp 19, 329-340.
Torkaman, J., Ashori, A., Momtazi, A.S., 2014. Using wood fiber waste, rice husk ash, and limestone powder waste as cement replacement materials for lightweight concrete blocks. Constr Build Mater 50, 432-436.
U.S.EPA, 2014. Wastes - Resource Conservation - Common Wastes & Materials. www.epa.gov/osw/conserve/materials/plastics.htm (assessed by 09/03/2015).
Uno, P.J., 1998. Plastic shrinkage cracking and evaporation formulas. Aci Mater J 95, 365-375.
Velis, C., 2014. Global recycling markets - plastic waste: A story for one player - China. . Report prepared by FUELogy and formatted by D-waste on behalf of International Solid Waste Association - Globalisation and Waste Management Task Force. ISWA, Vienna, September 2014. .
Viksne, A., Rence, L., Kalnins, M., Bledzki, A.K., 2004. The effect of paraffin on fiber dispersion and mechanical properties of polyolefin-sawdust composites. J Appl Polym Sci 93, 2385-2393.
Villain, F., Coudane, J., Vert, M., 1995. Thermal-Degradation of Polyethylene Terephthalate - Study of Polymer Stabilization. Polym Degrad Stabil 49, 393-397.
Vincent, T., Ozbakkaloglu, T., 2013. Influence of fiber orientation and specimen end condition on axial' compressive behavior of FRP-confined concrete. Constr Build Mater 47, 814-826.
Walling, F.B., Otts, L.E., 1967. Water Requirements of the Iron and Steel Industry. Geological Survey Water, Washington, the USA
Wang, Y.J., Zureick, A.H., Cho, B.S., Scott, D.E., 1994. Properties of Fiber-Reinforced Concrete Using Recycled Fibers from Carpet Industrial-Waste. J Mater Sci 29, 4191-4199.
Wang, Y.N., Hughes, B., Caspe, H., Amini, M., 2004. Devil's Slide Tunnels. North American Tunneling 2004, 605-611.
Wille, K., Tue, N.V., Parra-Montesinos, G.J., 2014. Fiber distribution and orientation in UHP-FRC beams and their effect on backward analysis. Mater Struct 47, 1825-1838.
Won, J.P., Jang, C.I., Lee, S.W., Lee, S.J., Kim, H.Y., 2010. Long-term performance of recycled PET fibre-reinforced cement composites. Constr Build Mater 24, 660-665.
Yang, J.M., Min, K.H., Shin, H.O., Yoon, Y.S., 2012. Effect of steel and synthetic fibers on flexural behavior of high-strength concrete beams reinforced with FRP bars. Compos Part B-Eng 43, 1077-1086.
Yehia, N.A.B., 2009. Fracture mechanics approach for flexural strengthening of reinforced concrete beams. Eng Struct 31, 404-416.
Yeo, S.Y., Lee, H.J., Jeong, S.H., 2003. Preparation of nanocomposite fibers for permanent antibacterial effect. J Mater Sci 38, 2143-2147.
Yin, S., Tuladhar, R., Collister, T., Combe, M., Sivakugan, N., 2015a. Mechanical Properties and Post-crack Behaviours of Recycled PP Fibre Reinforced Concrete. Concrete 2015, 30 August – 2 September, 2015, Melbourne, Australia.

Yin, S., Tuladhar, R., Combe, M., Collister, T., Jacob, M., Shanks, R., 2013. Mechanical properties of recycled plastic fibres for reinforcing concrete, In: Proceedings of the 7th International Conference Fibre Concrete, pp. 1-10. From: 7th International Conference Fibre Concrete, September 12-13 2013, Prague, Czech Republic.
Yin, S., Tuladhar, R., Shanks, R.A., Collister, T., Combe, M., Jacob, M., Tian, M., Sivakugan, N., 2015b. Fiber preparation and mechanical properties of recycled polypropylene for reinforcing concrete. J Appl Polym Sci 132, 41866.
Yin, S., Tuladhar, R., Shi, F., Combe, M., Collister, T., Sivakugan, N., 2015c. Use of macro plastic fibres in concrete: A review. Constr Build Mater 93, 180-188.
Yoo, D.Y., Min, K.H., Lee, J.H., Yoon, Y.S., 2014. Shrinkage and cracking of restrained ultra-high-performance fiber-reinforced concrete slabs at early age. Constr Build Mater 73, 357-365.
Yoo, D.Y., Park, J.J., Kim, S.W., Yoon, Y.S., 2013. Early age setting, shrinkage and tensile characteristics of ultra high performance fiber reinforced concrete. Constr Build Mater 41, 427-438.
ZCBL, 2013. ZCBL (Zero Carbon Building Ltd). Reinforcing Bar and Structural Steel Carbon Labelling Scheme for Construction Products Assessment Guide. Kowloon, Hong Kong. .
Zhang, B., Chen, J.B., Zhang, X.L., Shen, C.Y., 2011. Crystal Morphology and Structure of the beta-Form of Isotactic Polypropylene Under Supercooled Extrusion. J Appl Polym Sci 120, 3255-3264.
Zhao, X.W., Ye, L., 2011. Structure and properties of highly oriented polyoxymethylene produced by hot stretching. Mat Sci Eng a-Struct 528, 4585-4591.
Zheng, Z.H., Feldman, D., 1995. Synthetic Fiber-Reinforced Concrete. Prog Polym Sci 20, 185-210.
Zhijun, Z., Farhad, A., 2005. Determination of crack tip opening displacement of concrete by embedded fiber optic sensor. ICF 11, JRESEARCH PAPERS.
Zhong, C.F., Mao, B.Q., 2009. Structure and Isothermal Crystallization Behavior of Polypropylene Prepared at High Polymerization Temperature. J Appl Polym Sci 114, 2474-2480.
Zhou, C.B., Fang, W.J., Xu, W.Y., Cao, A.X., Wang, R.S., 2014. Characteristics and the recovery potential of plastic wastes obtained from landfill mining. J Clean Prod 80, 80-86.
Zi, G., Kim, J., Bazant, Z.P., 2014. Size Effect on Biaxial Flexural Strength of Concrete. Aci Mater J 111, 319-326.
Zollo, R.F., 1997. Fiber-reinforced concrete: an overview after 30 years of development. Cement Concrete Comp 19, 107-122.